

ความเกี่ยวข้องของคาทอลิกกับอะพอโทซิสม์ในกึ่งกลางคำที่ติดเชื่อไวรัสตัวแดงดวงขาว



นาย อาทิตย์ ชะลอศรีกุล

สถาบันวิทยบริการ

วิทยานิพนธ์นี้เป็นส่วนหนึ่งของการศึกษาตามหลักสูตรปริญญาวิทยาศาสตรมหาบัณฑิต

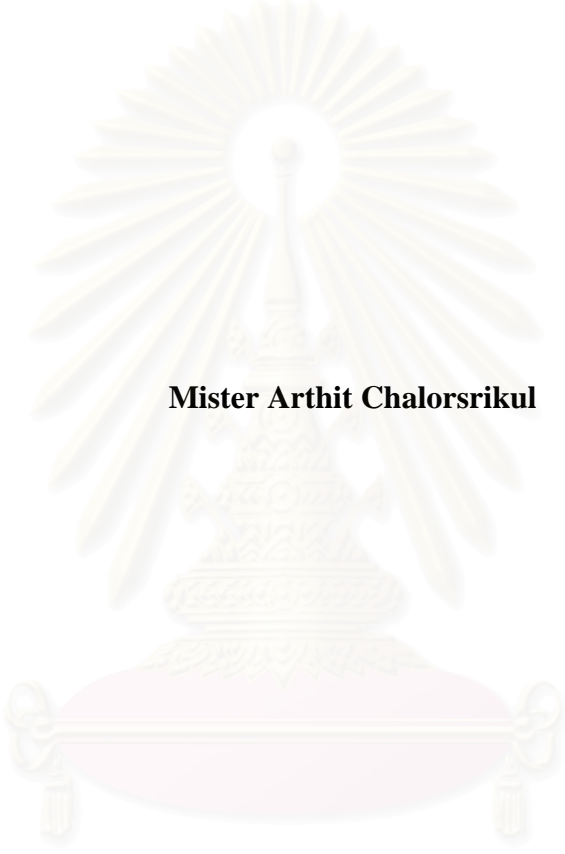
สาขาวิชาชีวเคมี ภาควิชาชีวเคมี

คณะวิทยาศาสตร์ จุฬาลงกรณ์มหาวิทยาลัย

ปีการศึกษา 2550

ลิขสิทธิ์ของจุฬาลงกรณ์มหาวิทยาลัย

**INVOLVEMENT OF CATHEPSIN IN APOPTOSIS OF THE BLACK TIGER  
SHRIMP INFECTED WITH WHITE SPOT SYNDROME VIRUS**



**Mister Arthit Chalorsrikul**

**A Thesis Submitted in Partial Fulfillment of the Requirements  
for the Degree of Master of Science Program in Biochemistry**

**Department of Biochemistry**

**Faculty of Science**

**Chulalongkorn University**

**Academic Year 2007**

**Copyright of Chulalongkorn University**

Thesis Title            INVOLVEMENT OF CATHEPSIN IN APOPTOSIS OF THE  
                                  BLACK TIGER SHRIMP INFECTED WITH WHITE SPOT  
                                  SYNDROME VIRUS  
By                            Mister Arthit Chalorsrikul  
Field of study            Biochemistry  
Thesis Advisor          Professor Anchalee Tassanakajon, Ph.D.  
Thesis Co-advisor      Siriporn Pongsomboon, Ph.D.

---

Accepted by the Faculty of Science, Chulalongkorn University in Partial  
Fulfillment of the Requirements for the Master's Degree

*S. Hannongbua*  
.....Dean of the Faculty of Science  
(Professor Supot Hannongbua, Ph.D.)

THESIS COMMITTEE

*Aran Incharoensakdi*  
.....Chairman  
(Professor Aran Incharoensakdi, Ph.D.)

*A. Tassanakajon*  
.....Thesis Advisor  
(Professor Anchalee Tassanakajon, Ph.D.)

*Siriporn Pongsomboon*  
.....Thesis Co-advisor  
(Siriporn Pongsomboon, Ph.D.)

*V. Rimphanitchayakit*  
.....Member  
(Associate Professor Vichien Rimphanitchayakit, Ph.D.)

*Teerapong Buaboocha*  
.....Member  
(Assistant Professor Teerapong Buaboocha, Ph.D.)

อาทิตย์ ชะลอศรีกุล: ความเกี่ยวข้องของคาเทปซินกับอะพอพโทซิสในกุ้งกุลาดำที่ติดเชื้อไวรัสตัวแดงดวงขาว. (INVOLVEMENT OF CATHEPSIN IN APOPTOSIS OF THE BLACK TIGER SHRIMP INFECTED WITH WHITE SPOT SYNDROME VIRUS) อ. ที่ปรึกษา: ศ.ดร.อัญชลี ทศนาขจร, อ. ที่ปรึกษาร่วม: ดร.สิริพร พงษ์สมบูรณ์, 99 หน้า.

จากรายงานก่อนหน้านี้นี้มีการตรวจพบการเกิดอะพอพโทซิสในกุ้งกุลาดำที่ติดเชื้อไวรัสตัวแดงดวงขาว โดยการเกิดอะพอพโทซิสอาจเป็นสาเหตุให้กุ้งที่ติดเชื้อตาย และมีรายงานว่าโปรตีนในกลุ่ม cathepsin สามารถกระตุ้นให้เกิดอะพอพโทซิสในสัตว์มีกระดูกสันหลังหลายชนิด สำหรับกุ้งกุลาดำที่ติดเชื้อไวรัสตัวแดงดวงขาวจะมีการแสดงออกของ mRNA ของ cathepsin L เพิ่มขึ้นในต่อมน้ำเหลือง ดังนั้นในงานวิจัยนี้จะศึกษาความเกี่ยวข้องระหว่าง cathepsin L กับการเกิดอะพอพโทซิสในกุ้งกุลาดำที่มีการติดเชื้อไวรัสตัวแดงดวงขาว การตรวจหาโปรตีน cathepsin L ด้วยเทคนิค Western blot ในเม็ดเลือด หัวใจ ดับ และต่อมน้ำเหลือง พบโปรตีนขนาด 28 กิโลดาลตัน ในดับเพียงอวัยวะเดียว ขณะที่ผลของ immunohistochemistry ใน cephalothorax พบ cathepsin L ใน B เซลล์ของดับ และใน spheroid ของต่อมน้ำเหลือง นอกจากนี้ระดับของโปรตีน cathepsin L ใน spheroid ของกุ้งกุลาดำที่ติดเชื้อไวรัสตัวแดงดวงขาว มีระดับลดลงที่ 24 ชั่วโมง เมื่อเปรียบเทียบกับกุ้งกุลาดำที่ฉีดด้วยน้ำเลี้ยงเชื้อไวรัสตัวแดงดวงขาว (LHM) การศึกษาความเกี่ยวข้องของ cathepsin L ต่อการเกิดอะพอพโทซิสในเซลล์ปฐมภูมิของต่อมน้ำเหลือง พบว่าเซลล์ที่มีการเติม actinomycin D และตัวยับยั้ง caspase 3 หรือ actinomycin D และตัวยับยั้ง cathepsin L มีเปอร์เซ็นต์การตายของเซลล์ลดลงเมื่อเทียบกับเซลล์ที่มีการเติม actinomycin D เพียงอย่างเดียว และยังพบว่าความเข้มข้นที่เหมาะสมของตัวยับยั้ง caspase 3 และ cathepsin L คือ 0.5 และ 1 ไมโครโมลาร์ ตามลำดับ อย่างไรก็ตามเมื่อทำการตรวจสอบการเกิดอะพอพโทซิสด้วยวิธี DNA laddering พบว่าลักษณะดีเอ็นเอที่มีการเกิดอะพอพโทซิสของเซลล์ที่เติม actinomycin D 40 นาโนโมลาร์ ทั้งที่มีการเติมและไม่ได้เติมตัวยับยั้ง จะมีขนาดประมาณ 200 คู่เบส จากผลการเลี้ยงเซลล์พบว่า cathepsin L เกี่ยวข้องกับการเกิดอะพอพโทซิส นอกจากนี้ procathepsin L ได้ถูกนำไปผลิตในระบบของ *E.coli* BL21(DE3) เพื่อยืนยันหน้าที่ของ cathepsin L แต่เนื่องจากรีคอมบิแนนต์ procathepsin L ไม่สามารถกระตุ้นตัวเองได้ในสภาวะกรด ทำให้ไม่สามารถเปลี่ยนเป็นรีคอมบิแนนต์ cathepsin L ที่ทำงานได้

ภาควิชา.....ชีวเคมี..... ลายมือชื่อนิสิต..... อาทิตย์ ชะลอศรีกุล.....  
 สาขาวิชา.....ชีวเคมี..... ลายมือชื่ออาจารย์ที่ปรึกษา..... อัญชลี ทศนาขจร.....  
 ปีการศึกษา.....2550..... ลายมือชื่ออาจารย์ที่ปรึกษาร่วม..... ศิริพร พงษ์สมบูรณ์.....

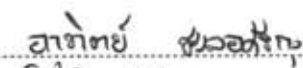
##4472568823: MAJOR BIOCHEMISTRY

KEY WORD: *Penaeus monodon* / IMMUNOHISTOCHEMISTRY / PRIMARY SHRIMP CELL CULTURE / CATHEPSIN L / WHITE SPOT SYNDROME VIRUS

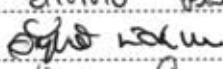
ARTHIT CHALORSRIKUL: INVOLVEMENT OF CATHEPSIN IN APOPTOSIS OF THE BLACK TIGER SHRIMP INFECTED WITH WHITE SPOT SYNDROME VIRUS. THESIS ADVISOR: PROF. ANCHALEE TASSANAKAJON, Ph.D., THESIS COADVISOR: SIRIPORN PONGSOMBOON, PhD., 99 pp.

Many studies suggest that apoptosis occurs following white spot syndrome virus (WSSV) infection in *Penaeus monodon* and might be the cause of death in viral infection. Among the molecules involved in apoptosis process, cathepsins have been reported to act as proapoptotic mediators of apoptosis in a variety of vertebrate species. In shrimp, cathepsin L mRNA was up-regulated in lymphoid organs after infection with WSSV. Since cathepsins seem to be interesting molecules, this study was aimed to verify the involvement of apoptosis function of cathepsin L in WSSV infected shrimp. Western blotting of the crude protein from haemocyte, heart, hepatopancreas and lymphoid organ revealed a single 28 kDa protein band of mature cathepsin L in hepatopancreas. Immunohistochemistry analysis in cephalothorax of *Penaeus monodon* found that the cathepsin L was detected mainly in B cells of hepatopancreas and in spheroid of lymphoid organ. Moreover, the cathepsin L level in lymphoid organ was found to be decreased at 24 h when compared with the control LHM-injected shrimp. The involvement of cathepsin L in apoptosis was further elucidated in the primary cell culture of lymphoid organ. The cells treated with actinomycin D and caspase-3 inhibitor or actinomycin D and cathepsin L inhibitor showed lower percentage of dead cells compared with the cells treated with actinomycin D only. The appropriate concentrations of caspase-3 and cathepsin L inhibitors for successful inhibition of apoptosis were 0.5 and 1  $\mu$ M, respectively. However, when the DNA laddering assay was performed to detect apoptosis, the characteristic apoptotic DNA ladder of approximately 200 bp was seen in all 40 nM actinomycin D treated cells with or without inhibitor as well as the control (untreated cells). As a result of cell culture assay, the study reveals an involvement in apoptosis of cathepsin L. Furthermore, in order to verify the function of cathepsin L, the procathepsin L was expressed in *E. coli* BL21(DE3) expression system. However, auto activation of the recombinant procathepsin L in acidic condition was unsuccessful, thus, the active cathepsin L was not obtained.

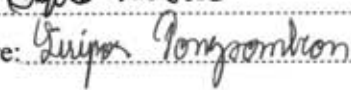
Department: Biochemistry

Student's signature: 

Field of study: Biochemistry

Advisor's signature: 

Academic year: 2007

Co-advisor's signature: 

## ACKNOWLEDGEMENTS

This study was carried out during the past four years at the Department of Biochemistry, Faculty of Science, Chulalongkorn University. I wish to express my deepest gratitude to my supervisor, Professor Dr. Anchalee Tassanakajon and my co-advisor, Dr. Siriporn Pongsomboon, for their excellent guidance, enthusiasm, instruction and support from the very beginning to the very end of my thesis. Especially I thank Professor Dr. Anchalee and Dr. Siriporn for endless patience and advice.

My gratitude is also extended to Professor Dr. Aran Incharoensakdi, Assistant Professor Dr. Vichien Rimphanitchayakit and Assistant Professor Dr. Teerapong Buaboocha for serving as thesis committee, for their available comments and useful suggestion.

My appreciation is also expressed to Professor Dr. Tim Felgel, Professor Dr. Paisarn Sithigorngul, Associate Professor Dr. Witoon Tirasophon, Dr. Premruethai Supungul, Dr. Kunlaya Somboonwiwat and Dr. Wanchai Assavalapsakul for warm support, instruction, lending helping, and interesting discussion.

Sincere thanks are also extended to all members and friends in R728, for lending a helping hand whenever needed, sharing the great time in laboratory, their warm assistance and friendship, at Department of Biochemistry Chulalongkorn University.

I wish to acknowledge to contributions of National Center of Genetic Engineering and Biotechnology (BIOTEC) for my financial support.

Last, but not least, I wish to thank my family for keeping my feet tightly on the ground and my mind away from science when I was at home. It's always good to be the family.

# CONTENTS

	<b>Page</b>
Abstract (Thai).....	iv
Abstract (English).....	v
Acknowledgements.....	vi
Contents.....	vii
List of Tables.....	x
List of Figures.....	xi
List of Abbreviations.....	xiii
Chapter I Introduction.....	1
1.1 General introduction.....	1
1.2 Taxonomy of <i>Penaeus monodon</i> .....	3
1.3 Morphology.....	4
1.4 Distribution and life cycle.....	6
1.5 Shrimp disease.....	9
1.5.1 Viral disease.....	9
1.5.2 White spot syndrome (WSS).....	10
1.6 Apoptosis.....	11
1.6.1 Pathways of apoptosis.....	12
1.7 Cathepsin.....	14
1.7.1 Cysteine cathepsins in apoptosis.....	15
1.9 Objective of the thesis.....	17
Chapter II Materials and Methods.....	18
2.1 Material.....	18
2.1.1 Equipments.....	18
2.1.2 Chemicals and reagents.....	19
2.1.3 Enzymes.....	21
2.1.4 Microorganisms.....	21
2.1.5 Kits.....	22
2.2 Samples.....	22

	<b>Page</b>
2.3 Preparation of WSSV infected shrimp.....	22
2.4 Diagnosis of WSSV.....	22
2.5 Immunohistochemistry.....	23
2.5.1 Tissue preparation for histology.....	23
2.5.2 Immunohistochemistry staining.....	24
2.6 Expression of CatL in the BL21(DE3) <i>E. coli</i> .....	25
2.6.1 Construction of recombinant pET-21a(+)-CatL.....	25
2.6.1.1 Preparation of DNA fragment containing CatL gene.....	25
2.6.1.2 Preparation of pET-21a(+) expression vector.....	26
2.6.1.3 Restriction enzyme digestion.....	27
2.6.1.4 Ligation.....	28
2.6.1.5 Electrotransformation.....	28
2.6.1.6 Isolation of the recombinant plasmid.....	28
2.6.2 Expression of recombinant CatL.....	29
2.6.2.1 Competent cell preparation.....	29
2.6.2.2 Calcium chloride transformation.....	29
2.6.2.3 Recombinant protein expression.....	29
2.6.3 Protein analysis.....	30
2.6.3.1 Sodium dodecyl sulfate-polyacrylamide gel electrophoresis (SDS-PAGE).....	30
2.6.3.2 Sample preparation.....	30
2.6.3.3 Analysis of the recombinant protein by SDS-PAGE..	30
2.6.3.4 Coomassie brilliant blue staining.....	31
2.6.4 Purification of recombinant protein.....	31
2.6.5 Detection of the purified recombinant protein by Western blot analysis.....	32
2.6.6 Molecular mass determination of recombinant CatL by using MALDI-TOF mass spectrometry.....	33

	<b>Page</b>
2.6.7 CatL activation.....	33
2.7 Preparation of the primary shrimp cell culture.....	34
2.8 Apoptosis induction by Actinomycin D.....	34
2.9 Detection of apoptosis using agarose gel electrophoresis.....	34
Chapter III Results.....	36
3.1 Immunohistochemical localization of cathepsin L protein.....	36
3.2 Immunohistochemical localization of WSSV.....	45
3.3 Recombinant expression of CatL in <i>Escherichia coli</i> expression system.....	48
3.3.1 Amplication of the truncated CatL gene.....	48
3.3.2 Construction of recombinant plasmid pGEM-T-CatL.....	48
3.3.3 Construction of recombinant plasmid pET-21a(+)-CatL.....	51
3.3.4 Recombinant protein expression in <i>Escherichia coli</i> BL21 (DE3).....	51
3.3.5 Solubility of the recombinant protein.....	51
3.4 Purification of the recombinant protein.....	54
3.5 Detection of recombinant protein using Western blot analysis.....	54
3.6 Molecular mass determination of the recombinant CatL by using MALDI-TOF mass spectrometry.....	54
3.7 Autocatalytic processing of procathepsin L.....	57
3.8 Primary lymphoid cell culture.....	59
3.9 Inhibition of apoptosis by Cas3 inhibitor and CatL inhibitor on AD induced apoptosis.....	59
3.10 Detection of apoptosis using agarose gel electrophoresis.....	62
Chapter IV Discussions.....	65
Chapter V Conclusions.....	72
References.....	73
Appendices.....	85
Biography.....	99

## List of Tables

		<b>Page</b>
Table 1.1	Thailand's exports of <i>P. monodon</i> in various countries.....	2
Table 3.1	Number of death cells counted by Trypan blue staining.....	62



สถาบันวิทยบริการ  
จุฬาลงกรณ์มหาวิทยาลัย

## List of Figures

	<b>Page</b>
Figure 1.1 Thai shrimp production between 2002 and 2006 and the prediction in 2007.....	2
Figure 1.2 Lateral view of the external morphology of <i>Penaeus monodon</i> (Anderson, 1993).....	5
Figure 1.3 Lateral view of the internal anatomy of a female <i>Penaeus monodon</i> (Primavera, 1993).....	7
Figure 1.4 Location of hematopoietic tissue and lymphoid organ of penaeid shrimp.....	8
Figure 1.5 The life cycle of <i>Penaeus monodon</i> shrimp (Baily-Brook, and Moss, 1992).....	8
Figure 1.6 Intrinsic and extrinsic apoptosis pathway in mammalian cells (Jeong et al. 2008).....	14
Figure 1.7 The role of cathepsin in apoptosis (Vasiljeva et al. 2008).....	17
Figure 2.1 Western transfer cassettes.....	32
Figure 3.1 SDS-PAGE (A) and Western blot analysis (B) in shrimp tissues with human CatL antibody.....	37
Figure 3.2 Immunohistochemical localization of CatL in multiple <i>P. monodon</i> cephalothoraxes tissues.....	38
Figure 3.3 Immunohistochemical localization of CatL in multiple <i>P. monodon</i> cephalothoraxes tissue.....	40
Figure 3.4 Immunohistochemical localization of CatL in multiple <i>P. monodon</i> cephalothoraxes tissues.....	41
Figure 3.5 Immunohistolocalization of CatL in hepatopancreas and lymphoid organ of normal shrimp.....	42
Figure 3.6 Light micrograph of CatL immunolocalization in hepatopancreas.....	43
Figure 3.7 Light micrograph of CatL immunolocalization in lymphoid organ.....	44

	<b>Page</b>
Figure 3.8	Immunohistochemistry of WSSV in hepatopancreas..... 46
Figure 3.9	Immunohistochemistry of WSSV in lymphoid organ..... 47
Figure 3.10	The nucleotide and deduced amino acid sequence of the cDNA clone encoding <i>Penaeus monodon</i> CatL from lymphoid organ (ABQ10739)..... 49
Figure 3.11	Agarose gel electrophoresis of PCR amplification product and the recombinant vector on 1.2 % agarose gel..... 50
Figure 3.12	The Coomassie stained 12 % SDS-PAGE analysis of CatL expressed in <i>Escherichia coli</i> BL21(DE3) at various time of induction..... 52
Figure 3.13	The SDS-PAGE analysis of soluble and inclusion protein fractions..... 53
Figure 3.14	Western blot analysis of purified CatL from <i>Escherichia coli</i> BL21(DE3)..... 55
Figure 3.15	MALDI-TOF mass spectrometric determination of molecular weight of the recombinant CatL..... 56
Figure 3.16	Acid autoactivation of crude CatL..... 58
Figure 3.17	Morphology of primary lymphoid cell culture..... 60
Figure 3.18	Morphology of the primary lymphoid cell of <i>P. monodon</i> after treated with actinomycin D..... 61
Figure 3.19	Percentage of mortal cells in AD induced apoptosis with or without inhibitors..... 63
Figure 3.20	Apoptotic DNA laddering from primary cell culture treated with AD..... 64
Figure 4.1	Multiple alignment of the deduced amino acid sequence of cathepsin L..... 67

## List of Abbreviations

AD	actinomycin D
Ala	aminoacid Alanine
BCIP	5-Bromo-4-Chloro-3'-Indolyphosphate p-Toluidine Salt
bp	base pair
BSA	bovine serum albumin
°C	degree Celcius
Cas3	caspase 3
CatD	cathepsin D
CatL	cathepsin L
CTAB	cetyl trimethylammonium bromide
DNA	deoxyribonucleic acid
dNTP	deoxyribonucleotide triphosphate
<i>E. coli</i>	<i>Escherichia coli</i>
EDTA	ethylene diamine tetraacetic acid
EtBr	ethidium bromide
EST	Expressed Sequence Taq
h	hour
His	histidine
hpi	hour-post injection
IgG	immunoglobulin G
IHC	immunohistochemistry
IPTG	isopropyl-beta-D-thiogalactopyranoside
kb	kilobase
KCl	potassium chloride
kDa	kilodalton
KH <sub>2</sub> PO <sub>4</sub>	potassium dihydrogen phosphate
LB	luria broth
LHM	lobster haemolymph medium

LO	lymphoid organ
LOS	lymphoid organ spheroid
LT	lymphoid organ tubule
Lum	lumen
<i>Lv</i>	<i>Litopenaeus vanamei</i>
M	molar
MALDI	matrix-assisted laser desorption/ionization
MCS	multiple cloning sites
<i>M. ensis</i>	<i>Metapenaeus ensis</i>
ml	millilitre
MgCl <sub>2</sub>	magnesium chloride
mg	milligram
mM	millimolar
Na <sub>2</sub> HPO <sub>4</sub>	disodium hydrogen orthophosphate
NaOH	sodium hydroxide
NBT	nitroblue tetrazolium chloride
ng	nanogram
Ni	nickel
nM	nanomolar
NRS	normal rabbit serum
O.D.	optical density
ORF	open reading frame
PAGE	polyacrylamide gel electrophoresis
PBS	phosphate buffered saline
PCR	polymerase chain reaction
<i>Pm</i>	<i>Penaeus monodon</i>
pmol	picomole
RNA	ribonucleic acid
RNase A	ribonuclease A
SDS	sodium dodecyl sulfate
TOF	time-of-flight

$\mu\text{g}$	microgram
$\mu\text{l}$	microlitre
$\mu\text{M}$	micromolar
$\mu\text{m}$	micrometer
UV	ultraviolet
Val	amino acids valine
WSSV	white spot syndrome virus



สถาบันวิทยบริการ  
จุฬาลงกรณ์มหาวิทยาลัย

# CHAPTER I

## INTRODUCTION

### 1.1 General introduction

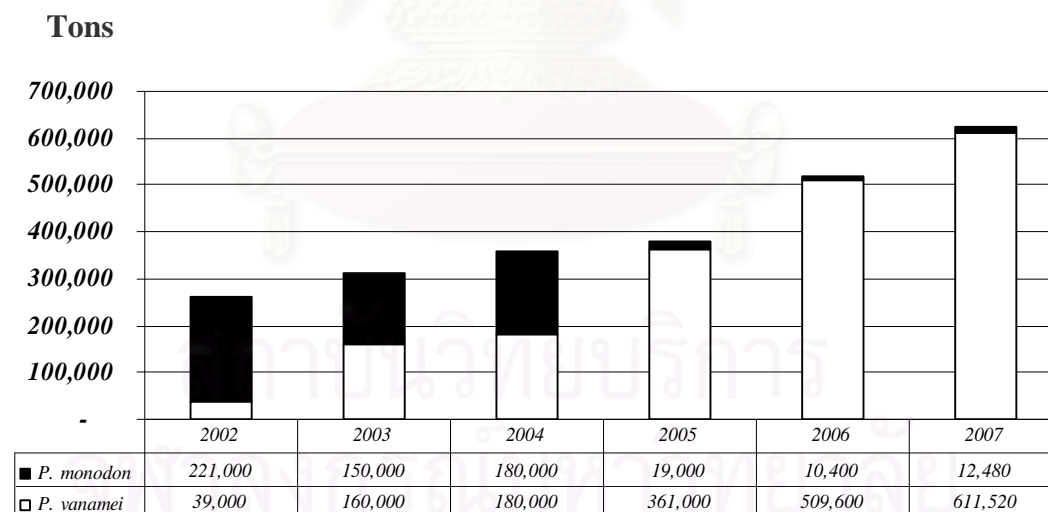
For the trading of aquaculture produces, shrimp and prawn as a group were the second highest reported value worth US\$10.6 billion. For single species, the highest reported value was US\$5.9 billion for the pacific white shrimp (*Litopenaeus vannamei*), followed by Atlantic salmon (*Salmo salar*), silver crap and black tiger shrimp (*Penaeus monodon*) (Source: FAO Aquaculture Newsletter No. 38, 2007). Thailand is one of the top ten countries in aquaculture production of aquatic animals, and shrimp is one of our highest value productions. Black tiger shrimp, *P. monodon*, and the pacific white shrimp, *L. vannamei*, are the two major shrimp species exported to various countries. Before the year 2000, Thailand was the world's leading shrimp producer of *P. monodon*. In 2002, however, the production, as compared to 2001, decreased about 40 percent to approximately 160,000 tons due to infectious diseases at the beginning of the year, unfavorable weather, high salt concentration in water, slow shrimp growth rates, low yield per area. The worst of it is that the black tiger shrimp production of Thailand fell down from 180,000 tons in 2004 to 19,000 tons in 2005 (Fig 1.1). In 2007, the prediction of black tiger shrimp production will be 12,480 tons while that of white shrimp will be 611,520 tons.

Due to the serious problems of the black tiger shrimp, the species mainly cultured in Thailand had switched to the white shrimp, *L. vannamei*. The exotic species, *L. vannamei*, was imported for aquaculture instead of the native one like *P. monodon* (Fig 1.1). The main reasons behind the importation of *L. vannamei* had been the poor performance, slow growth rate and disease susceptibility of the *P. monodon* shrimp virtually everywhere in Thailand. However, the total Thai shrimp production was not affected as it was compensated by the increased production of the white shrimp (Fig 1.1).

**Table 1.1** Thailand's exports of *P. monodon* in various countries

Country	2003		2004		2005		2006	
	Quantity	Value	Quantity	Value	Quantity	Value	Quantity	Value
USA	37,701	12,157	20,593	5,878	12,147	2,992	15,302	3,613
Japan	15,238	5,381	11,672	3,961	6,662	2,261	2,523	802
Canada	5,453	1,767	3,345	1,109	1,966	578	2,019	531
Singapore	2,366	612	1,042	201	379	65	238	38
Korea	5,141	1,345	4,994	1,244	3,704	864	2,769	664
Taiwan	1,886	515	2,825	469	1,469	381	456	145
Australia	2,669	718	1,365	371	296	108	317	107
Hong Kong	516	140	666	217	589	169	618	142
China	361	74	612	136	646	102	582	71
Total	73,334	23,341	49,303	14,307	29,168	7,900	25,420	6,298

Quantity = tons Value = million baht (Source: The Customs Department)

**Figure 1.1** Thai shrimp production between 2002 and 2006 and the prediction in 2007

[Source: FAO Fishstat (2006)]

The advantages of *L. vannamei* include its rapid growth rate, tolerance of high stocking density, tolerance of low salinities and temperatures, lower protein requirements (and, therefore, the production costs), certain disease resistance (if specific pathogen resistant stocks are used), and high survival during larval rearing. There are, however, also disadvantages to the importation of *L. vannamei*, including its ability to act as a carrier of various exotic viral pathogens. *L. vannamei* is a known carrier of *Baculovirus penaei* (BP), infectious hypodermal and hematopoietic necrosis virus (IHHNV), Reo-like virus (REO) and Taura Syndrome virus (TSV). These viruses can be transmitted to the native wild penaeid shrimp populations, and thus increases the concern over the spreading of diseases by the release of infected shrimps from culture facilities (Overstreet et al. 1997). Because the first signs of Taura Syndrome Virus (TSV) in Thai *L. vannamei* and *Macrobrachium rosenbergii* has been observed (Briggs et al. 2004), there is also the possibility of viral outbreak on the cultured *L. vannamei* as in Latin America. Although TSV is not reported to have affected indigenous cultured or wild shrimp populations, insufficient time and research have been conducted on this issue and there is a need for caution. TSV is a highly mutable virus, capable of mutating into more virulent strains capable of infecting the other shrimp species. In addition, some other viruses are probably imported along with the *L. vannamei*, for example, a new LOVV-like virus, have been implicated in causing the slow growth problems currently being encountered in the culture of indigenous *P. monodon*.

Due to the above problems, the native shrimp should be improved to gain resistance to the pathogens and rapid growth rate. Researches in *P. monodon* must be continued in various fields concerning the shrimp immunity, pathology, physiology and genetics, aquaculture, etc.

## **1.2 Taxonomy of *Penaeus monodon***

*Penaeus monodon*, the giant tiger shrimp, is a shrimp species that was classified into the largest phylum in the animal kingdom, the Arthropoda. The taxonomic definition of *Penaeus monodon* is as follows (Fast et al. 1992):

**Phylum** Arthropoda  
**Subphylum** Crustacea  
**Class** Malacostraca  
**Subclass** Eumalacostraca  
**Order** Decapoda  
**Suborder** Natantia  
**Infraorder** Penaeidea  
**Superfamily** Penaeoidea  
**Family** Penaeidae Rafinesque, 1985  
**Genus** *Penaeus* Fabricius, 1798  
**Subgenus** *Penaeus*  
**Species** *monodon*

**Scientific name:** *Penaeus monodon* (Fabricius), 1798

**Common name:** Jumbo tiger prawn, Giant tiger prawn, Blue tiger prawn, Leader prawn, Panda prawn (Australia), Jar-Pazun (Burma), Bangkear (Cambodia), Ghost prawn (Hong Kong), Jinga (India, Bombay region), Udang windu (Indonesia), Ushi-ebi (Japan), Kamba ndogo (Kenya), Kalri (Pakistan), Sugpo (Philippines), Grass shrimp (Taiwan), Kung kula-dum (Thailand), Timsa (Vietnam).

**FA.O. Names:** Giant tiger prawn, Crevette gigante tigre, Camaron tigre gigante.

### 1.3 Morphology

The shrimp body includes three regions: head, thorax, and abdomen (Fig 1.2). Each body region possesses appendages specialized for different functions. The head (five somites) and thorax (eight somites) are fused into a cephalothorax, which is completely covered by the carapace. Many internal organs, such as gills, digestive system, reproductive system and heart located in thorax are protected by carapace, while the muscles concentrate in the abdomen. The pleura of the cephalothorax form the branchiostegite or gill cover. The carapace has characteristic ridges (carinae) and grooves (sulci). The rostrum is always prominent, with a high median blade bearing dorsal teeth and, in some genera, ventral teeth as well. The compound eyes

are stalked and laterally mobile and the somites of the head bear, in order, pairs of antennules, antennae, mandibles, maxillae 1 and maxillae 2 (not visible in Figure 1.2). The thorax has three pairs of maxillipeds and five pairs of pereopods (legs), the first three being chelate and used for feeding, and the last two simple (non-chelate) and used for walking. The abdomen consists of six somites, the first five with paired pleopods (walking legs) (Bell et al. 1988; Baily-Brook et al. 1992) and the sixth with uropods. The mouth is situated ventrally and the cephalic appendages surrounding it, plus the first and second maxillipeds and sometimes the third as well may be referred to collectively as the "mouth parts". The anus is on the ventral surface of the telson towards its base (Dall et al. 1990).

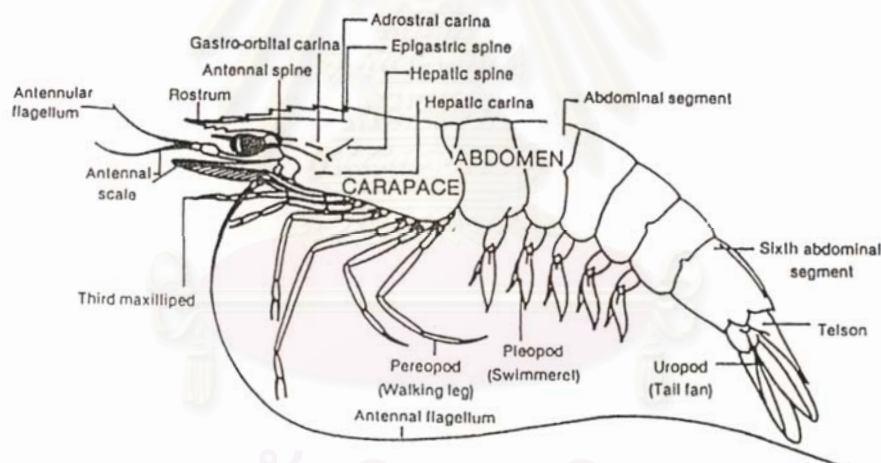


**Figure 1.2** Lateral view of the external morphology of *Penaeus monodon* (Anderson 1993).

The cuticle, which is secreted by an epidermal cell layer, consists of chitin and protein in which calcium carbonate and calcium phosphate have been deposited. The epidermis detaches from the inner cuticle layer and begins to secrete a new cuticle, while the old cuticle is molted. After molting the new cuticle is soft and is stretched to accommodate the increased sized of the shrimp.

The black tiger shrimp has the following characteristic coloration: carapace and abdomen are transversely banded with red and white, the antennae are grayish

brown, and the pereopods and pleopods are brown with crimson fringing setae. In shallow brackishwaters or when cultured in ponds, the color changes to dark and, often, to blackish brown (Moton, 1981:cited in (Solis 1988)).

The internal morphology of penaeid shrimp is very well developed (Fig 1.3). Muscular, digestive, circulatory, respiratory, nervous, and reproductive systems are all present. Many sorts of muscles control movements of the body such as walking, crawling, burrowing, swimming, feeding, and breathing. The digestive system is complex, in which parts of the tract are differentiated into a foregut, a midgut, and a hindgut. The circulatory system consists of a heart, dorsally located in the cephalothoraxes, with branching arteries conducting blood to the various organs. Gills are responsible for respiration process. The nervous system consists of two ventral nerve cords, a dorsal brain, and a pair of ganglia for each somite. Hepatopancreas connects to the gastrointestinal tract via the primary duct. It occupies a large portion of the cephalothoraxes in penaeid shrimp and functions on absorption of nutrients, storage of lipids and production of digestive enzymes (Johnson 1980). One of the haemolymph vessels that leave the heart ends in the lymphoid organ where the haemolymph is filtered. This organ consists of two distinct lobes, each located ventro-lateral to the junction of the anterior and posterior stomach chambers. The lymphoid lobes are apposed slightly dorso-anterior to the ventral hepatopancreatic lobe. The haemocytes are produced in haematopoietic tissue. The hematopoietic tissue consists of densely packed lobules located at different parts of the shrimp anterior region. The first one is hematopoietic tissue surrounding the lateral arterial vessel, which joins the anterior recurrent artery at the base of the rostrum. The second one located within the first maxilliped. The third one is the second maxilliped hematopoietic tissue. The last one is epigastric hematopoietic tissue located dorsal to the anterior stomach chamber and just ventral to the dorsal cuticle. Lymphoid organ and haematopoietic tissue are shown in Figure 1.4.

#### **1.4 Distribution and life cycle**

The black tiger shrimp is mainly found throughout the Indo-Pacific region. Northern part of Indo-Pacific region ranges from Japan and Taiwan, Eastern region

distributes toward Tahiti. For southern and western part, it distributes to Australia and Africa, respectively. The development of penaeid shrimps includes several distinct stages in various habitats (Fig 1.5). Brackish shore is a preferable area for juveniles. The adults migrate to deeper offshore areas that have higher salinity, where mating and reproduction occur. Females produce between 50,000-1,000,000 eggs per spawning (Rosenberry 1997). Larvae hatching from the fertilized eggs pass through a series of moults and metamorphic stages before becoming adulting-like (juveniles). After one day, the eggs hatch into the first stage, nauplius. The nauplii feed on their egg-yoke reserves for a few days and develop into the protozoeae. Around 4-5 days, the protozoeae will metamorphose into mysis by feeding on algae. The mysis feed on algae and zooplankton and then develop into early postlarvae (PLs), which the

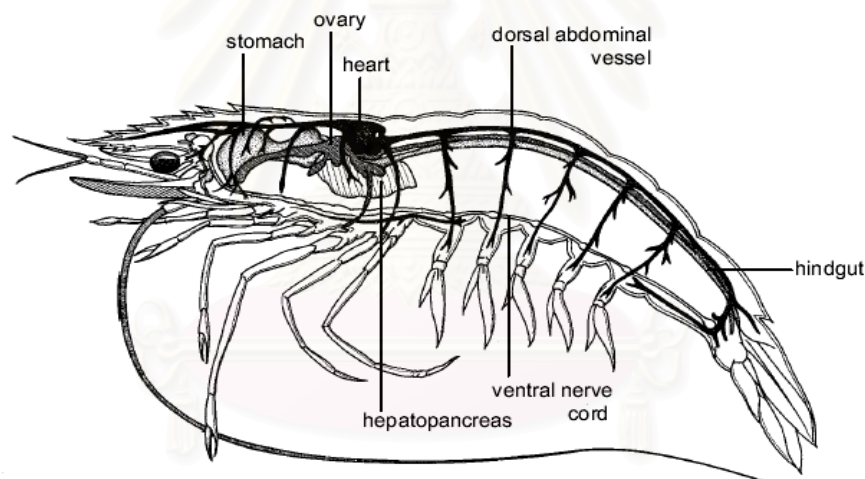


**Figure 1.3 Lateral view of the internal anatomy of a female *Penaeus monodon***  
(Primavera 1990).

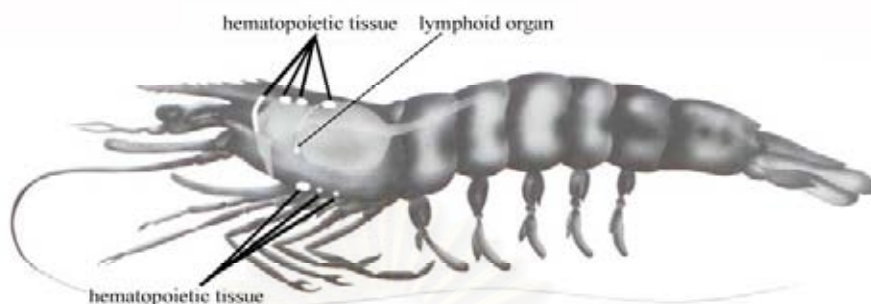


**Figure 1.4** Location of hematopoietic tissue and lymphoid organ of penaeid shrimp.

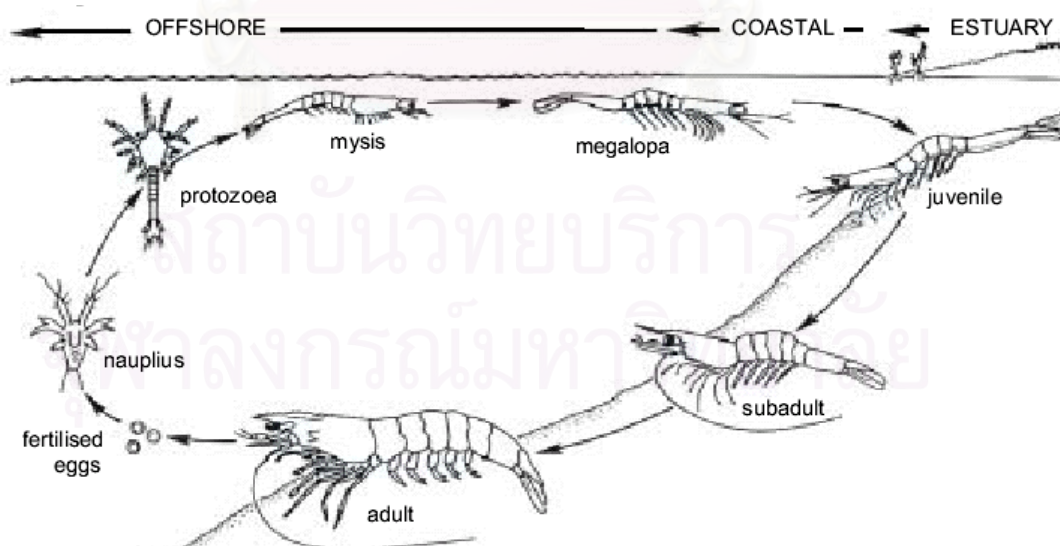


**Figure 1.5** The life cycle of *Penaeus monodon* shrimp (Baily-Brook et al. 1992).

development time is 6-15 days (Solis 1988). Transition from juvenile to sub adult takes 135-255 days and subsequently completion of sexual maturity occurs within 10 months. The larvae inhabit plankton-rich surface waters offshore, with a coastal migration as they develop.

## **1.5 Shrimp diseases**

Diseases are the biggest obstacle to the future of shrimp farming. Viral and bacterial outbreaks have decimated the industries in many countries. At present, white spot syndrome virus and bacteria in Vibrionacea family are considered significant causative agents of infectious diseases in Thailand. Diseases affect the economic viability and long-term sustainability of the shrimp farming industry. They cause great loss of shrimp production. Therefore, the prevention and control of diseases are a priority for shrimp production. To deal with this problem, besides the development of farm management, shrimp immunity and defense effectors responded to the pathogens should be elucidated.

### **1.5.1 Viral disease**

The shrimp farming industry in Thailand has encountered a severe problem from viral infectious disease for over a decade. There are 7 families of viral pathogens including Parvoviridae, Baculoviridae, Iridoviridae, Picornaviridae, Rhabdoviridae, and Togaviridae identified in penaeid shrimp (Jittivadhna 2000). Four major viruses, in order with the greatest to the least economic impact, are white spot syndrome virus (WSSV), yellow head virus (YHV), infectious hypodermal and hematopoietic necrosis virus (IHHNV), hepatopancreatic parvo-like virus (HPV) and monodon baculovirus (MBV). HPV, IHHNV and MBV infections are related to the impeding of shrimp growth (Sukhumsirichart et al. 2002; Chayaburakul et al. 2004). The virus species that cause high mortality of *P. monodon* are WSSV and YHV, causative agents of white spot syndrome (WSS) and yellow-head (YH) diseases, respectively (Mohan et al. 1998; Sithigorngul et al. 2000; Sukhumsirichart et al. 2002; Soowannayan et al. 2003; Wongteerasupaya et al. 2003; Kiatpathomchai et al. 2004).

The outbreak of these viruses results in a great deal of loss in the shrimp industry in several countries including Thailand.

### **1.5.2 White spot syndrome (WSS)**

White spot syndrome (WSS) is one of the most important viral diseases, which affects most of the commercially cultivated marine shrimp species, not just in Asia but globally (Chou et al. 1995; Lightner 1996; Flegel 1997; Lotz 1997; Span 1997). Lightner (1996) called this virus white spot syndrome baculovirus (WSSV). This virus belongs to a new virus family, the Nimaviridae, and the genus *Whispovirus* (van Hulten et al. 2001; Mayo 2002). WSSV has a large circular double-stranded DNA genome of 292,967 bp (van Hulten et al. 2001); however, different genome sizes have been reported from diverse virus isolates (Chen et al. 2002). The virion contains one nucleocapsid with a typical striated appearance and five major and at least other 39 structural proteins (van Hulten et al. 2001; van Hulten et al. 2001; Huang et al. 2002; Tsai et al. 2006; Sanchez-Martinez et al. 2007). It is believed that the envelop proteins play important roles in virus infection. Therefore, many researchers have now focused on the analyses of envelop proteins (Zhang et al. 2004; Wu et al. 2005).

The affected shrimp exhibit white patches or spots on the inside surface of the carapace and the shell accompanied by reddish to pinkish red discoloration of the body. The disease affects the on-growing juvenile shrimp of all ages and sizes. Histological changes observed from the affected shrimp show wide spread cellular degeneration and severe nuclear hypertrophy in most tissue derived from ectodermal and mesodermal origin, especially from subcuticular shell epithelium, gill epithelium, subcuticular stomach epithelium, lymphoid organ, connective tissue, hematopoietic tissue and nervous tissues (The ASEAN Fisheries Sub-Working group, 1998). The other clinical sign of this disease is a rapid reduction in food consumption of shrimp. Mortality was low during the initial two to three days. Mass mortality occurs within seven to ten days of the first clinical signs. Very few of the WSSV-infected shrimp survived the disease. Shrimp, which survive, are suspected to be life-long carriers of WSSV. Nevertheless, mechanism of WSSV infection is still unknown. Recently, WSSV envelope protein VP187 was found to interact with the

shrimp integrin. It is believed that  $\beta$ -integrin may function as cellular receptor for WSSV infection (Wikstrom et al. 2007).

To minimize damage from WSSV infection, detection of virus at an early stage is necessary. Several diagnostic methods have been described such as PCR (Tapay et al. 1999), in situ hybridization (Wang et al. 1998), miniarray (Quere et al. 2002), observation of tissues subjected to fixation or negative staining (Inouye et al. 1994), immunological methods using monoclonal and polyclonal antibodies to WSSV or their component proteins and recently developed method (Poulos et al. 2001), a reverse passive latex agglutination (RPLA) method (Okumura et al. 2005).

Recently, the WSSV subunit vaccine, the WSSV envelop proteins VP19 and VP28, had been tested. The VP19 and VP28 fused to maltose binding protein (MBP) gave significantly better protection against infection (Witteveldt et al. 2005). The other researches to control of WSSV infection is the use of antiviral proteins. A 170-amino acid peptide with a C-type lectin-like domain from a *PmAV* cDNA of WSSV-resistant *P. monodon* was shown to possess a strong antiviral activity in virus infected fish cell line (Luo et al. 2003). In 2004, Zhang and co-workers showed that hemocyanin from the *P. monodon* had non-specific antiviral properties. In addition, interferon-like protein from haemocytes of the virus-resistant *M. japonicus* was found to have also the non-specific antiviral ability by inhibiting the SGIV (grouper iridovirus) in GP cells (grouper embryo cells) (He et al. 2005).

## 1.6 Apoptosis

Apoptosis is a way of eliminating a cell from an organism without eliciting a major host inflammatory and/or immune response. The main difference from necrosis is the absence from the environment of cellular constituents of the dying cells, which induce a host response. In multicellular organisms, apoptosis is essential for development, tumor suppression, immune function and maintenance of homeostasis. The morphological changes of cells undergoing apoptosis include plasma membrane blebbing, condensation of cytoplasm and increase in cell density (pyknosis), a half-moon or crescent shape. Simultaneously the nuclear chromatin becomes compact, segregates and forms sharply delineated masses along the nuclear envelope. The

nucleus splits into discrete fragments (karyorrhexis) and finally, the cell splits into a cluster of membrane bound apoptotic bodies, each containing a variety of organelles. Apoptotic bodies are ingested by nearby cells and macrophages before they cause an inflammatory reaction. The morphologically visible process of apoptosis takes a few hours, and the majority of the time is spent on the degradation within the phagocytic cells. Apoptosis contrasts with necrosis, which is a passive and accidental form of cell death. In necrosis the cell swells, the cell membrane is disrupted, and the nuclear and cytosolic structures are demolished, causing an inflammatory reaction in the neighboring cells (Kerr et al. 1972; Wyllie et al. 1980; Galluzzi et al. 2007)

Apoptosis has been detected in several viral target tissues of shrimp such as haemocyte, hematopoietic tissue and lymphoid organ (Khanobdee et al. 2002; Wongprasert et al. 2003; Hameed et al. 2006; Anantasomboon et al. 2008). Based on morphological and biochemical analysis, it has been suggested that viral infections may induce apoptosis in shrimp. Khanobdee et al. (2002) regarded the widespread and progressive occurrence of apoptosis in *P. monodon* infected with yellow head virus (YHV) as a major cause of dysfunction and death of the host. Wu and Muroga (2004) revealed that high mortality of WSSV infection in *P. japonicus* was accompanied by a high incidence of apoptosis. These results supported the earlier proposal by Flegel and Pasharawipas (1998) that apoptosis might be implicated in shrimp death as a result of viral infection. On the other hand, Wongprasert et al. (2003) reported that cells displaying nuclear condensation and fragmentation characteristic of apoptosis did not contain WSSV virions while those containing WSSV virions were not apoptotic.

### 1.6.1 Pathways of apoptosis

Cell death through apoptosis is known to occur through two primary pathways (Fig 1.6), an extrinsic pathway involving death receptors, and an intrinsic pathway via members of the Bcl-2 family (Adams et al. 1998). The extrinsic pathway uses the classical death receptors such as Fas (CD95/APO1), TNF Receptor1, and TRAIL Receptors. Engagement of these receptors triggers a now well-defined process of recruitment of proteases known as caspases (cysteine-dependent aspartate-cleaving proteases). In the case of Fas, oligomerization by its ligand causes recruitment of the

adaptor protein FADD (Fas-associated via death domain) through interactions between the death domains (DD) found in each protein (Krueger et al. 2003). FADD then recruits caspase-8 through their common death effector domains (DED). Homodimerization of caspase-8 results in its activation through sequential cleavage at critical aspartate residues. Fully active caspase-8 then cleaves downstream targets such as the Bcl-2 family member Bid to form truncated Bid or tBid (Li et al. 1998). tBid localizes to the outer mitochondrial membrane where it promotes oligomerization of another Bcl-2 member, Bax, which results in breakdown of the mitochondria and release of cytochrome *c* and Smac/Diablo (Li et al. 1998). Cytochrome *c* engages a complex containing Apaf-1 and caspase-9 that in the presence of ATP forms a large molecular weight complex of active caspase-9 known as the apoptosome (Cain et al. 2000). The apoptosome can then activate the effector caspases, such as caspase-3 and caspase-6 that ultimately lead to breakdown of cellular components. Among these is cleavage of an inhibitor of caspase-activated DNase (ICAD) that allows the DNase to degrade DNA. This process is fundamental to various assays of DNA breaks. In parallel with the extrinsic death pathway, the intrinsic pathway ultimately engages the same mitochondria-initiated downstream death pathways. In this case the cascade is initiated by any of a variety of sensors that detect cellular stress. The initiators in this case include a panel of Bcl-2 family members that contain only the BH3 domain (so-called BH3-only proteins) (Strasser 2001). These pro-apoptotic Bcl-2 family members are located throughout the cell somewhat as sentinels that detect cellular perturbations. Upon their activation they induce aggregation and activation of Bax or Bak, which then feeds into the mitochondrial death pathway described above. Activation of the intrinsic death pathway may occur in the form of DNA damage by UV irradiation that activates p53 and then two BH3-only proteins, Puma and Noxa. Glucocorticoids similarly activate Puma and Bim that are critical to induction of cell death by steroids. In fact most chemotherapeutic agents ultimately engage a BH3-only protein in the process of killing cells. As a consequence of these pathways, several death assays measure mitochondrial integrity or membrane potential. Additional assays might assess cleavage of caspases or their substrates. Given the localization of many Bcl-2 family members at the mitochondria, considerable interest is now developing over the

concept that these proteins may function as well in some normal metabolic pathways. An early and somewhat overlooked study from the Korsmeyer laboratory showed that increased expression of Bcl-2 in T lymphocytes decreased their production of the growth cytokine IL-2 and resulted in somewhat reduced proliferative capacity following stimulation of the T cell antigen receptor (TCR) (Linette et al. 1996) Bcl-2-deficient T cells manifested the opposite phenotype. More recent studies suggest that this may function via regulation of calcium signaling (White et al. 2005) Other studies suggest that BAD may regulate glucokinase activity in mitochondria and that BAD-deficient  $\beta$  - islet cells are less responsive with insulin secretion to glucose levels (Wikstrom et al. 2007) In a similar manner, caspase-8 has been shown to be critical to growth of various cell types including T lymphocytes (Chun et al. 2002; Salmena et al. 2003; Taatjes et al. 2008)

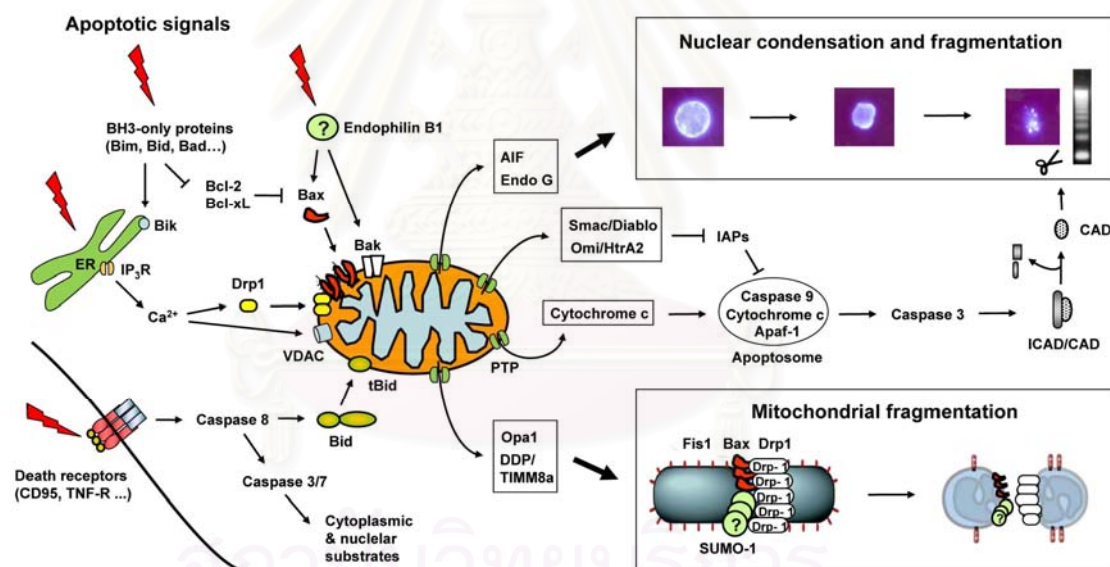


**Figure 1.6 Intrinsic and extrinsic apoptosis pathway in mammalian cells (Jeong et al. 2008)**

## 1.7 Cathepsin

Eleven human cysteine cathepsins have been identified: cathepsins B, C (J, dipeptidyl peptidase I), F, H, K (O, O2), L, O, S, V (L2), W (lymphopain) and X (P, Y, Z) (Rossi et al. 2004). All have been biochemically characterized except cathepsins

O and W (Turk et al. 2000; Vasiljeva et al. 2007). Cysteine cathepsins share a common fold of the papain-like structure and are synthesized as inactive zymogens that are activated by proteolytic removal of the N-terminal propeptide (Turk et al. 2002). Most of them are endopeptidases, with cathepsins H and B also being an aminopeptidase and a carboxydipeptidase, respectively (Musil et al. 1991; Vasiljeva et al. 2003). The only true exopeptidases are the aminodipeptidase cathepsin C and carboxymonopeptidase cathepsin X (Turk et al. 2003). Cysteine cathepsin activity is regulated by several mechanisms that comprise regulation of synthesis, zymogen processing, inhibition by endogenous inhibitors (e.g. cystatins) and pH stability (Turk et al. 2000). For many years cysteine cathepsins were believed to be localized exclusively in lysosomes, however, it is clear now that cathepsins including their splice variants are also found in other cellular and extracellular compartments, including the nucleus (Goulet et al. 2004; Goulet et al. 2007), extracellular milieu (Roshy et al. 2003; Jane et al. 2006) and plasma membrane (Jane et al. 2006; Lechner et al. 2006), where they fulfil important functions. Besides their main function as a lysosomal protein recycling machine, the cathepsins have been shown to play roles in a variety of physiological and pathological processes (Turk et al. 2002; Vasiljeva et al. 2007). Cysteine cathepsins are involved in major histocompatibility complex (MHC) class II-mediated antigen presentation by generation of the antigenic peptides and by processing the MHC class II invariant chain, thereby participating in the maturation of the MHC class II complex. Cathepsins also play a role in bone remodelling, precursor protein activation (e.g. prohormones), keratinocyte differentiation, etc. In addition, cysteine cathepsins have also been demonstrated to participate in several pathological conditions such as tumour progression and metastasis, rheumatoid arthritis and osteoarthritis, and atherosclerosis (Vasiljeva et al. 2007).

### **1.7.1 Cysteine cathepsins in apoptosis**

Recently, cysteine cathepsins have attracted considerable attention as potential mediators of apoptosis. It is well established that massive lysosomal rupture would induce necrotic autolysis of cells (cellular necrosis), a process mediated by the lysosomal cathepsins and other “acidic” hydrolases. On the other hand, more

selective release of cysteine cathepsins as a consequence of limited lysosome damage has been suggested to lead to apoptosis, as also demonstrated in L-leucyl-L-leucine methyl ester -induced apoptosis in HeLa cells (Cirman et al. 2004). Whereas lower concentrations of this lysosomotropic agent induced apoptotic cell death, the use of higher concentrations resulted in necrotic cell death with no caspase activation observed. However, despite numerous reports on their involvement in apoptosis, the mechanism(s) are still not clear, except that they need to be released into the cytosol in order to exert their proapoptotic activity. Several models for the release of lysosomal cathepsins into the cytosol have been proposed, mostly based on the mode of lysosomal membrane permeabilization (Fig 1.6) (Tardy et al. 2006; Stoka et al. 2007). Most of these stimuli directly target the lysosomal membrane, either through lysosomal destabilization or through lysosomal membrane permeabilization. These include bile salts (Roberts et al. 1997), sphingosine (Kagedal et al. 2001), reactive oxygen species (Zhao et al. 2003), polyclonal antithymocyte globulins (Michallet et al. 2003), L-leucyl-L-leucine methyl ester (Thiele et al. 1990; Cirman et al. 2004), microtubule stabilizing agents (Broker et al. 2004), cold ischemia-warm reperfusion (Baskin-Bey et al. 2005), or hexadecylphosphocholines (Paris et al. 2007). Furthermore, it is now well established that lysosomal permeabilization could occur in response to specific signalling processes induced by death ligands such as tumour necrosis factor  $\alpha$  (TNF- $\alpha$ ) (Guicciardi et al. 2000) and TNF-related apoptosis inducing ligand (TRAIL) (Nagaraj et al. 2006; Garnett et al. 2007). Once released into the cytosol, cysteine cathepsins can induce liberation of cytochrome c from the mitochondria, which was suggested to proceed through the cleavage of pro-apoptotic factors, such as Bid (Stoka et al. 2001). It was shown that almost all cysteine cathepsin endopeptidases are capable of cleaving Bid in the flexible loop to its truncated form (Cirman et al. 2004). Furthermore, experimental induction of early lysosomal destabilization by treating cells with the lysosomotropic agent L-leucyl-L-leucine methyl ester induced cleavage of Bid and cytochrome c release from mitochondria (Cirman et al. 2004). However, alternative pathways have been proposed (Guicciardi et al. 2005). There is also evidence for a role of cathepsins in the execution of cell death independent of caspase activation, which results in an

apoptosis-like morphology (Foghsgaard et al. 2001; Li et al. 2005; Vasiljeva et al. 2008).

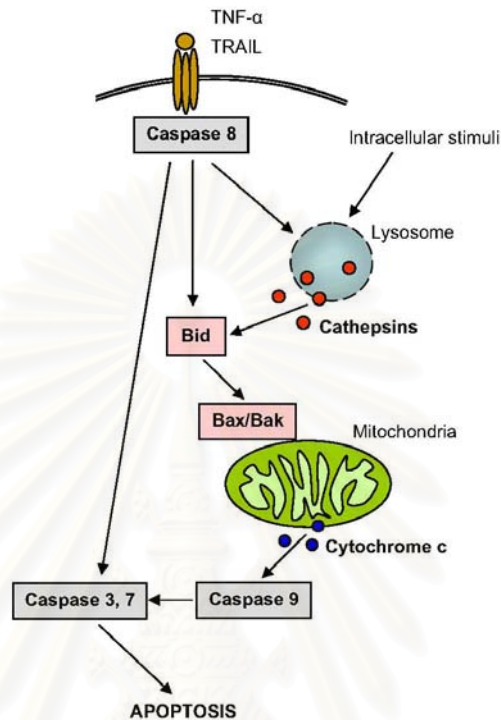


**Figure 1.7 The role of cathepsin in apoptosis (Vasiljeva et al. 2008)**

## 1.8 Objective of the study

From the *P. monodon* EST project (<http://pmonodon.biotec.or.th>), it was found that genes in the cathepsin family including cathepsin L and cathepsin B were predominant in the lymphoid organ cDNA libraries. Expression analysis of CatL mRNA by quantitative real-time RT-PCR showed up regulation of CatL mRNA in the lymphoid organ from WSSV injected *P. monodon*. Moreover, lymphoid organ of shrimps have been proposed to play important role in defense against bacterial and viral infection. Thus, it is interesting to investigate the role of cathepsin in the lymphoid organ.

The objectives of this research are to localization CatL in cephalothoraxes of *Penaeus monodon* and examined the change of CatL enzyme in shrimp injected with WSSV using immunohistochemistry and to study the CatL function in mediated apoptosis using primary shrimp cell culture prepared from lymphoid organ.

## **CHAPTER II**

### **MATERIALS AND METHODS**

#### **2.1 Material**

##### **2.1.1 Equipments**

-80 °C Freezer (Revco)

-20 °C Freezer (Whirlpool)

24 well cell culture cluster, flat bottom with lid (Costar)

96 well cell culture cluster, flat bottom with lid (Costar)

Autoclave Model MLS-3750 (SANYO Labo autoclave.)

Automatic micropipette P10, P20, P100, P200, and P1000 (Gilson Medical Electrical S.A.)

CX31 Biological microscope (Olympus)

Disposable sterile filter systems 0.22 µm Polyethersulfone (Corning, USA)

ECLIPSE TS100 inverse microscope (Nikon, Japan)

Hybridization oven (Hybrid, USA)

Incubator 30 °C (Heraeus)

Incubator 37 °C (Mettler)

Laminar airflow biological safety cabinets class II A2 Model 1285 Ref 6 (Thermo)

Laminar airflow biological safety cabinets class II Model NU-440-400E (NuAire, Inc., USA)

Microcentrifuge tubes 0.6 ml and 1.5 ml (Bio-RAD Laboratories, USA)

Minicentrifuge (Costar, USA)

Nipro disposable syringe (Nissho)

Orbital shaker SO3 (Stuart Scientific, Great Britain)

PCR Mastercycler (Eppendorf AG, Germany)

PCR thin wall microcentrifuge tubes 0.2 ml (Axygen® Scientific, USA)

PCR workstation Model # P-036 (Scientific Co., USA)

pH meter (TOLEDO)

Pipette boy ACU (Integra biosciences)  
 Pipette tips 10, 20, 100 and 1000  $\mu$ l (Axygen® Scientific, USA)  
 Poly-L-lysine coated slide (Sigma-Aldrich)  
 Power supply, Power PAC 3000 (Bio-RAD Laboratories, USA)  
 Refrigerated centrifuge Model Avanti™ J30-I (Beckma Coulter)  
 Refrigerated microcentrifuge MIKRO 22R (Hettich Zentrifugen, Germany)  
 Sonicator Vibra-Cell (Sonics & Materials, USA)  
 Spectrophotometer DU650 (Beckman, USA)  
 Spectrophotometer: Gene Quant Pro  
 Sterile disposable plastic pipettes 5, and 10 ml (Costar, USA)  
 Stirring hot plate (CERAMAG Midi, KIKA® works, USA)  
 Touch mixer Model # 232 (Fisher Scientific, USA)  
 Trans-Blot® SD (Bio-RAD Laboratories)  
 Transilluminator 2011 Macrovue (LKB)  
 Vacuum pump (Bio-RAD Laboratories)

### **2.1.2 Chemicals and reagents**

100 mM dATP, dCTP, dGTP, and dTTP (Promega)  
 2-mercaptoethanol, C<sub>2</sub>H<sub>6</sub>OS (Fluka)  
 5-bromo-4-chloro-3-indolyl-beta-D-galactopyranoside (X-Gal) (Fermentas)  
 Absolute ethanol, C<sub>2</sub>H<sub>5</sub>OH (BDH)  
 Acetic acid glacial, CH<sub>3</sub>COOH (BDH)  
 Acrylamide, C<sub>3</sub>H<sub>5</sub>NO (Merck)  
 Actinomycin D (Sigma)  
 Agarose (Sekem)  
 Ammonium persulfate, (NH<sub>4</sub>)<sub>2</sub>S<sub>2</sub>O<sub>8</sub> (USB)  
 Anti-His antibody (GE healthcare)  
 Anti-human cathepsin L antibody (R&D Systems)  
 Bacto agar (Difco)  
 Bacto tryptone (Merck)  
 Bacto yeast extracts (Scharlau)  
 BCIP (5-bromo-4-chloro-indolyl phosphate) (Sigma)

Boric acid,  $\text{BH}_3\text{O}_3$  (Merck)

Bromophenol blue (BDH)

Caspase 3 Inhibitor II (Calbiochem)

Cathepsin L Inhibitor I (Calbiochem)

Chloroform,  $\text{CHCl}_3$  (Merck)

Coomassie brilliant blue R-250,  $\text{C}_{45}\text{H}_{44}\text{N}_3\text{O}_7\text{S}_2\text{Na}$  (Sigma)

DePeX mounting medium (BDH)

Diaminobenzidine (Sigma)

Dimethyl sulfoxide (DMSO),  $\text{C}_6\text{H}_6\text{SO}$  (Amresco)

di-Sodium hydrogen orthophosphate anhydrous,  $\text{Na}_2\text{HPO}_4$  (Carlo Erba)

Ethidium bromide (Sigma)

Ethylene diamine tetraacetic acid (EDTA), disodium salt dihydrate (Fluka) Ficoll™  
-400 (Amersham)

Fetal bovine serum (Gibco BRL)

Formaldehyde,  $\text{CH}_2\text{O}$  (BDH)

GeneRuler™ 100bp DNA Ladder

Glucose (Merck)

Glycerol,  $\text{C}_3\text{H}_8\text{O}_3$  (BDH)

Glycine  $\text{NH}_2\text{CH}_2\text{COOH}$  (Scharlau)

Hydrochloric acid,  $\text{HCl}$  (Merck)

Isoamylalcohol (Merck)

Isopropanol,  $\text{C}_3\text{H}_7\text{OH}$  (Merck)

Isopropyl-beta-D-thiogalactopyranoside (IPTG) (Fermentas)

Leibovitz's L-15 Medium with L-glutamine (Gibco)

Levamisol (Sigma)

Methanol,  $\text{CH}_3\text{OH}$  (Merck)

Minimum Essential Medium (Gibco)

N, N, N', N'-tetramethylethylenediamine (TEMED) (BDH)

N, N'-methylene-bisacrylamide,  $\text{C}_7\text{H}_{10}\text{N}_2\text{O}_2$  (USB)

Nitroblue tetrazolium (NBT) (sigma)

Phenol crystals,  $\text{C}_6\text{H}_5\text{OH}$  (Carlo Erba)

Prestained protein molecular weight marker (Fermentas)  
 Protease Inhibitor mix (Amersham Biosciences)  
 Protrans® nitocellulose transfer membrane (Schleicher & Schuell)  
 Sodium acetate, CH<sub>3</sub>COONa (Carlo Erba)  
 Sodium chloride, NaCl (BDH)  
 Sodium citrate, Na<sub>3</sub>C<sub>6</sub>H<sub>5</sub>O<sub>7</sub> (Carlo Erba)  
 Sodium dihydrogen orthophosphate, NaH<sub>2</sub>PO<sub>4</sub>.H<sub>2</sub>O (Carlo Erba)  
 Sodium dodecyl sulfate, C<sub>12</sub>H<sub>25</sub>O<sub>4</sub>SNa (Sigma)  
 Sodium hydrogen carbonate, NaHCO<sub>3</sub> (BDH)  
 Sodium hydroxide, NaOH (Eka Nobel)  
 TRIreagent (Molecular biology)  
 Tris-(hydroxy methyl)-aminomethane, NH<sub>2</sub>C(CH<sub>2</sub>OH)<sub>3</sub> (USB)  
 Triton® X-100 (Merck, Germany)  
 Trypan blue (BDH)  
 Tryptic soy broth (Difco)  
 Tween™-20 (Fluka)  
 Whatman 3 MMTM filter paper (Whatman)

### 2.1.3 Enzymes

*Nhe* I (Biolabs)  
*Pfu* DNA polymerase (Promega)  
 Proteinase K (Sigma)  
 RNase A (USB)  
*Taq* DNA polymerase (Fermentas)  
*Xho* I (Biolabs)

### 2.1.4 Microorganisms

*Escherichia coli* BL21(DE3) (Novagen) Genotype; F<sup>-</sup> *ompT hsdS<sub>B</sub>(r<sub>B</sub><sup>-</sup>m<sub>B</sub><sup>-</sup>) gal dcm*  
 (DE3)  
*Escherichia coli* XL1 blue Genotype; *recA1 endA1 gyrA96 thi-1 hsdR17 supE44*  
*relA1 lac* [F *proAB lacI<sup>f</sup> ZΔM15 Tn10* (Tet<sup>R</sup>)]

### 2.1.5 Kits

Nucleospin® Extraction Kit (MACHEREY-NAGEL, Germany)

pGEM®-T Easy Vector System I (Promega corporation, USA)

QIAprep® Spin Miniprep Kit (QIAGEN GmbH, Germany)

## 2.2 Samples

Twenty grams of body weight of sub-adults *P. monodon* (approximately 3 month-old) were purchased from local farms. Then, these *P. monodon* were divided into 2 experimental groups. For the first group, the shrimp were injected with Lobster haemolymph medium (LHM), while the second ones were injected with white spot syndrome virus (WSSV). Both groups were acclimatized in aquaria controlling of salinity (15 ppt) and ambient temperature ( $28 \pm 4$  °C) at least 1 day before start the experiments.

## 2.3 Preparation of WSSV infected shrimp

WSSV stock solution was kindly provided by Charoenpokphand Group of Companies. The virus stock was dissolved with LHM buffer and kept at -80 °C. Shrimps were injected with 100 µl of a 1:100 dilution (LHM) of viral stock solution into the ventral 4<sup>th</sup> abdominal segment. The control shrimps was injected with 100 µl of LHM buffer

## 2.4 Diagnosis of WSSV

The WSSV-infection shrimps were analyzed by modified method using PCR technique according to Kiatpathomchai et al. (2001). The advantage of this procedure is that it could be detected both the existence and the severity of WSSV infection. Firstly, a gill of shrimp *P. monodon* was crushed up in 200 µl of lysis buffer (0.05 N NaOH and 0.025 % sodium dodecyl sulphate), followed by incubation in boiling water for 5 min and then immediately incubated on ice. After a brief centrifugation at 7,500 rpm for 5 min, 1 µl of the supernatant was used as the template for PCR amplification. The 25 µl of PCR reaction contained 1 µl of cDNA template, 1.25 mM

of each dNTPs, 1.5 mM MgCl<sub>2</sub>, 1x PCR buffer (10 mM Tris-HCl pH 8.8, 50 mM KCl and 0.1 % TritonX-100), 1 U of Taq DNA polymerase, 10 pmol of the forward primer, (F1: 5'-AGA GCC CGA ATA GTG TTT CCT CAG C-3') and reverse primer (R3: 5'-AAC ACA GCT AAC CTT TAT GA G-3'), amplifying a 250 bp fragment of WSSV DNA. The PCR reaction was followed by 2 successive cycling protocols of (1) 90 °C for 3 min, 60 °C for 30 s and 72 °C for 30 s, followed by (2) 35 cycles of 90 °C for 30 s, 60 °C for 30 s and 72 °C for 30 s, and the final extension step was 72 °C 5 min. The PCR product was run on 2 % w/v agarose gel electrophoresis and was analyzed by ethidium bromide staining.

## **2.5 Immunohistochemistry**

### **2.5.1 Tissue preparation for histology**

Tissues from juvenile shrimp were prepared by dissecting the cephalothoraxes. The dissected tissues were immediately fixed in freshly prepared Davidson's AFA fixative solutions (220 ml of formaldehyde 37 %, 315 ml of absolute ethanol, 115 ml of Glacial acetic acid, and 350 ml of water) incubated at 4 °C for 24 h. To ensure an adequate supply of fixative; a rule of thumb is that a minimum of approximately 10x their volume of fixative should be used for each specimen (e.g. the ratio of a shrimp volume to fixative is 10 ml to 100 ml). Subsequently, the specimens were transferred to 70 % ethanol, where it can be stored for an indefinite period. The cuticle was slit before transferred to 70 % ethanol. A history of the specimen at number of specimen and the collection time post-infection was recorded by using soft-lead pencil on paper. The tissues were dehydrated 3 times in 70 % ethanol at room temperature for 20 min, 3 times in 90 % ethanol room temperature for 20 min, 3 times in 100 % ethanol room temperature for 20 min, and 3 times in 70 % ethanol at room temperature overnight. The dehydrated fixed tissues were embedded in paraplast by incubating as following: 3 times in xylene for 20 min at room temperature, 12 h (minimum) in xylene at room temperature, 12 h in a solution (v/v) of xylene/Paraplast at 60 °C, and 3 times in Paraplast 1 h at 60 °C. To prepare Paraplast blocks, the sections were cut approximately 5 µm and mounted sections on poly-L-lysine coated slide and stored them at 4 °C until use.

### 2.5.2 Immunohistochemistry staining

For the five micrometer-thick paraffin sections, elimination of paraffin and hydration was carried out by consecutive baths in xylene; 2 baths of 15 min, 96 % ethanol; 2 baths of 5 min, 70 % ethanol; 2 baths of 5 min, 30 % ethanol; 2 baths of 5 min. The slides were equilibrated immediately for 1 h at room temperature in PBS buffer (137 mM of NaCl, 2.7 mM of KCl, 4.3 mM of  $\text{Na}_2\text{HPO}_4 \cdot 7\text{H}_2\text{O}$ , and 1.4 mM of  $\text{KH}_2\text{PO}_4$  pH 7.4), then incubated for 10 min in new PBS and subsequently pre-incubated with buffer A containing 1 % of Normal Rabbit Serum (NRS), 1 % of BSA, and 0.1 % of Triton X-100 (PBS/NRS/BSA/Triton X-100) for 1 h at room temperature. Five hundred microliters of goat anti-cathepsin L (5  $\mu\text{g}/\text{ml}$ ) and mouse anti-vp28 antibody dissolved in PBS/NRS/BSA/Triton X-100 solution with dilution fold at 1:1000 were overlaid onto the section. The sample was incubated overnight at 4 °C for detecting the cathepsin L (CatL) and WSSV in the shrimp tissue, respectively. After incubation, the sections were washed 4 times for 10 min each with TBS buffer. After that, the secondary antibody, alkaline phosphatase-conjugated rabbit anti-goat IgG and alkaline phosphatase-conjugated rabbit anti-mouse IgG (Jackson Immunoresearch), diluted 1:1000 with PBS/NRS/BSA/Triton X-100, were added to the section for 3 h at room temperature. After washing 2 times for each 5 min with TBS, the sections were equilibrated in buffer B containing 0.1 M Tris-HCl, 100 mM NaCl, 50 mM  $\text{MgCl}_2$  pH 9.5 for 10 min. Immunodetection was performed by incubating the slides in the dark at room temperature with 500  $\mu\text{l}$  of detection solution containing 375  $\mu\text{g}/\text{ml}$  of NBT, (nitroblue tetrazolium), 188  $\mu\text{g}/\text{ml}$  of BCIP (5-bromo-4-chloro-indolyl phosphate), and 1 mM of levamisole, 0.1 M Tris-HCl pH 9.5, 50 mM  $\text{MgCl}_2$ , and 0.9 % NaCl. The slides were washed by TBS buffer for 10 min to stop the reaction and rinsed briefly with distilled water. The slides were mounted with a DePeX mounting medium, and then examined under a light microscope (Olympus).

## 2.6 Expression of CatL in the BL21(DE3) *E. coli*

### 2.6.1 Construction of recombinant pET-21a(+)-CatL

#### 2.6.1.1 Preparation of DNA fragment containing CatL gene

The pGEM<sup>®</sup>-T-easy vector containing *Penaeus monodon* CatL (EF213115) was used as template. The two restriction sites, namely *Nhe* I and *Xho* I were incorporated at the 5'-ends of primers 1 and 2, respectively which were then incorporated into the PCR product. The primer was designed in order to delete the putative signal sequence of the CatL. The sequences of each primer set are listed below. The 30 µl of PCR reaction containing 25 ng of DNA template, 0.45 µM of each primer, 0.2 mM of each dNTP and 0.45 unit of *Pfu* polymerase (Promega) was performed followed by 30 cycles of denaturation at 95 °C for 30 s, annealing at 60 °C for 30 s and extension at 72 °C for 2.0 min. The intensities of PCR products were analyzed by gel electrophoresis. The size of the product was compared with standard a Gene Ruler<sup>™</sup> 100 bp DNA ladder Plus (Fermentas). The two restriction sites, namely *Nhe* I and *Xho* I were then incorporated at the 5'-ends of both primers 1 and 2, respectively.

#### 1. Forward primer 1 with *Nhe* I site.

*Nhe* I  
5'-ACTAGCTAGCGTGTCCTTTTCTCCGTTGTTCTG-3'

#### 2. Reverse primer 2 with *Xho* I site

*Xho* I  
5'-CCGCCGCTCGAGGACAAGAGGGAAGGAGGCGG-3'

The amplified CatL gene was purified by phenol-chloroform precipitation (see Appendix A). After ethanol precipitation, the DNA pellet was dissolved in 40 µl of TE buffer.

The purified CatL gene was tailed with an adenine nucleotide prior to start ligation into the pGEM<sup>®</sup>-T Easy vector (see appendix E). The recombinant plasmid was transformed into *Escherichia coli* strain XL1-Blue using electroporation technique as described in Materials and Methods 2.6.1.5. The transformants grown on the 100 µg/ml ampicillin agar plates were selected using blue white colony screening.

A single white colony of *E. coli* strain XL1-Blue harboring a recombinant plasmid was then cultivated in 1.5 ml LB broth containing 100 µg/ml ampicillin incubated at 37 °C on rotary shaker overnight. Then recombinant plasmids were isolated and restricted with two enzymes, namely *Nhe* I and *Xho* I incubated at 37 °C overnight. The digested fragments were analyzed by 1.2 % agarose gel electrophoresis. The expected fragment approximately 1,005 bp was purified using Nucleospin extraction kit (MACHEREY-NAGEL).

Briefly, a section of agarose gel (approximately 100 mg) containing the 1,005 bp DNA fragment was excised and then transferred to a clean 1.5 ml microcentrifuge tube. Three hundred microlitres of NT1 buffer was added into the tube. The sample was incubated at 50 °C for 5-10 min with occasional vortexing until a piece of gel was melted. A NucleoSpin extract column was placed into a 2 ml collecting tube. The sample was loaded into the column and centrifuged at 10,000×g for 1 min. The flow-through was discarded. Five hundred microlitres of NT2 buffer was added into the column and centrifuged as describe above. Six hundred microlitres of NT3 buffer was added into the column and centrifuged according to previous step. The flow-through was discarded. The column was then centrifuged at 11,000×g for 2 min to remove NT3 buffer. The column was placed into a clean 1.5 ml microcentrifuge tube. Forty microlitres of elution buffer NE was added into the column and leaved at room temperature for 1 min. The column was centrifuged at 11,000×g for 1 min. The flow-through containing the DNA fragment was then stored at 4 °C until used. The concentration of DNA was determined by 1.2 % agarose gel electrophoreses and the expected protein size was estimated compared to 100 bp DNA ladder standard under the UV transilluminator. The DNA fragment containing the *CatL* gene was subsequently ligated to expression vector, pET-21a(+).

#### **2.6.1.2 Preparation of pET-21a(+) expression vector**

The expression vector used in this experiment was pET-21a(+) as shown in (see appendix F), the structure of vector comprised of *lac* operator (*lacO*), ribosome binding site (rbs), initiation ATG, multiple cloning site (MCS), polyhistidine region (6×His), T7 terminator, f1 origin, ampicillin resistance gene (β-lactamase), pBR322 origin and *lac* repressor gene (*lacI*). The cloning sites for construction *CatL* recombinant plasmid gene were *Nhe* I and *Xho* I.

A single colony containing the pET-21a(+) plasmid was inoculated into 1.5 ml of LB broth containing 100 µg/ml of ampicillin. The culture was grown at 37 °C and shaken on rotary shaker at 250 rpm overnight. The plasmid was extracted using QIAprep® Spin Miniprep Kit. Briefly, the culture was transferred to 1.5 ml microcentrifuge tube and centrifuged at 800×g for 5 min. The supernatant was discarded. The pellet was resuspended in 250 µl of Buffer P1. Two hundred and fifty microlitres of Buffer P2 was added and mixed gently by inverting the tube 4-6 times. Three hundred and fifty microlitres of Buffer N3 was added and the tube was gently inverted immediately for 4-6 times. The sample was centrifuged for 10 min at 17,900×g in a table-top microcentrifuge. The supernatant liquid was loaded into the QIAprep spin column and centrifuged as described above. The flow-through was discarded. Five hundred microlitres of Buffer PB was added into the column and centrifuged for 1 min. The flow-through was discarded. Seven hundred and fifty microlitres of Buffer PE was added and centrifuged for 1 min. The flow-through was discarded and centrifuged for an additional 1 min to remove residual wash buffer. The QIAprep column was then placed in a clean 1.5 ml microcentrifuge tube. Finally, forty microlitres of elution buffer (EB) was added to the center of QIAprep spin column, let stand for 1 min and centrifuged for 1 min. The pET-21a(+) was cut with two restriction enzymes, namely *Nhe* I and *Xho* I and then the fragments were purified by using phenol-chloroform extraction. After ethanol precipitation, the DNA pellet was dissolved in 40 µl TE buffer. The concentration of DNA was determined by 1.2 % agarose gel electrophoreses. The expected size was estimated compared to 100 bp DNA ladder standard under the UV transilluminator. The digested pET-21a(+) was used for the cloning of CatL gene.

### 2.6.1.3 Restriction enzyme digestion

Since the expression vector pET-21a(+) and CatL gene products contains *Nhe* I and *Xho* I restriction sites, both were specifically restricted digested with these two enzymes. Approximately 20 µg DNA was digested in a 50 µl reaction volume containing 1× NE buffer 2 (10 mM Tris-HCl, pH 7.9, 10 mM MgCl<sub>2</sub>, 50 mM NaCl, and 1 mM dithiothreitol), 10 units of *Nhe* I (Biolabs), 20 units of *Xho* I (Biolabs) and 100 µg of BSA. The reaction was incubated at 37 °C overnight.

#### 2.6.1.4 Ligation

A suitable molecular ratio between vector and inserted DNA in the mixture of cohesive-end ligation is usually 1:3. To calculate the appropriate amount of PCR product (insert) used in the ligation reaction, the following equation was used:

$$\frac{\text{ng of vector} \times \text{kb size of insert}}{\text{kb size of vector}} \times \text{insert: vector molar ratio} = \text{ng of insert}$$

The 10 µl ligation reaction was composed of 1 µl of 10× T4 DNA ligase buffer, 1 unit of T4 DNA ligase (USB), 10 ng of *Nhe* I and *Xho* I digested pET-21a(+) and 4 ng of *Nhe* I and *Xho* I digested amplified CatL gene. Sterile distilled water was added to make the final volume of 10 µl. The reaction was mixed, briefly spun for 30 s and incubated at 16 °C for an overnight. One microlitre of the ligation mixture was transformed into competent *Escherichia coli* strain XL1 blue.

#### 2.6.1.5 Electrotransformation

The competent cells were gently thawed on ice. Forty microlitres of cell suspension were mixed with 1 µl of the ligation mixture, mixed well and placed on ice for 1 min. The cells were transformed by electroporation using an ice-cold 0.2 cm cuvette (25 µF, 200 Ω, 2.50 kV Gene pulser apparatus, Bio-RAD). After one pulse was applied, the cells were immediately resuspended to 1 ml of SOC medium (2 % (w/v) Bacto tryptone, 0.5 % (w/v) Bacto yeast extract, 10 mM NaCl, 2.5 mM KCl, 10 mM MgCl<sub>2</sub>, 10 mM MgSO<sub>4</sub> and 20 mM glucose). The cell suspension was incubated at 37 °C on the rotary shaker at 250 rpm for 1.30 h. The cell suspension was spread on the LB agar plates containing 100 µg/ml ampicillin and incubated at 37 °C overnight. After incubation, colonies were randomly selected for plasmid DNA isolation.

#### 2.6.1.6 Isolation of the recombinant plasmid

The recombinant plasmid containing CatL gene was selected by restriction enzyme digestion using *Nhe* I and *Xho* I. The digested plasmid was analyzed by 1.2 % agarose gel electrophoresis. The size of DNA fragment was compared with standard DNA ladder (1 kb DNA ladder, Fermentas). The clone containing the corrected DNA fragment of approximately 1,005 bp was selected. DNA sequencing was performed to

confirm the correct junction of the vector and inserted DNA as well as the sequence of the CatL gene.

## **2.6.2 Expression of recombinant CatL**

A recombinant pET-21a(+)*CatL* was transformed into an expression host *Escherichia coli* strain BL21(DE3) carrying the gene for T7 RNA polymerase under *lacUV5* control.

### **2.6.2.1 Competent cell preparation**

The competent cells were freshly prepared using calcium chloride treatment. A single colony of *Escherichia coli* strain BL21(DE3) was inoculated into 2 ml of LB. Then the culture was grown overnight at 37 °C with shaking at 250 rpm. Four hundred microlitres of culture was inoculated into 10 ml of LB broth and incubated at 37 °C until the optical density at 600 nm (OD<sub>600</sub>) reached 0.2-0.6 (about 2-3 h). Cells were then chilled on ice for 10 min and harvested by centrifugation at 5,000×g for 5 min at 4 °C. The pellet was washed with 1/2 volume of the ice-cold 10 mM CaCl<sub>2</sub> and centrifuged as described above. The pellet was resuspended with 1/20 volume of the ice-cold 0.1 M CaCl<sub>2</sub> and left on ice at least 30 min.

### **2.6.2.2 Calcium chloride transformation**

A hundred microlitres of competent cells were gently mixed with 2 µl of recombinant pET-21a(+)*CatL* and placed on ice for 30 min. The mixture was incubated for 1 min at 42 °C immediately and then 0.9 ml LB broth was added. The cell suspension was incubated with shaking at 250 rpm for 1 hour. After incubation, the 20 µl of the cell suspension was spread on LB agar plates containing 100 µg/ml of ampicillin and incubated at 37 °C overnight. The single colonies were selected for protein expression.

### **2.6.2.3 Recombinant protein expression**

After the recombinant pET-21a(+)*CatL* was established in the expression host, *Escherichia coli* BL21(DE3), the expression of the *CatL* proteinase gene was induced by addition of IPTG into the growing culture medium. Firstly, a single colony from a freshly streaked plate was picked, inoculated into 2 ml LB broth containing 100 µg/ml of ampicillin and incubated with shaking at 37 °C until the optical density at 600 nm (OD<sub>600</sub>) reaches 0.6-1.0. The cell suspension was inoculated into 50 ml LB medium containing 100 µg/ml of ampicillin. The culture was incubated with shaking at 37 °C

until the OD<sub>600</sub> reached 0.6. IPTG was then added from a 100 mM stock to a final concentration of 1 mM for induction. The culture was incubated further with shaking for 0, 1, 2, 3 and 4 h, respectively. An aliquot of 1 ml of the culture was sampled at each time point. The cell pellet was kept by centrifugation at 8,000×g for 10 min. The supernatant was discarded. The cell pellet was stored at -80 °C until required for further analysis.

### **2.6.3 Protein analysis**

#### **2.6.3.1 Sodium dodecyl sulfate-polyacrylamide gel electrophoresis (SDS-PAGE)**

SDS-PAGE was conducted in a discontinuous system. The gel solutions were prepared as shown in Appendix B. After the glass plates and spacers were assembled, the components of the separation gel solution were mixed thoroughly and pipetted into the gel plate setting. Then a small amount of distilled water was carefully layered over the top of the 12 % separation gel solution to ensure that a flat surface of gel would be obtained. When the polymerization was completed, the water was poured off. The 5 % stacking gel solution was prepared, mixed thoroughly and poured on the top of the separating gel. A comb was placed in position with excess gel solution overflowing the front glass plate. After the stacking gel was polymerized, the comb was removed and the wells were rinsed with distilled water to remove excess unpolymerized acrylamide.

#### **2.6.3.2 Sample preparation**

Protein samples were resuspended in 1×sample buffer (12 mM Tris-HCl, pH 6.8, 5 % glycerol, 0.4 % SDS, 2.88 mM 0.02 % bromophenol blue, and 2-mercaptoethanol) and were then boiled for 5 min in capped microtubes. After centrifugation at 10,000×g for 5 min, the samples were kept at 0 °C until loaded onto a gel.

#### **2.6.3.3 Analysis of the recombinant protein by SDS-PAGE**

After boiling, the protein samples and the prestained protein marker were loaded into the wells. Electrophoresis was conducted in 1× protein running buffer [25 mM Tris-HCl, pH 8.3, 192 mM glycine, 0.1 % (w/v) SDS] at constant current of 18 mA/gel until the tracking dye (bromophenol blue) reached the bottom of the

separation gel. The gels were either stained with 0.1 % (w/v) Coomassie brilliant blue R250 or Western blotted.

#### **2.6.3.4 Coomassie brilliant blue staining**

The gel was placed in Coomassie blue staining solution [0.1 % (w/v) Coomassie brilliant blue R250, 10 % (v/v) acetic acid, 45 % (v/v) methanol] at room temperature with gentle shaking for 1 h, immersed in destaining solution [10 % (v/v) acetic acid, 10 % (v/v) methanol] and incubated at room temperature with agitation for 1-3 h. Destaining solution was replaced regularly to assist the removal of stain. The gel was then placed between the two sheets of cellophane over the glass plate before air-dried at room temperature.

#### **2.6.4 Purification of recombinant protein**

A few microlitres of cell suspension from a glycerol stock was inoculated into 20 ml LB medium containing 100 µg/ml of ampicilin and incubated with shaking at 37 °C until the OD<sub>600</sub> reached 0.6-1.0. The cell suspension was transferred into 1 liter LB medium. The culture was incubated with shaking at 37 °C until the OD<sub>600</sub> reaches 0.6. IPTG was then added from a 100 mM stock to a final concentration of 1 mM for induction. The culture was further incubated for 4 h with shaking. The cells were harvested by centrifugation at 5,000×g for 5 min at 4 °C. The supernatant was removed and the cell pellet was resuspended in PBS. The solution was freezed at -80 °C and thawed at room temperature by repeated freezing and thawing for 3 times. The cell lysate was then sonicated with the Vibra-Cell sonicator (80 % amplitude 1 min 3x times). The inclusion bodies was collected by centrifugation at 12,000×g for 20 min, washed twice with 1 % Triton X-100, and PBS, and then solubilized in 3 ml of 50 mM Tris-HCl buffer pH 8 containing 6 M urea and 20 mM imimidazole at room temperature overnight. The insoluble material was removed by centrifugation as the previous step and the supernatant was stored at 4 °C until further used.

Ni-NTA agarose (Pharmlingen) was gently resuspended in 6×His washing buffer (50 mM Tris-HCl, 300 mM NaCl, 10 % glycerol, 6 M urea and 20 mM imimidazole, pH 8) and packed into a column (1×5 cm). The column was washed with 5 bed volumes of 6×His washing buffer. The recombinant protein, which was solubilized in 50 mM Tris-HCl containing 6 M urea and 20 mM imimidazole pH 8,

was applied to the column at a flow rate of 5 ml/h. The column was washed with 6×His washing buffer until the absorbance at 280 nm of eluate was less than 0.01. After washing, the column was eluted with 6×His elution buffer (50 mM Tris-HCl, 300 mM NaCl, 10 % glycerol, 6 M urea and 100 mM imidazole pH 8) until the eluate absorbance at 280 nm was zero. The eluted protein was pooled and slowly dialysed against PBS.

### 2.6.5 Detection of the purified recombinant protein by Western blot analysis

The purified recombinant proteins were separated on the two 12 % SDS-PAGE gels as described in section 2.6.3.1-2.6.3.3. The gel slab was removed from the glass plates and incubated for 10 min in a tank-blotting buffer (48 mM Tris, pH 9.2, 39 mM glycine and 20 % methanol). The nitrocellulose membrane was activated in methanol for 3 min. The activated membrane and 6 sheets of filter papers were soaked into tank-blotting buffer for 15 min. The first 3 sheets were laid on the Trans-Blot<sup>®</sup> SD (Bio-Rad). The air bubbles were eliminated. Then the membrane, the gel and 3 sheets of filter paper left were laid on respectively like sandwich model. Finally the lid of the machine was closed. (Fig 2.1)

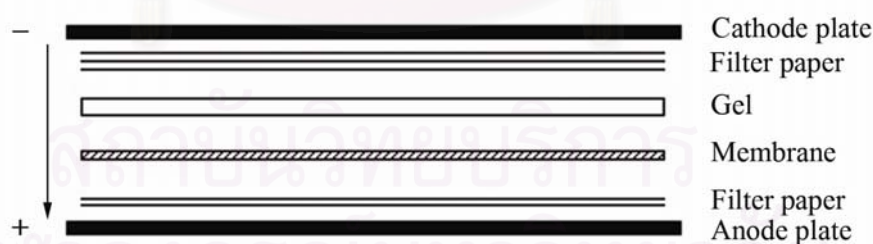


**Figure 2.1 Western transfer cassettes**

Protein transfer was performed at constant electricity of 90 mA for 1 hour. After that, the membrane was then incubated overnight with blocking buffer (5 % (w/v) BSA, 0.05 % (v/v) Tween 20 in PBS buffer) at room temperature. The membrane was washed 3 times for each 10 min with PBS-Tween buffer (0.05 % (v/v) Tween 20 in PBS buffer, pH 7.5). Then the membrane was then incubated with first

antibody namely either mouse anti-His antibody for His-tag fused protein detection or goat anti-human CatL antibody for specific binding detection of CatL in PBS buffer (1 % (w/v) BSA, 0.05 % (v/v) Tween 20) at the dilution ratio of 1:1,500 at 37 °C for 1 h. After that the membrane was washed 3 times for each 10 min in PBS-Tween buffer at room temperature. Subsequently, the membrane was then incubated with secondary antibody, namely rabbit anti-mouse and anti-goat IgG conjugated alkaline phosphatase solution at 1:5,000 dilution ratio diluted in the same buffer as primary antibody incubated for 1 hour at room temperature. The membrane was washed 3 times for each 10 min in PBS-Tween buffer at room temperature. The expected protein was detected by transferring the membrane into NBT/BCIP solution (375 µg/ml of NBT, 188 µg/ml of BCIP, 0.1 M Tris-HCl, pH 9.5, 50 mM MgCl<sub>2</sub>, and 0.9 % NaCl) until the positive band was appeared. Finally, the chromogenic reaction was stopped by rinsing the membrane twice with water.

#### **2.6.6 Molecular mass determination of recombinant CatL by using MALDI-TOF mass spectrometry**

MALDI-TOF Mass spectrometry is a technique for accurate determination of protein molecular mass. It was performed in the commercial facility of the Proteomic Service Center, Bioservice Unit (BSU) (BIOTEC, Pathumthani, Thailand).

#### **2.6.7 CatL activation**

The crude CatL was autolytic degraded under acidic condition. The method was modified from Kramer et al. (2007). The crude protein was dissolved in 100 mM sodium acetate buffer pH 4.0 containing 2 mM EDTA and 2 mM DTT and incubated at 30 °C for 30 min. Then, the protein solution was adjusted pH to 3.5 by adding 50 mM sodium acetate buffer pH 3.0 and incubated at 37 °C for 0, 30 and 60 min. The reaction was stopped by precipitated protein with absolute ethanol. The autocatalytic function of the protein was analyzed by running on SDS-PAGE.

## 2.7 Preparation of the primary shrimp cell culture

The primary culture of *Penaeus monodon* lymphoid cells was prepared as described by Tirasophon et al. (2005). Briefly, lymphoid tissues collected from approximately 100 sub-adult shrimps were washed in a washing medium (2x Leibovitz's L-15 medium containing 100 IU/ml penicillin, 100 mg/ml streptomycin, 15 % fetal bovine serum, and 5 % lactalbumin). The tissues were minced into 1-2 mm cubes in working medium (2x Leibovitz's L-15 supplemented with 15 % fetal bovine serum, 1 % glucose, 5 g/L NaCl, 100 IU/ml penicillin and 100 mg/ml streptomycin (Wang et al. 2004). To remove the large cell debris, the cell suspensions were stood at room temperature for 10-15 min. Subsequently, the upper solution, here after called lymphoid cell solution, was transferred and seeded to 96-well plates at density of either  $1 \times 10^5$  cells per 150  $\mu$ l or  $1 \times 10^6$  cells per 1 ml in micro centrifuge tube. Lymphoid cell solution was allowed for cell attachment for 6 h at 28 °C.

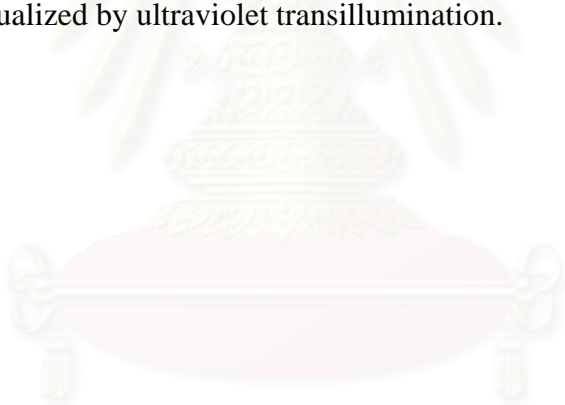
## 2.8 Apoptosis induction by Actinomycin D

The cells were divided into six experimental conditions. In the third and fourth conditions, the cells were cultivated in working media in the presence of 1  $\mu$ M or 0.5  $\mu$ M caspase-3 (Cas3) inhibitors (Calbiochem) for two hours before adding 40 nM actinomycin D (AD). In the fifth and sixth conditions, the CatL inhibitor (Calbiochem) was added instead of Cas3 inhibitor. In the first and second conditions, the cells were cultivated in working media for two hours and then replaced by adding a working media in the absence (control) or in the presence of 40 nM AD.

## 2.9 Detection of apoptosis using agarose gel electrophoresis

Apoptotic DNA fragments were isolated by using the modified conventional phenol/chloroform extraction method, as described by Sambrook et al. (2001). Primary lymphoid cells in microcentrifuge tube were centrifuged at 800xg 4 °C for 5 min. The cell pellets were collected and lysed with 500  $\mu$ l lysis buffer (50 mM Tris-HCl pH 9.0, 100 mM EDTA, 50 mM NaCl, 200 mM sucrose and 2 % sodium dodecyl sulfate). After that 70  $\mu$ g/ml proteinase K and 200  $\mu$ g/ml RNase A-free DNase were then added. The mixture was incubated at 37 °C for 1 h and then transferred to 65 °C

for two hours. To remove contaminated carbohydrate and protein, 100  $\mu$ l of 5 M NaCl and 80  $\mu$ l of CTAB/NaCl solution were added and the mixture was incubated at 65 °C for 10 min. Subsequently, one volume of chloroform-isoamyl alcohol (24:1) was added to the samples followed by further centrifugation at 14,000 rpm at 4 °C for 20 min. The supernatant was collected and then resuspended with one volume of phenol-chloroform-isoamyl alcohol (25:24:1) and 0.5 volume chloroform respectively. The DNA was precipitated by the addition of 2 volumes of absolute ethanol and 0.1 volume of 3 M ammonium acetate pH 5.5. The mixture was incubated for 30 min at -20 °C. The DNA was recovered by centrifugation at 12,000 rpm for 10 min. Pellets were air dried and resuspended in TE buffer (10 mM Tris-HCl, pH 8.0, 1 mM EDTA). To remove contaminated RNA, 500  $\mu$ g/ml DNase free RNase A was added into the solution and incubated at 37 °C for two hours. The extracted DNA was analyzed by running on 2 % agarose gel electrophoresis, stained with ethidium bromide and visualized by ultraviolet transillumination.



สถาบันวิทยบริการ  
จุฬาลงกรณ์มหาวิทยาลัย

## CHAPTER III

### RESULTS

#### 3.1 Immunohistochemical localization of cathepsin L protein

Previously, it was found that cathepsin L (CatL) transcript was abundantly expressed in the lymphoid organ cDNA libraries of the black tiger shrimp. To further investigate the role of CatL in the shrimp lymphoid organ, the localization and distribution of CatL enzyme were examined by immunohistochemistry (IHC). Due to unavailability of antibody against shrimp CatL, goat anti-recombinant human CatL antiserum was used for immunohistochemical localization of CatL protein in the shrimp tissues. First, cross-reactivity of anti-human CatL antibody to shrimp cathepsin L was determined using Western blot analysis. The presence of CatL was examined in haemocyte lysate, heart, hepatopancreas and lymphoid organs (Fig 3.1). The 36-kDa mature human cathepsin L and the 50-kDa pro human cathepsin D (CatD) were used as positive and negative controls, respectively. From the results of SDS-PAGE and Western blot analysis, a single band of about 28 kDa, presumably representing the shrimp CatL was only found in hepatopancreas. Positive signal was absent in pro human CatD protein indicated specificity of the antibody to the CatL.

To localize shrimp CatL in cephalothorax, the tissues from lobster haemolymph medium (LHM) and WSSV injected *P. monodon* were cut and fixed in Davidson's fixative solution for 24 h before processing for paraffin sectioning. Serial sections (5  $\mu$ m thickness) were prepared and processed for indirect immuno-alkaline phosphatase staining using goat anti-recombinant human CatL antiserum followed by alkaline phosphatase-conjugate rabbit anti-goat IgG. The sections were detected by colorimetric reaction using NBT/BCIP as substrate. The slides were counter stained with eosin Y. Sections were examined under light microscope. The color of positive CatL should have dark blue, heavy stain or purple color while negative stain has pink or red color of eosin Y.

In the immunolocalization assays, positive staining was found in various tissues such as segmental ganglia (Fig 3.2 A), supraesophageal ganglion (Fig 3.2 B),

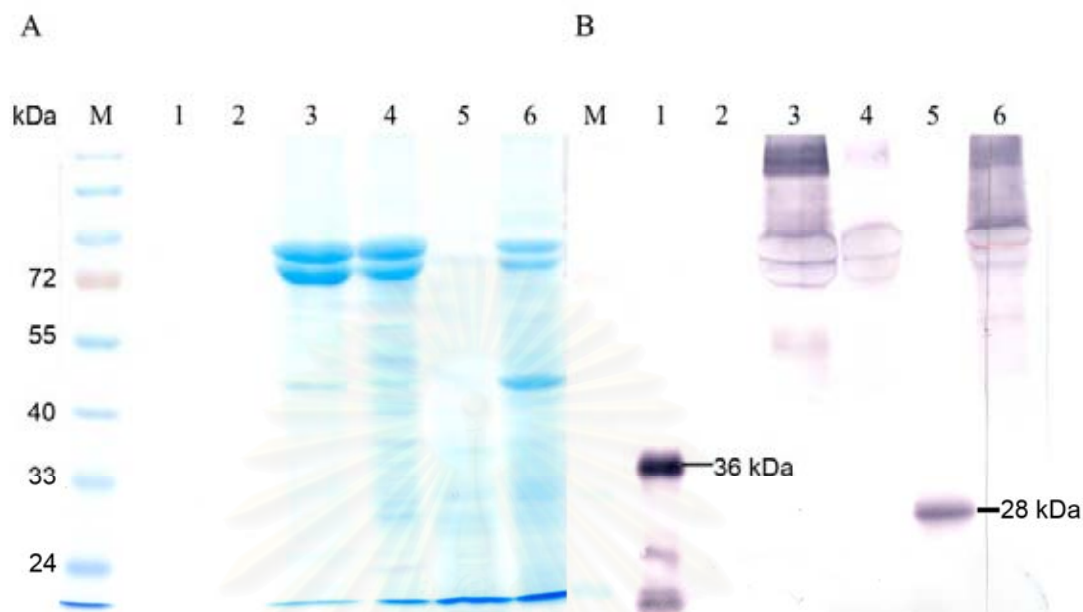


**Figure 3.1 SDS-PAGE (A) and Western blot analysis (B) in shrimp tissues with human CatL antibody.** Fifty-microgram proteins extracted from each tissue and forty-nanograms of human CatL and D were separated in 12 % SDS-PAGE and blotted onto a nitrocellulose membrane. The CatL was detected with anti-human CatL antibody, rabbit anti goat human CatL conjugated with alkaline phosphatase and visualized by colorimetric reaction using NBT/BCIP as substrates.

Lane M : Protein marker

Lane 1 : Mature human CatL

Lane 2 : Pro human CatD

Lane 3 : Haemocyte lysate protein

Lane 4 : Heart protein

Lane 5 : Hepatopancreas protein

Lane 6 : Lymphoid protein

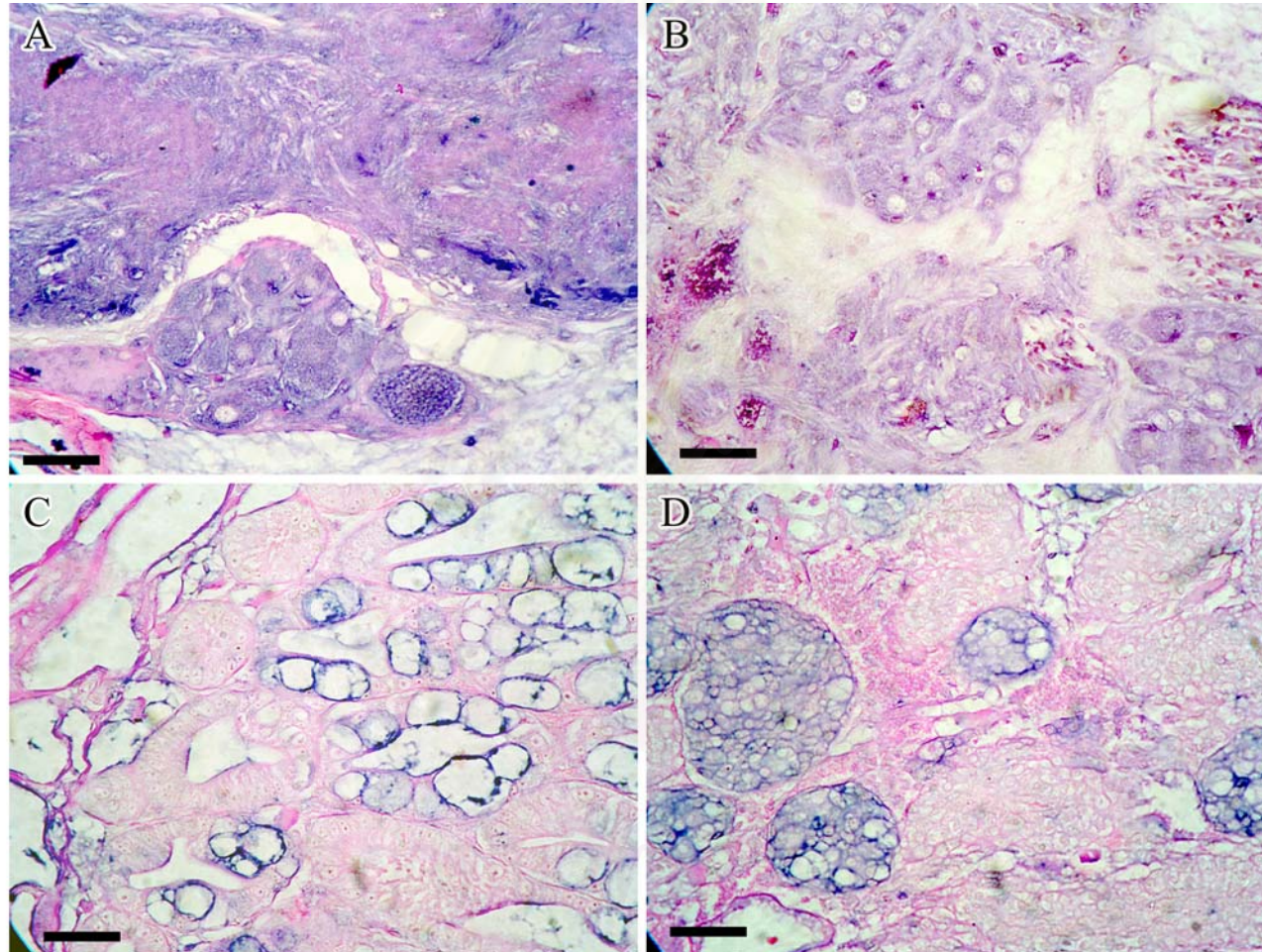


**Figure 3.2 Immunohistochemical localization of CatL in multiple *P. monodon* cephalothorax tissues.** All samples were incubated with goat anti-CatL (5  $\mu\text{g/ml}$ ) followed by alkaline phosphatase-conjugated rabbit anti-goat IgG (1:1,000) and detected by colorimetric method using NBT/BCIP substrate. Positive CatL shows dark blue or purple color. (A) segmental ganglia, (B) supraesophageal ganglion, (C) hepatopancreas and (D) lymphoid organ. All tissues were counter stained with eosin Y. Magnification 400x. Scale bar 50  $\mu\text{m}$ .

hepatopancreas (Fig 3.2 C) lymphoid organ (Fig 3.2 D), hematopoietic tissue (Fig 3.3 A), haemolymph in muscle near oral region (Fig 3.4 C), haemocytes in heart, anterior aorta and hepatopancreas (Figs 3.3 B, C and D). Positive CatL also established in connective tissue (Fig 3.4 D), and septum of vas deferens but no staining could be observed in testis (Figs 3.4 A and B). Shrimp CatL was heavy stained in the hepatopancreas and lymphoid organ, consequently the distribution in the hepatopancreas and lymphoid organ were studied in detail.

In hepatopancreas, CatL was mostly observed in the epithelial cells of hepatopancreas (Figs 3.5 A and 3.6), mainly in the B-cells. No staining could be observed in the other cell types: E-, F- and R-cells. CatL was localized inside the large vacuole of the hepatopancreas B-cell. Heavy stain was observed in the central region of the vacuole and in the margin region in close contact with the limiting membrane of the large vacuole. The amount and color intensity of positive B-cell was used to compare the difference in the CatL between LHM and WSSV injected *P. monodon* in time course analysis (Fig 3.6). No different staining intensity and amount of positive B-cell was observed between the two groups. However, the intensity of positive B-cell was decreased at 24 h and unchanged at 48 and 84 h when compared with the control of normal shrimp (Fig 3.5 A).

In general, lymphoid organ comprises of lymphoid organ tubule (LT) with a central haemal lumen (Lum) and lymphoid organ spheroid (LOS). Normal shrimp comprises only LT whereas LOS can be observed in infected shrimp (van de Braak et al. 2002). In this study, LOS was found in both LHM and WSSV injected shrimp at the same amount indicated that they may be exposed to microbial infection, as shrimp live in an environment enriched with microorganisms. The immunoreactivity of CatL in the lymphoid organ exhibited the positive signal mainly in lymphoid organ spheroid (LOS) (Figs 3.5 B and 3.7) whereas lymphoid tubule (LT) showed less intensity around the edge of lymphoid tubule. Time course analysis of CatL in lymphoid organ after WSSV injection showed a decrease of color intensity at 24 h when compared with those of the LHM-injected shrimp (Fig 3.7) and the normal shrimp (Figs 3.5 B and 3.7). The signal intensity increased and returned to the same intensity level as the control groups at 48 h and 84 h.

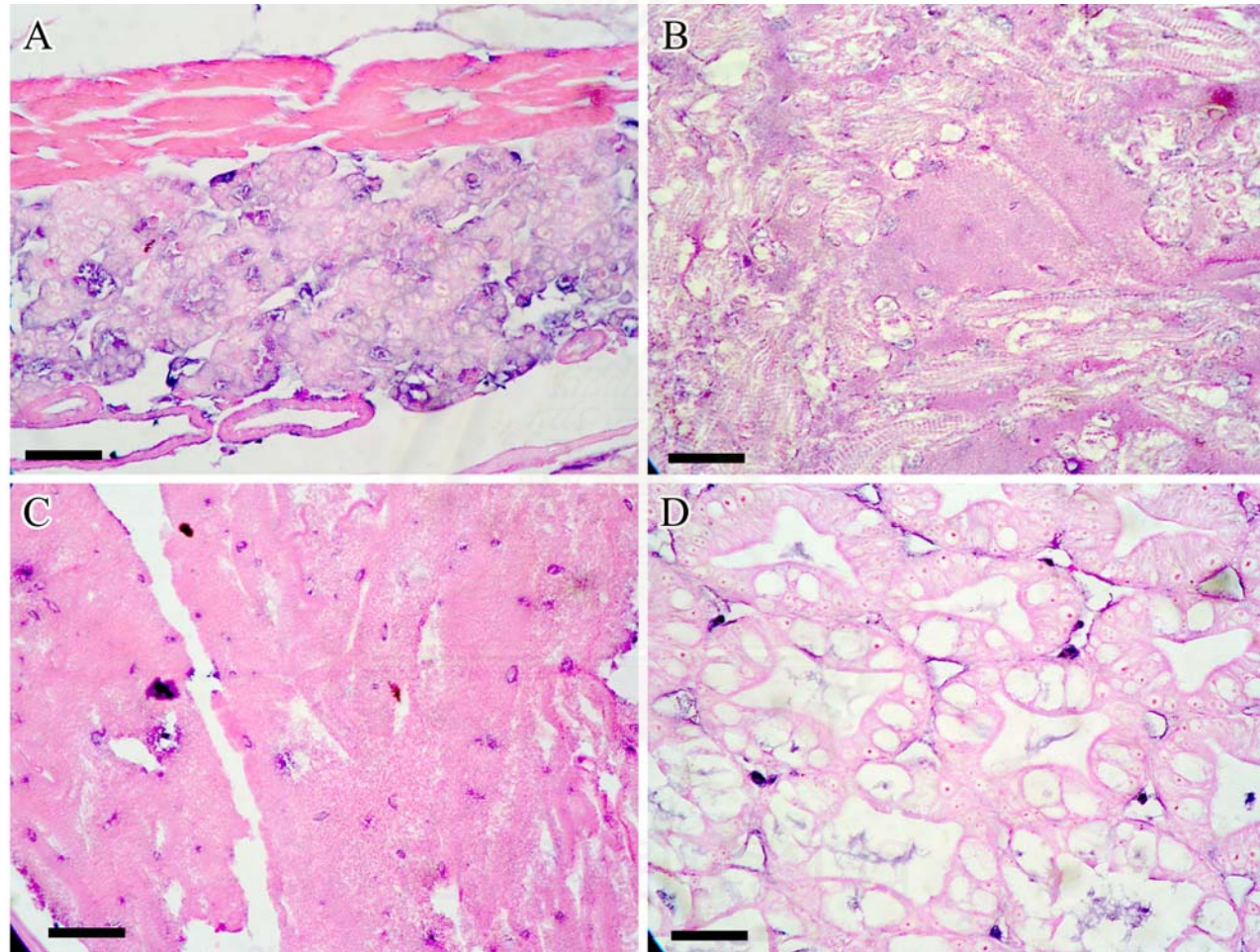


**Figure 3.3 Immunohistochemical localization of CatL in multiple *P. monodon* cephalothorax tissue.** All samples were incubated with goat anti-CatL (5  $\mu\text{g/ml}$ ) followed by alkaline phosphatase-conjugated rabbit anti-goat IgG (1:1,000) and detected by colorimetric method using NBT/BCIP substrate. Positive CatL shows dark blue or purple color. (A) hematopoietic tissue. Haemocytes were positive in heart (B), anterior aorta (C) and hepatopancreas (D). All tissues were counter stained with eosin Y. Magnification 400x. Scale bar 50  $\mu\text{m}$ .

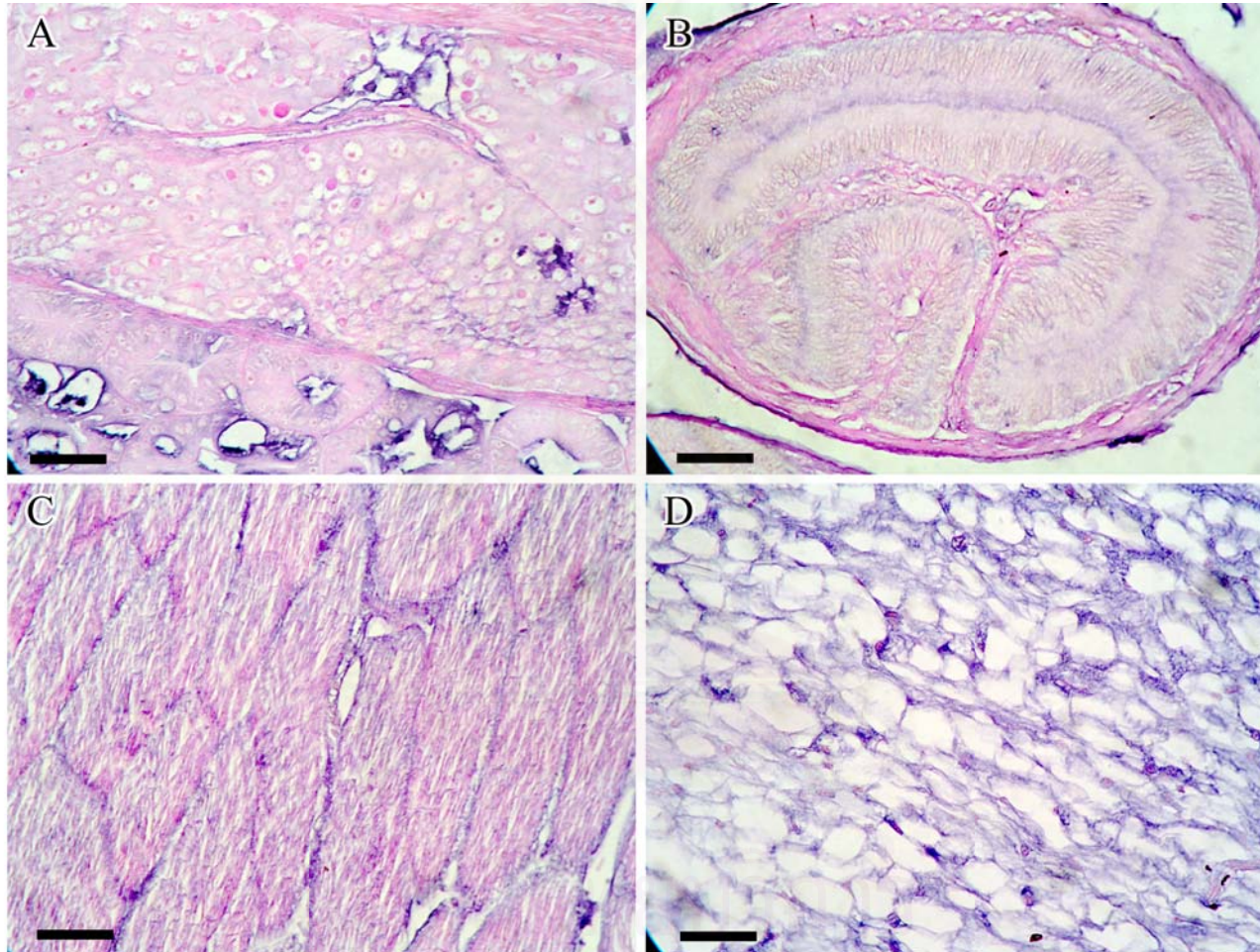


**Figure 3.4 Immunohistochemical localization of CatL in multiple *P. monodon* cephalothorax tissues.** All samples were incubated with goat anti-CatL (5  $\mu\text{g/ml}$ ) followed by alkaline phosphatase-conjugated rabbit anti-goat IgG (1:1,000) and detected by colorimetric method using NBT/BCIP substrate. Positive CatL shows dark blue or purple color. The positive CatL was detected in septum of vas deferens (B), haemolymph in muscle near oral region (C) and connective tissue (D). No immunoreactive staining was detected in the testis (A). All tissues were counter stained with eosin Y. Magnification 400x. Scale bar 50  $\mu\text{m}$ .

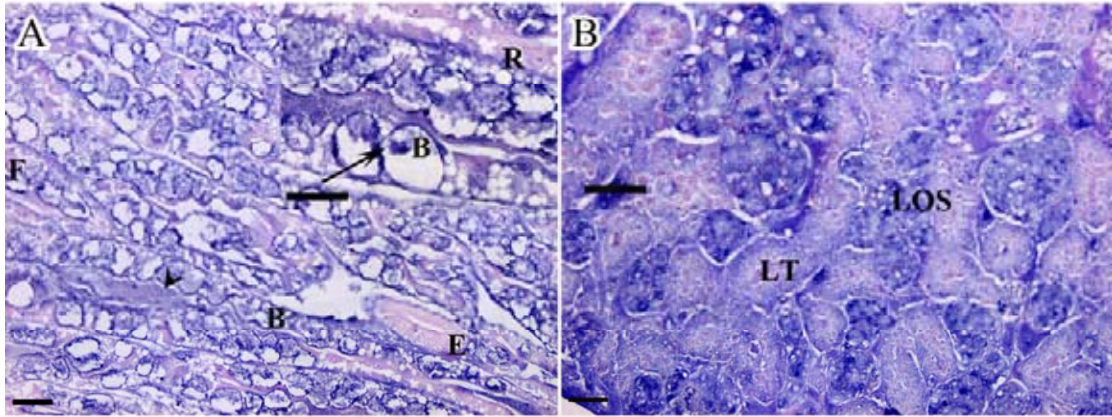


**Figure 3.5 Immunohistocalization of CatL in hepatopancreas and lymphoid organ of normal shrimp.** (A) Longitudinal sections of the hepatopancreatic tubules and (B) lymphoid organ. Dark blue color indicates positive in vacuole of B cell (arrow), hepatopancreatic lumen (arrow head) and in LOS of lymphoid organ. The sections were counterstained with eosin Y. B, B-cell; E, E-cell; F, F-cell; R, R-cell; LOS, lymphoid spheroid; LT, lymphoid tubule. Magnification: 200x. Scale bar 50  $\mu$ m.

สถาบันวิทยบริการ  
จุฬาลงกรณ์มหาวิทยาลัย

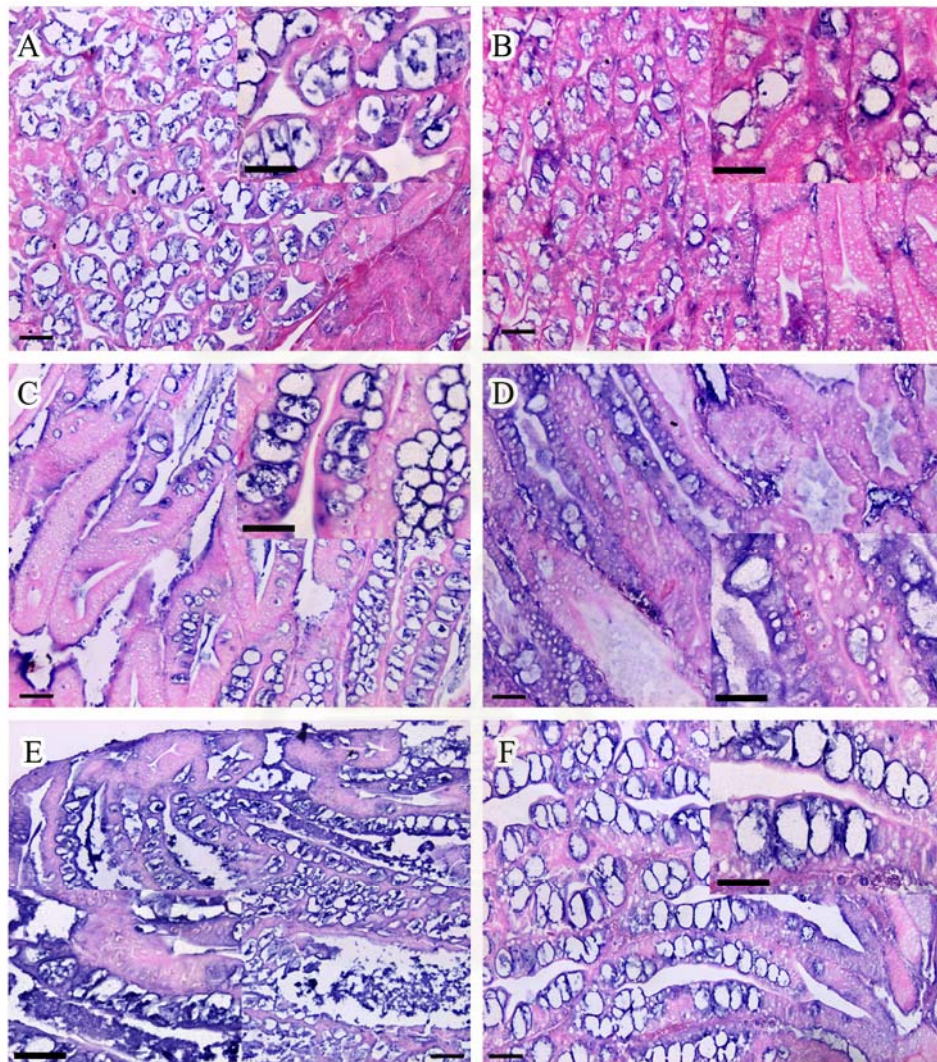


**Figure 3.6** Light micrograph of CatL immunolocalization in hepatopancreas. The longitudinal sections of shrimp hepatopancreas injected with WSSV (right column) and the control LHM (left column) at 24 h (A and B), 48 h (C and D) and 84 h post infection (E and F). Positive immunoreactions have dark blue or purple color of insoluble NBT-diformazan. Eosin Y counterstained; 200 x; Scale bar: 50  $\mu$ m.

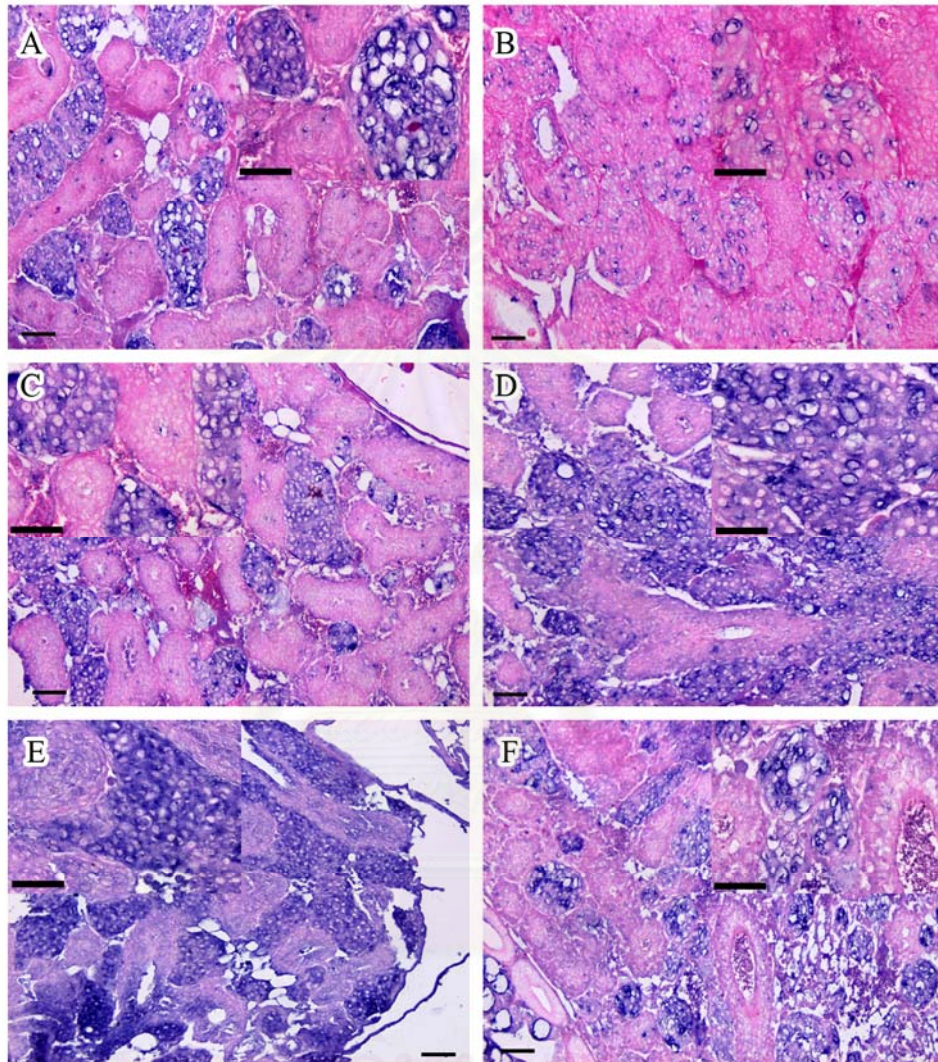


**Figure 3.7 Light micrograph of CatL immunolocalization in lymphoid organ.**

The longitudinal sections of shrimp lymphoid organs injected with WSSV (right column) and control LHM (left column) at 24 h (A and B), 48 h (C and D) and 84 h (E and F). Positive immunoreactions have dark blue or purple color of insoluble NBT-diformazan. Eosin Y counterstained; 200 x; Scale bar: 50  $\mu$ m.

### 3.2 Immunohistochemical localization of WSSV

To examine the site of WSSV infection, the immunohistolocalization of WSSV was done using the anti-VP28 antibody kindly provided by Prof. Paisarn Sithigorngul from Srinakharinwirot University. VP28 is a major envelop protein of WSSV. The tissues sections of LHM and WSSV injected shrimps were incubated with anti-VP28 antibody followed with alkaline phosphatase-conjugated rabbit anti-mouse IgG. The sections were detected by colorimetric reaction using NBT/BCIP as substrate. The slides were counter stained with eosin Y. WSSV was found in heart, stomach, gill, connective tissue, hepatopancreas and lymphoid organ of WSSV injected shrimp whereas no positive signal was observed in all LHM injected shrimps (data not shown). In hepatopancreas, the apparent staining levels were increased significantly from 24 h to 48 h (Fig 3.8) while the levels of positive signals were declined at 84 h (Fig 3.8 F). In all positive hepatopancreas, the signals were found in the region of the interspaces of hepatopancreas tube. The trend of WSSV detection in lymphoid organ was the same as in hepatopancreas and no positive signals of WSSV was observed in all LHM injected groups. The WSSV was found in the stromal matrix and haemal sinuses of LT (Fig 3.9). The positive signal was increased from 24 to 84 h. No positive signal of WSSV was observed in LOS.

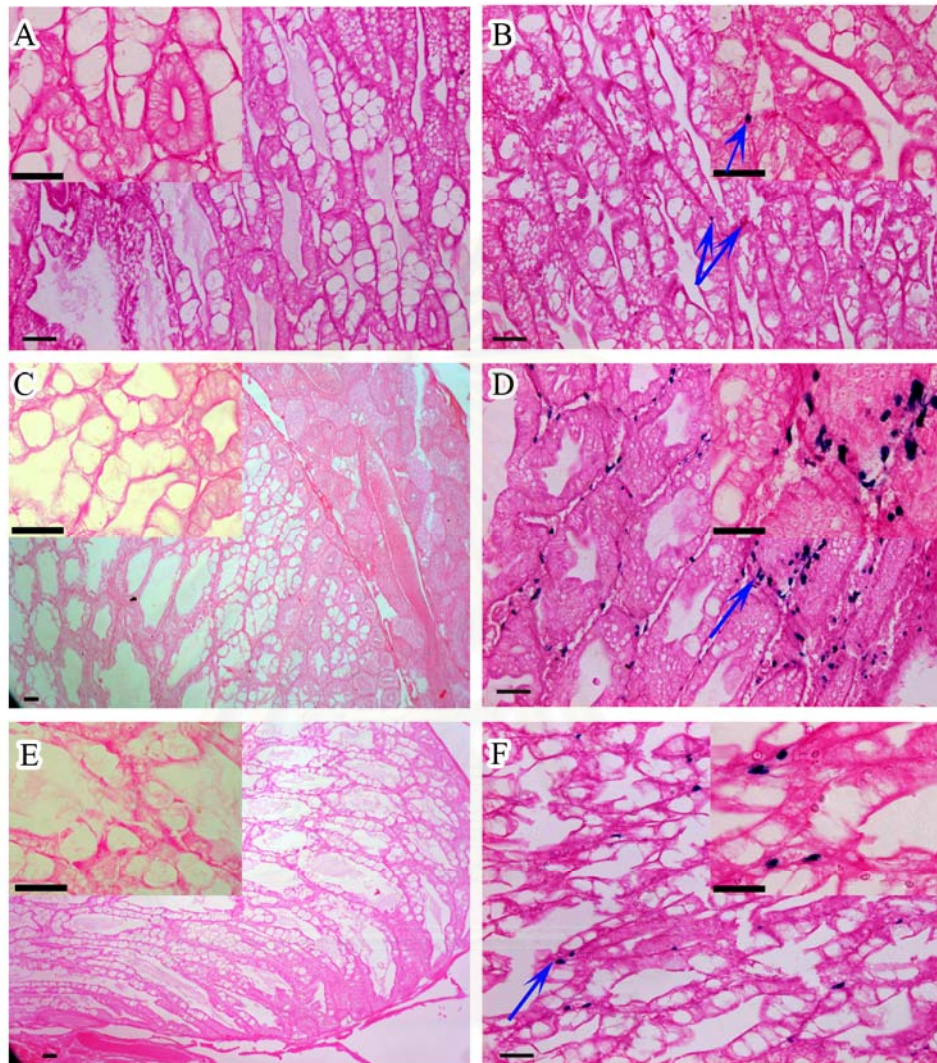


**Figure 3.8 Immunohistochemistry of WSSV in hepatopancreas.** Longitudinal section of hepatopancreas from LHM (left column) and WSSV infected shrimp (right column) at 24 (A and B), 48 (C and D) and 84 h (E and F) were incubated with mouse anti-VP28 antibody followed by rabbit anti-mouse conjugated with alkaline phosphatase. Detection was achieved by colorimetric method using NBT/BCIP substrate and counter stained with eosin Y. Blue arrows indicate WSSV. A, B, D and F magnification 200x, C and E magnification 100x. Scale Bar: 50  $\mu$ m.

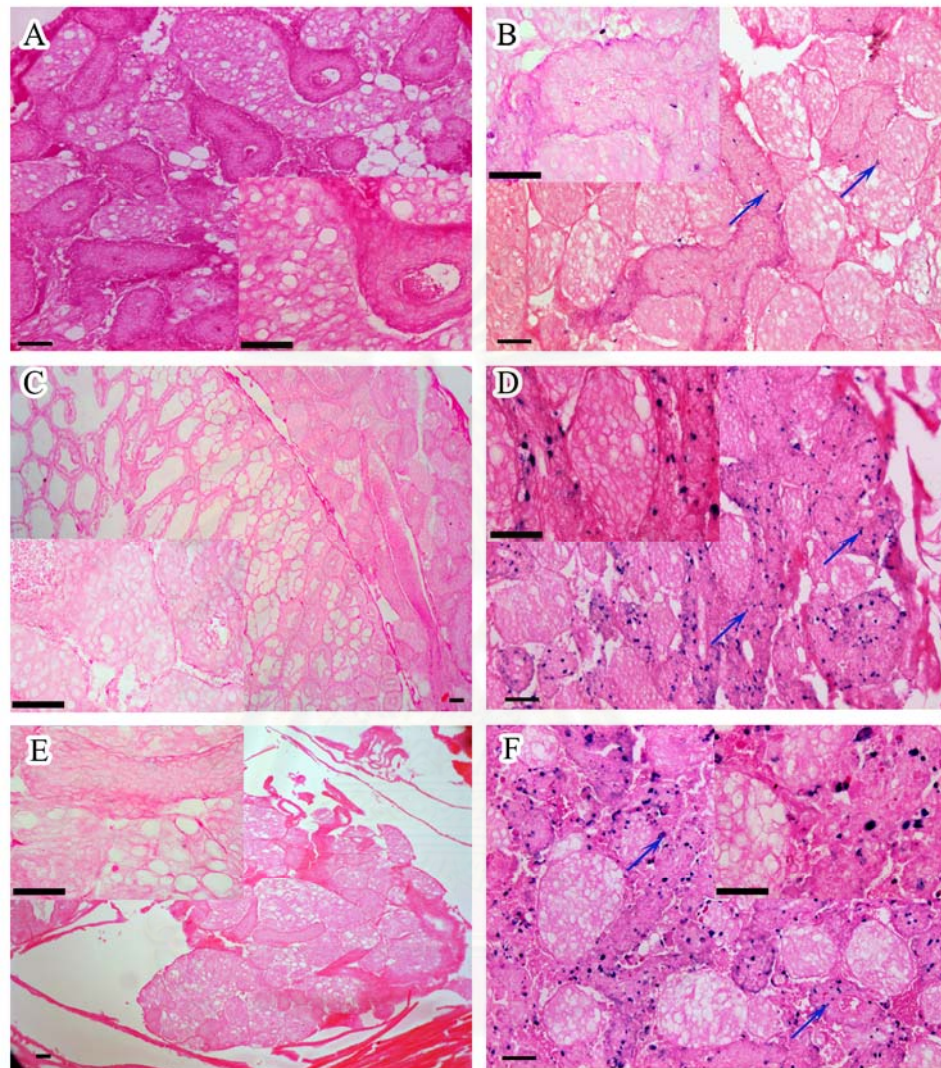


**Figure 3.9 Immunohistochemistry of WSSV in lymphoid organ.** Longitudinal section of lymphoid organ from LHM (left column) and WSSV infected shrimp (right column) at 24 (A and B), 48 (C and D) and 84 h (E and F) were incubated with mouse anti-VP28 antibody followed by rabbit anti-mouse conjugated with alkaline phosphatase. Detection was achieved by colorimetric method using NBT/BCIP substrate and counter stained with eosin Y. Blue arrows indicate WSSV. A, B, D and F magnification 200x, C and E magnification 100x. Scale Bar: 50  $\mu$ m.

### 3.3 Recombinant expression of CatL in *Escherichia coli* expression system

The *P. monodon* CatL from lymphoid organ (GenBank accession no. EF213115) was used as the template for cloning and expression. The sequence of lymphoid CatL consists of an open reading frame of 1,120 bp coding for a protein of 341 amino acids (Fig 3.10). The deduced amino acid of CatL was used to predict the signal peptide using SignalP prediction server (Nielsen et al. 1997). The putative signal cleavage site is between amino acid Ala18 and Val19. Two oligonucleotides were designed. The 5' oligonucleotide was designed such that the signal peptide was excluded and a restriction site *Nhe* I was included (5'-ACTAGCTAGCGTGTCCTTTTTCTCCGTTGTTCTG-3') for the cloning into pGEM<sup>®</sup>-T Easy vector and subsequently into the pET-21a(+) expression vector. The 3' oligonucleotide was designed to include the *Xho* I site (5'-CCGCCGCTCGAGGACAAGAGGGAAGGAGGCGG-3') for cloning into the *Xho* I site of pGEM<sup>®</sup>-T Easy vector and the pET-21a(+) expression vector. The latter cloning resulted in the fusion of the C-terminal of CatL to the His.Taq<sup>®</sup> sequence.

#### 3.3.1 Amplification of the truncated CatL gene

The 5'-terminal truncated CatL gene was constructed by PCR amplification using the cDNA clone (EF213115) as a template and the two oligonucleotide primers described above. The resulting PCR product was separated on a 1.2 % agarose gel and a specific 1,005-bp fragment of expected size was observed (Fig 3.11 A)

#### 3.3.2 Construction of recombinant plasmid pGEM-T-CatL

The 1,005-bp PCR fragment was purified and ligated into pGEM<sup>®</sup>-T easy vector. After ligation, the reaction mixture was transformed to *Escherichia coli* stain XL1 Blue. The recombinant clone was first selected with LB agar plate containing ampicillin, X-Gal and IPTG. White colonies were randomly selected and cultured in LB medium containing 100 µg/ml ampicillin. The plasmids were extracted from the selected colonies and cut with *Nhe* I and *Xho* I. The digested plasmids were analyzed on 1.2 % agarose gel electrophoresis (Fig 3.11 B). The clone containing the 1,005-bp inserted DNA was selected for augmentation and named pGEM-T-Cat L. After restriction digestion and electrophoresis of the clone, the 1,005-bp inserted DNA was purified from the agarose gel for further ligation into pET-21a(+).

```

CATTAGAAGATGGAAATCTTAAGTGTAGCAGTACTTGTGGCCGTTGTGGCATCCACATCG 60
      M K F L S V A V L V A V V A S T S 17
GCCGTGTCCTTTTTCTCCGTTGTTCTGGAGGAATGGGAAGCTTCAAGCTTGAGCATAGC 120
A V S F F S V V L E E W E A F K L E H S 37
AAGAAGTACGACTCAGAGGTCGAGGAGTCATTCCGCATGAAGATCTTCACGGAGAACAAG 180
K K Y D S E V E E S F R M K I F T E N K 57
CACAAGATTGCCAACCAACAAGGGCTTTGCACAAGGACACCACACTTACAAACTCAGT 240
H K I A N H N K G F A Q G H H T Y K L S 77
ATGAACAAATATGGAGATATGCTCCACCATGAGTTCGTCTCTACCATGAATGGCTTCCGT 300
M N K Y G D M L H H E F V S T M N G F R 97
GGAAACCACACTGGGGGTTACAAGAACAACCGTGCTTACACCGGAGCCACCTTCATTGAG 360
G N H T G G Y K N N R A Y T G A T F I E 117
CCTGATGATGATGTGCAGCTTCCCAAGAATGTTGACTGGAGGACCAAGGGAGCCGTCACA 420
P D D D V Q L P K N V D W R T K G A V T 137
CCTATCAAGGACCAGGGCCAGTGTGGCTCTTGCTGGGCGTTCTGCCACTGGTGCCTG 480
P I K D Q G Q C G S C W A F S A T G A L 157
GAGGGCCAGACATTCCGCAAGACTGGTCAGCTGGTGAGCCTCTCGGAGCAGAACCTGGTG 540
E G Q T F R K T G Q L V S L S E Q N L V 177
GACTGCTCTCGCAAGTTTGGCAACAATGGTTGCAACGGTGGACTCATGGACAATGCCTTC 600
D C S R K F G N N G C N G G L M D N A F 197
GAGTACGTCAAGGAGAATGGCGGCATCGACACTGAGGAGAGCTACCCATATGATGCAGAG 660
E Y V K E N G G I D T E E S Y P Y D A E 217
GACGAGAAATGCCATTACAATCCCCGAGCTGCTGGTGCCGAGGACAAGGGCTTCGTTGAC 720
D E K C H Y N P R A A G A E D K G F V D 237
GTGCGCGAGGGAAGCGAACATGCACTGAAGAAGGCTGTTGCCACCGTTGGCCAGTGTCT 780
V R E G S E H A L K K A V A T V G P V S 257
GTGGCTATTGATGCATCTCATGAGTCATTCCAGTTCTACAGCCATGGTGTATACATTGAA 840
V A I D A S H E S F Q F Y S H G V Y I E 277
CCCGAATGCTCCCTGAGATGCTTGACCACGGTGTCCCTTGTGTTGGCTATGGCATGAC 900
P E C S P E M L D H G V L V V G Y G I D 297
GATGATGGCAGACTACTGGCTGGTAAAGAACTCCTGGGGTACAACCTGGGGTGATCAG 960
D D G T D Y W L V K N S W G T T W G D Q 317
GGCTACGTTAAGATGGCCCGCAACCGTGACAACAGTGTGGCATTGCCTCCTCCGCCTCC 1020
G Y V K M A R N R D N Q C G I A S S A S 337
TTCCCTCTTGTCTAGAGTAAAAAAATCATGAAGTTACAGTTAATGTTTACTCTAGATCA 1080
F P L V * 341
TTTTCTTTCCCATGAAGCTACAGTTATGTTTACCCTAGCTCATTCTTTCCCTTGCTCT 1140
GGTGGGTTAATGCTCTCAATACATACAGCAAGCAATATTTCTGAATTCTGAGCACTAGAC 1200
CTTGCTTTGCAT 1212

```

**Figure 3.10** The nucleotide and deduced amino acid sequences of the cDNA clone encoding *Penaeus monodon* CatL from lymphoid organ (ABQ10739). The initiation (ATG) and termination (TAG) codons are shown in bold faces. The signal peptide and the propeptide region are underlined and shaded in gray, respectively. The active site cysteine, histidine and asparagine residues are highlighted in black.

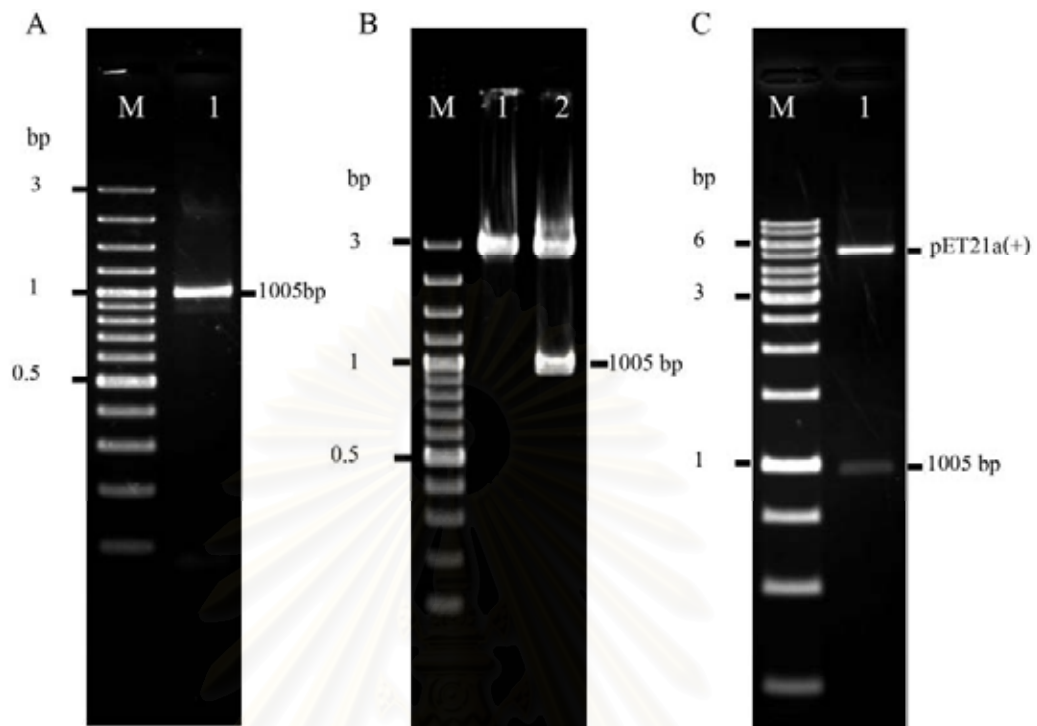


**Figure 3.11** Agarose gel electrophoresis of PCR amplification product and the recombinant vector on 1.2 % agarose gel.

(A) PCR amplification product of truncated segment of the CatL

Lane M : Standard DNA ladder (100 bp marker)

Lane 1 : Amplified CatL gene product

(B) Verification of pGEM-T Easy vector containing CatL

Lane M : Standard DNA ladder (100 bp marker)

Lane 1 : pGEM-T Easy vector/*Nhe I/Xho I*

Lane 2 : pGEM-T-cat L/*Nhe I/Xho I*

(C) Verification of pET-21a(+) vector containing CatL gene

Lane M : Standard DNA ladder (1 Kbp marker)

Lane 1 : pET-21a(+)-CatL/*Nhe I/Xho I*

### 3.3.3 Construction of recombinant plasmid pET-21a(+)-CatL

The truncated CatL insert excised from the pGEM-T-CatL using *Nhe* I and *Xho* I was subsequently cloned into pET-21a(+) expression vector at the *Nhe* I and *Xho* I sites. This plasmid vector carries a C-terminal His.Tag® sequence. After ligation, the reaction mixture was transformed to *Escherichia coli* strain XL1 Blue. The recombinant clone was selected with LB agar plate containing 100 µg/ml ampicillin. The plasmids were extracted from the selected colonies and cut with *Nhe* I and *Xho* I. The digested plasmids were analyzed on 1.2 % agarose gel electrophoresis (Fig 3.11 C). The correct construct was named pET-21a(+)-Cat L.

### 3.3.4 Recombinant protein expression in *Escherichia coli* BL21(DE3)

Recombinant plasmid pET-21a(+)-CatL were transformed into an *Escherichia coli* BL21(DE3) to test for the induction of CatL synthesis. After induction with 1 mM isopropyl-beta-D-thiogalactopyranoside (IPTG) for 0, 1, 2, 3 and 4 hours, the cells were harvested by centrifugation. The cells were then solubilized with the SDS-PAGE loading buffer and analyzed by electrophoresis on a 12 % SDS-PAGE. Cultures containing the plasmid pET-21a(+)-CatL without IPTG induction were used as a negative control. Following staining of the gels with Coomassie brilliant blue, an approximately 37 kDa protein was induced in the host cell lysate containing pET-21a(+)-CatL but absent in that negative control (Fig 3.12). The protein was detected after 1 hour of induction. At 4 hours of induction, the intensity of 37 kDa protein band was enough for further studies, and then this condition was used to prepare the recombinant protein for further characterization.

### 3.3.5 Solubility of the recombinant protein

The induced protein was suspected to be insoluble in the form of inclusion bodies. To verify the notion, the culture was grown, induced with IPTG for 4 hours and harvested by centrifugation. The cell pellet was completely frozen and thawed. The PBS buffer was added, and the cell suspension was sonicated and centrifuged at 12,000 g to separate the inclusion bodies and soluble fraction. The cell lysate of *Escherichia coli* and insoluble proteins were analyzed by electrophoresis on a 12 % SDS-PAGE. An approximately 37-kDa protein band was observed mainly in the insoluble protein fraction (Fig 3.13) and probably accounted for more than 80 % of

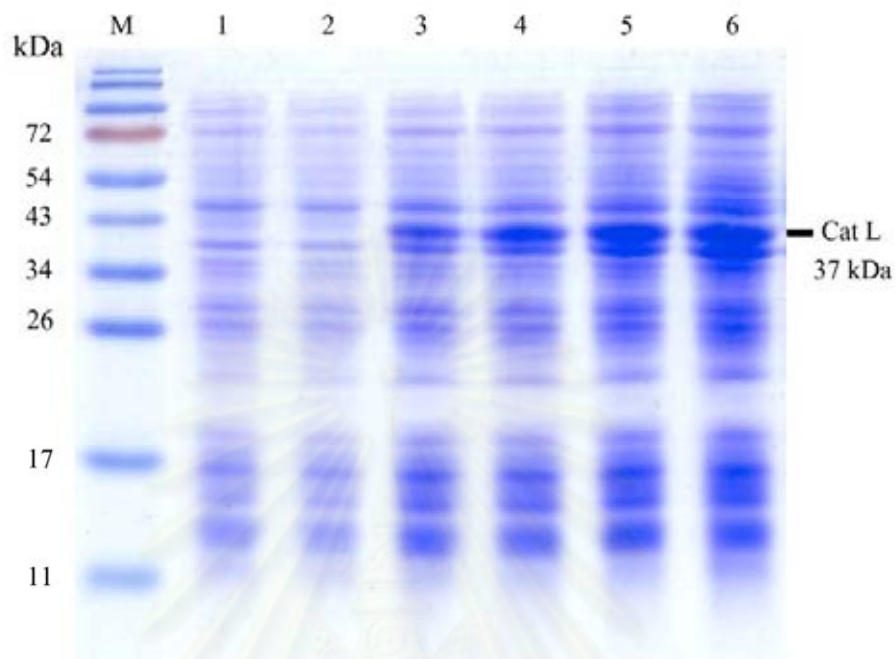


**Figure 3.12** The Coomassie stained 12 % SDS-PAGE analysis of CatL expressed in *Escherichia coli* BL21(DE3) at various time of induction. *E. coli* BL21(DE3) contained pET 21a(+)-CatL was cultivated in LB medium and induced the expression of protein with 1 mM IPTG. The medium was sampling every hour during 4 hours.

Lane M : Prestained protein marker (Fermentas)

Lane 1 : *E. coli* lysate of the cells containing recombinant plasmid pET 21(+)-CatL without induction at 0 h.

Lanes 2-6 : *E. coli* lysates of the cells containing recombinant plasmid pET21(+)-Cat L at 0, 1, 2, 3 and 4 h of induction, respectively.

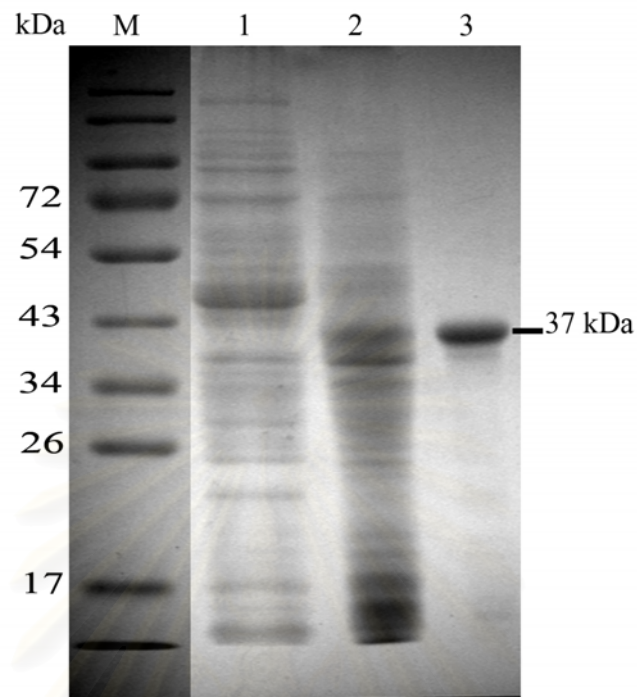


**Figure 3.13 The SDS-PAGE analysis of soluble and inclusion protein fractions.**

The IPTG induced *E. coli* cells were lysed by sonication and centrifuged at 12,000 g to separate the inclusion bodies and soluble fractions. Proteins were analyzed on 1.2 % SDS-PAGE and stained with Coomassie blue.

Lane M : Prestained protein marker (Fermentas)

Lane 1 : Soluble protein of *E. coli* lysate

Lane 2 : Insoluble protein of *E. coli* lysate

Lane 3 : Purified recombinant CatL

the expressed protein. The protein was thus expressed and aggregated in the cells as inclusion bodies.

### **3.4 Purification of the recombinant protein**

The inclusion bodies of CatL proteinase were solubilized in 50 mM Tris-HCl, pH 8, containing 6 M urea and was applied to a Ni-NTA agarose column as described in section 2.6.4 The unbound proteins were eluted from the Ni-NTA agarose column with 6xHis wash buffer. The bound proteins were then eluted with 6xHis elution buffer containing 100 mM imidazole. The bound fractions containing the 37 kDa protein were pooled and dialysed slowly against PBS. The protein was renatured upon dialysis.

### **3.5 Detection of recombinant protein using Western blot analysis**

Since the CatL gene was fused to the His tag at its C-terminus, the induced protein can be identified using Western blot analysis. The expressed His tagged protein was specifically detected using Anti-His.Taq antibody and a second antibody tagged with alkaline phosphatase and confirmed with anti human CatL antibody. The protein bands were localized in the gels with colorimetric method using NBT/BCIP as substrate. The approximately 37 kDa protein band was detected (Fig 3.14). This indicated that the CatL protein was successfully expressed in the host cell.

### **3.6 Molecular mass determination of the recombinant CatL by using MALDI-TOF mass spectrometry**

The molecular mass of recombinant CatL was determined by using MALDI-TOF mass spectrometry. The MALDI-TOF spectra of the recombinant CatL was shown in Fig 3.15. This result showed that the molecular mass of the recombinant CatL was 37,483.190 Da.

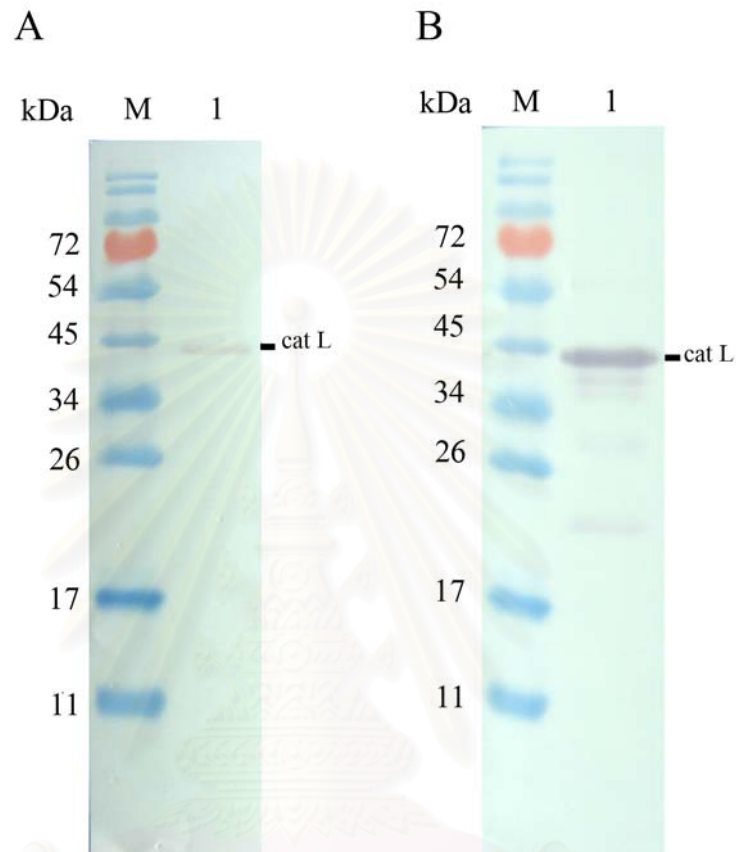


**Figure 3.14 Western blot analysis of purified CatL from *Escherichia coli* BL21(DE3).** Purified CatL was subjected to 12 % SDS-PAGE and transferred to nitrocellulose membrane. The membrane was incubated with mouse anti-His.Tag antibody (A) and goat anti-human CatL antibody (B) and then rabbit anti-mouse and anti-goat IgG conjugated with alkaline phosphatase. Detection was achieved by colorimetric method using NBT/BCIP as substrate.

Lane M : Prestained protein marker (Fermentas)

Lane 1 : Purified recombinant CatL

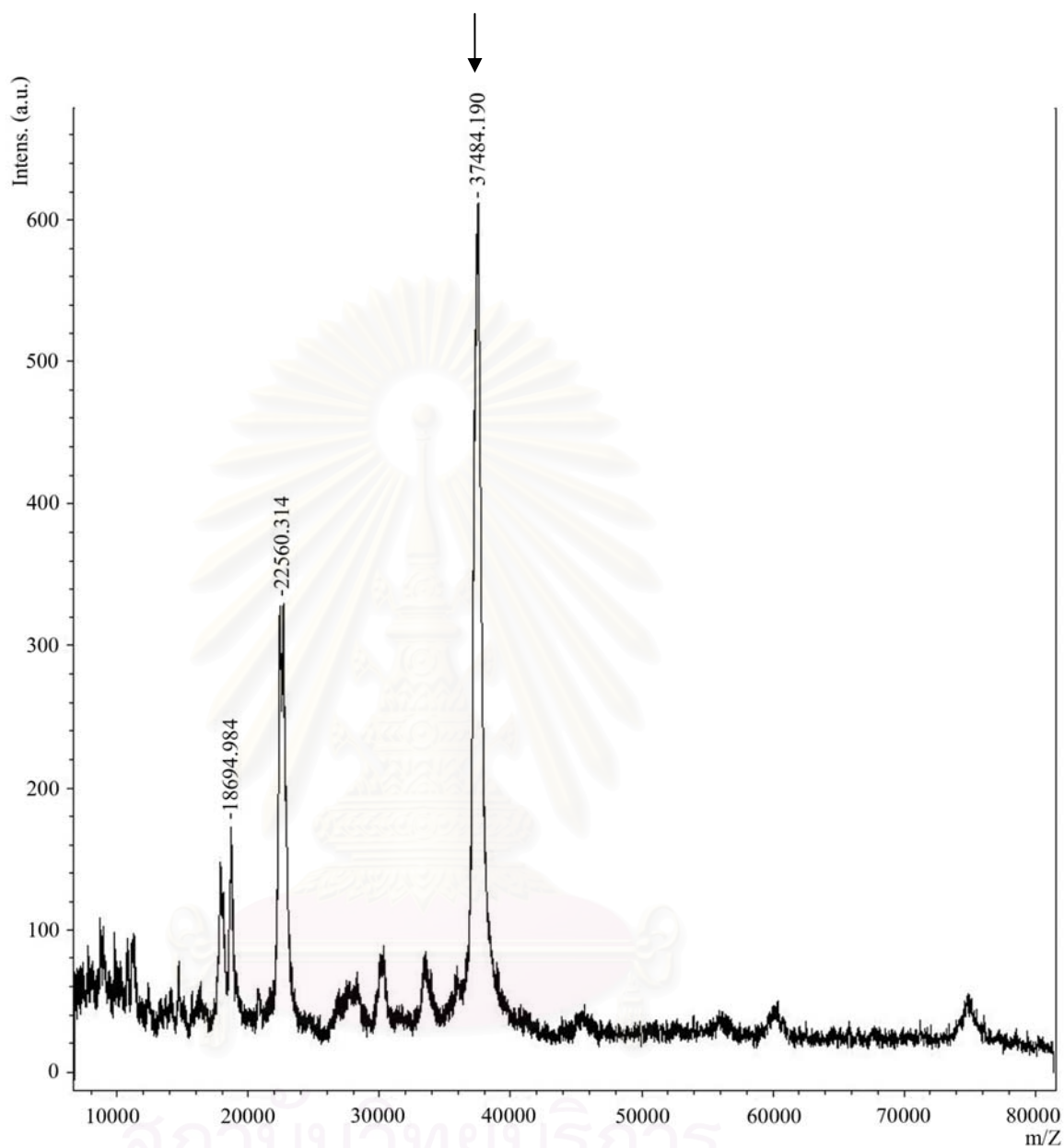


**Figure 3.15 MALDI-TOF mass spectrometric determination of molecular weight of the recombinant CatL.** The peak of the recombinant CatL is indicated by arrow.

### 3.7 Autocatalytic processing of procathepsin L

The deduce amino acid sequence of *P. monodon* CatL (*PmCatL*) (accession no. EF213115) revealed the presence of two motifs. The first motif was inhibitor I29 found near the N-terminal region and the next motif was peptidase C1A. The nucleotide sequence of *PmCatL* was subjected to similarity search against protein database of NCBI by using the BLASTX. The result showed that the *PmCatL* had the highest similarity (80.5 %) to cathepsin-L-like cysteine peptidase 02 from *Tenebrio molitor* (*TmCatL*). The *TmCatL* was expressed as the zymogens form and the zymogens were auto activated to mature enzyme at slightly acidic condition (Cristofolletti et al. 2005). To obtain the active CatL containing only a peptidase C1A motif, the crude proteins from the inclusion bodies were dissolved in sodium acetate buffer, pH 4.0 at 30 °C for 30 min. The proteins were then activated by adjust the pH to 3.5 and future incubated at 37 °C for 30 and 60 min. After incubation, the proteins were subjected to SDS-PAGE analysis, no change in the size of the recombinant CatL was observed (Fig 3.16) indicating that the acid activation was unsuccessful.

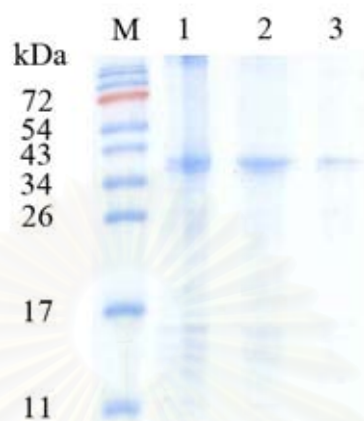


**Figure 3.16 Acid autoactivation of crude CatL.** The crude CatL was incubated in 100 mM sodium acetate buffer pH 3.5 at 37 °C for 30 and 60 min. The proteins were analyzed by 12 % SDS-PAGE and stained with Coomassie blue.

Lane M : Prestained protein marker (Fermentas)

Lane 1 : Crude CatL

Lanes 2-3: Crude CatL incubated in 100 mM sodium acetate pH 3.5 for 30 and 60 min, respectively.

### 3.8 Primary lymphoid cell culture

To investigate the involvement of CatL in apoptosis, actinomycin D (AD) was used to induce cell death and CatL inhibitor was added to the apoptotic induced cell culture. Caspase-3 (Cas3) inhibitor was used as the positive control.

Lymphoid organs were isolated from *Penaeus monodon* and washed in a washing medium (see 2.7). Lymphoid tissues were cut into 1-2 mm<sup>3</sup> cubes in working medium, followed by incubating at room temperature for 10-15 min to remove large cell debris. Cells were then seeded at  $1 \times 10^5$  cells per 150  $\mu$ l of 96-well plates. The cells were grown at 28 °C for 6 h to ensure that the cells were attached to the plates. Lymphoid cells formed a monolayer of round and some fibroblast-like cells of different size (Fig 3.17 A). Further incubation for another 6 h resulted in more fibroblast-like cells (Fig 3.17 B) than round cells.

### 3.9 Inhibition of apoptosis by Cas3 inhibitor and CatL inhibitor on AD induced apoptosis

To investigate the effect of CatL on the apoptotic process, the cells were treated with two concentrations, 0.5  $\mu$ M or 1  $\mu$ M, of CatL or Cas3 inhibitors for two hours before adding 40 nM AD followed by further incubation for 12 h. The cells were compared with normal (untreated group) and AD treated cells. After 12 h of incubation, the morphology of lymphoid cells was investigated under phase contrast microscope and the number of cell death was counted by staining with 0.4 % Trypan blue. The dead cells were stained with Trypan blue.

The apoptotic body was highest in the cells treated with 40 nM AD (Fig 3.18 B). The level of apoptotic body was decreased in cells treated with 40 nM AD+Cas3 inhibitor (Figs 3.18 C and D) or 40 nM AD+CatL inhibitor (Figs 3.18 E and F) whereas the apoptotic body was not observed in the untreated group.

Total cells at 12 h after AD treatment were counted and the number of cells death were determined by Trypan blue staining and reported in Table 3.1. The number of death cells and total cells were used to calculate the percentage of death cells. The high percentages of dead cells were found in the cells treated with 40 nM AD compared with the untreated cells.

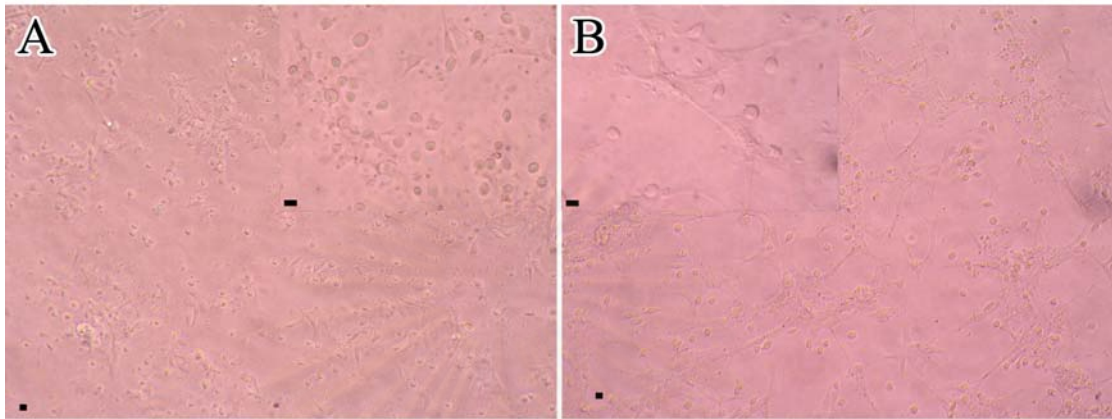


**Figure 3.17 Morphology of primary lymphoid cell culture.** Lymphoid cells were separated from lymphoid organ and seeded at  $1 \times 10^5$  cell/ $150 \mu\text{l}$ . (A) cell monolayer showed approximately 80 % round cells after incubation for 6 h at  $28^\circ\text{C}$ . (B) fibroblast-like cells were found after incubation for 12 h. Phase contrast microscopy, 200x, and scale bar,  $10 \mu\text{m}$ .

สถาบันวิทยบริการ  
จุฬาลงกรณ์มหาวิทยาลัย

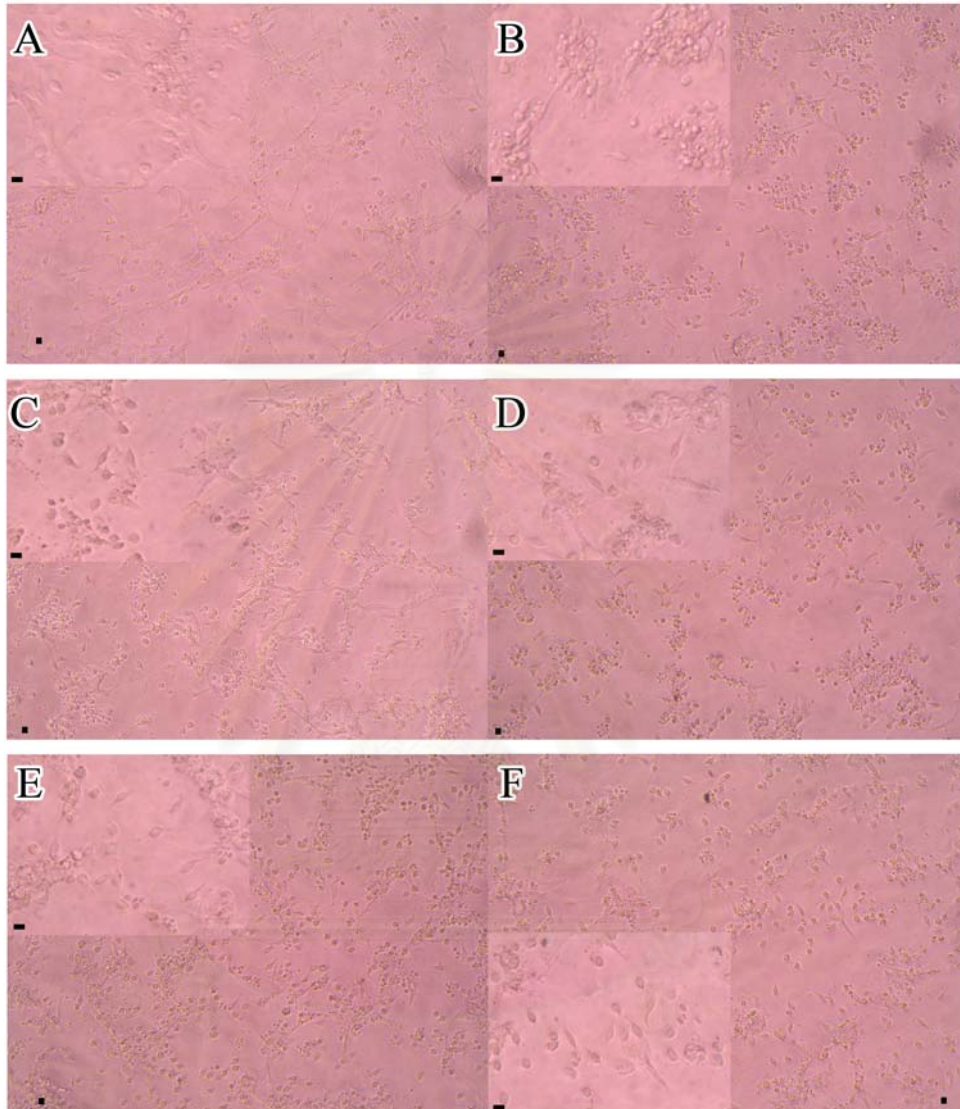


**Figure 3.18** Morphology of the primary lymphoid cells of *P. monodon* after treated with actinomycin D. At 12 h after AD treated, the morphology of cells was observed under phase contrast microscope. (A) untreated cell, (B) cell treated with 40 nM AD, (C) cells treated with 40 nM AD and 0.5  $\mu$ M Cas3 inhibitor, (D) cells treated with 40 nM AD and 1  $\mu$ M Cas3 inhibitor, (E) cells treated with 40 nM AD and 0.5  $\mu$ M CatL inhibitor, (F) cells treated with 40 nM AD and 1  $\mu$ M CatL inhibitor. Magnification: x200. Scale Bar: 10  $\mu$ m.

**Table 3.1 Number of death cells counted by Trypan blue staining.**

conditions	Total cells	No. of dead cells	Percent death cells
normal 1	429	40	9.0
normal 2	451	61	13.7
normal 3	457	42	9.4
40 nM AD 1	312	93	20.9
40 nM AD 2	415	102	22.9
40 nM AD 3	388	98	22.0
0.5 uM cas-3 inhibitor + 40 nM AD 1	364	20	4.5
0.5 uM cas-3 inhibitor + 40 nM AD 2	374	26	5.8
0.5 uM cas-3 inhibitor + 40 nM AD 3	415	45	10.1
1 uM cas-3 inhibitor + 40 nM AD 1	418	83	18.6
1 uM cas-3 inhibitor + 40 nM AD 2	368	65	14.6
1 uM cas-3 inhibitor + 40 nM AD 3	339	52	11.7
0.5 uM cat-L inhibitor + 40 nM AD 1	310	60	13.5
0.5 uM cat-L inhibitor + 40 nM AD 2	325	64	14.4
0.5 uM cat-L inhibitor + 40 nM AD 3	312	78	17.5
1 uM cat-L inhibitor + 40 nM AD 1	392	38	8.5
1uM cat-L inhibitor + 40 nM AD 2	441	34	7.6
1uM cat-L inhibitor + 40 nM AD 3	413	48	10.8

The cells treated with AD+Cas3 or AD+CatL inhibitors showed lower percentage of dead cells compared with the cells treated with AD only. The cells treated with 1  $\mu$ M Cas3 or 0.5  $\mu$ M CatL inhibitors have the percentage of dead cell nearly equal to the non-treated cells (Fig 3.19).

### 3.10 Detection of apoptosis using agarose gel electrophoresis

To confirm the death of cells in AD treatment, the DNA laddering assay was performed to detect apoptosis. The lymphoid cells were grown at  $1 \times 10^6$  cells/ 1 ml in microcentrifuge tube instead of 96-well plates. The apoptotic DNA fragment was extracted by conventional phenol/chloroform extraction method with some modification. The characteristic apoptotic DNA ladder of approximately 200 bp could be seen in all 40 nM AD treated cells with or without inhibitor as well as the control (untreated cells) (Fig 3.20).

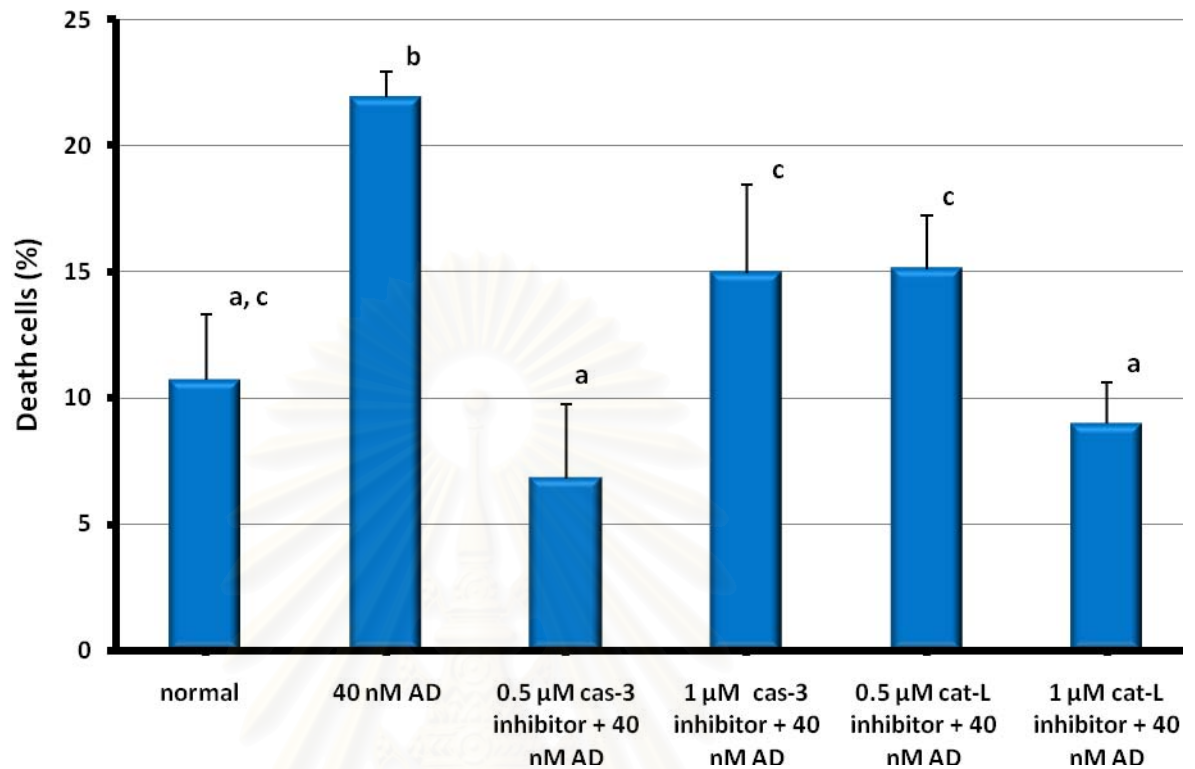


**Figure 3.19 Percentage of mortal cells in AD induced apoptosis with or without inhibitors.** Bar graph demonstrating the effect of Cas3 inhibitors and CatL inhibitor on AD induced cell death. The primary lymphoid cells were exposed to 40 nM AD for 12 h in the presence of Cas3 or CatL inhibitors. Cell counts were performed and expressed as a percentage of cell death. Different letters between groups indicate significant differences ( $P < 0.05$ ).

สถาบันวิทยบริการ  
จุฬาลงกรณ์มหาวิทยาลัย

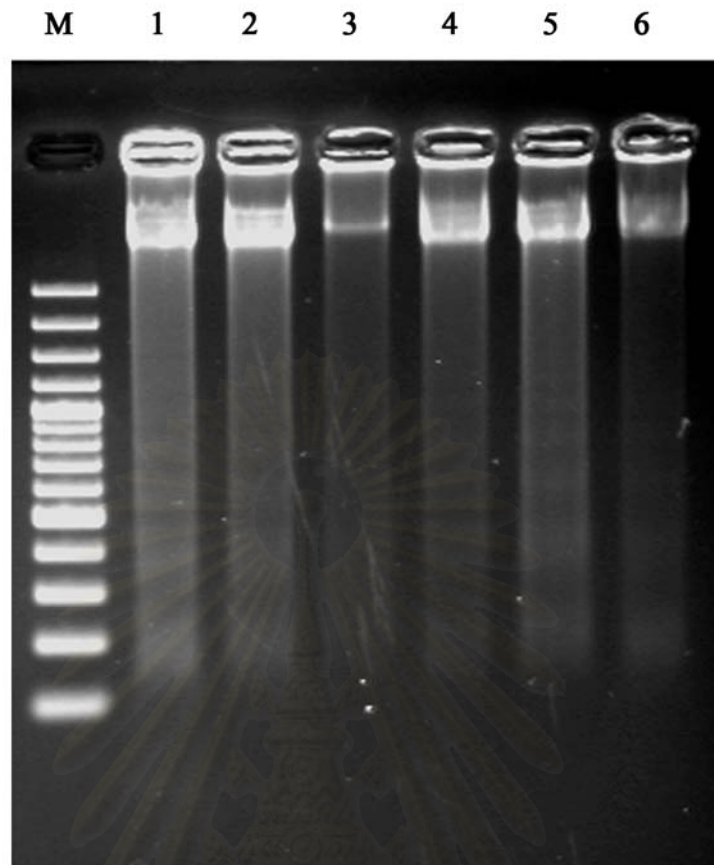


**Figure 3.20 Apoptotic DNA laddering from primary cell culture treated with AD.** Fragmented DNA was extracted and analyzed on 2 % agarose gel containing EtBr.

Lane M : 100 bp ladders plus (Fermentas)

Lane 1 : Normal primary lymphoid cells (control)

Lane 2 : Primary lymphoid cells treated with 40 nM AD

Lane 3 : Primary lymphoid cells treated with 40 nM AD and 0.5  $\mu$ M Cas3 inhibitor

Lane 4 : Primary lymphoid cells treated with 40 nM AD and 0.5  $\mu$ M CatL inhibitor

Lane 5 : Primary lymphoid cells treated with 40 nM AD and 1  $\mu$ M Cas3 inhibitor

Lane 6 : Primary lymphoid cells treated with 40 nM AD and 1  $\mu$ M CatL inhibitor

## CHAPTER IV

### DISCUSSIONS

The aquaculture of shrimp has been threatened by the severe outbreak of pathogenic microorganisms. The diseases have caused a decrease in shrimp production. The most devastating shrimp pathogen is the white spot syndrome virus (WSSV). WSSV is extremely virulent and the infection results in a rapid mortality of the infected animals. In 1996 and 1997, the loss from the outbreaks of WSSV was estimated at approximately 1 billion US dollars (Flegel 2006). Upon WSSV infection, the occurrence of apoptosis has long been observed. Apoptosis has been detected in several viral target tissues of shrimp, and the level of apoptosis seems to increase as WSSV progresses towards shrimp death (Sahtout et al. 2001; Wongprasert et al. 2003; Wu et al. 2004). Apoptosis is induced in multicellular organisms by internal as well as external signals, so at least two major pathways can be identified: the intrinsic pathway, which is controlled by mitochondrial membrane permeabilization, and extrinsic pathway, in which a death receptor triggers the apoptotic cascade. The central players in both pathways are the caspase. Recently, lysosomal cysteine cathepsins have attracted considerable attention as potential mediators of apoptosis in a variety of animal model (Chwieralski et al. 2006).

Five types of cathepsin were indentified from Expressed Sequence Tags (ESTs) analysis of *P. monodon* lymphoid organ cDNA libraries (Tassanakajon et al. 2006). Cathepsin L was found at the highest frequency (86 clones), followed by cathepsin B (49 clones), cathepsin A (4 clones), cathepsin D (4 clones) and cathepsin C (3 clones).

In the previous study, expression level of CatL mRNA in the lymphoid organ from WSSV injected *P. monodon* was determined by a quantitative real-time RT-PCR. After WSSV injection, the CatL transcript was up-regulated within 6 hpi (Pongsomboon unpublished data). From these reasons, CatL might be involved in the shrimp immunity.

In this research, the shrimp CatL was further characterized for its localization in different tissues and investigated for its function in mediated apoptosis. CatL

protein has been reported in gastrointestinal juice (Laycock et al. 1989) and in hepatopancreas of Greasy-back shrimp (*M. ensis*) (Hu et al. 2007). CatL cDNA has been cloned from hepatopancreas of American lobster (*Homarus americanus*) (Laycock et al. 1991), the shrimps *Penaeus vannamei* (Le Boulay et al. 1996) and *M. ensis* (Hu et al. 2004). It has also been cloned from the stomach of Norway lobster (*Nephrops norvegicus*) (Le Boulay et al. 1995). From amino acid pairwise alignment between CatL from *P. monodon* and *M. ensis* showed 68.2 % identity and 71.1 % identity of conserve C1A peptidase domain alignment (Fig 4.1).

In this research, anti-human CatL antibody was used instead of antibody of shrimp CatL because the commercial anti-shrimp Cat antibody was unavailable. The identity between human and shrimp CatL was 67.9 % at conserved domain, C1A (Fig. 4.1). To investigate the cross reactivity of the anti-human CatL antibody to shrimp CatL, Western blot analysis was performed. The result showed that this antibody specifically reacted to the shrimp CatL. Therefore, the anti human CatL antibody was used to identify the CatL in the immunohistochemistry assay. A 28-kDa band corresponding to the mature enzyme was found in the hepatopancreas. It is well known that CatL is activated at acidic pH by the removal of the pro sequence (Jerala et al. 1998; Menard et al. 1998; Kramer et al. 2007). The acidic environment in hepatopancreas probably made mature enzyme in the main form. The presence of mature CatL in the hepatopancreas was in agreement with the previous study in *M. ensis* (Hu et al. 2004).

In this study, the immunohistochemistry was performed to investigate the localization of CatL in shrimp cephalothoraxes. The result of immunohistological localization showed that the positive signal was found mainly in hepatopancreas and lymphoid organ. In the previous report, CatL was a digestive enzyme because it was predominantly expressed in the hepatopancreas of *P. monodon* (Le Boulay et al. 1996; Hu et al. 2007). Hepatopancreas was responsible for synthesis of many digestive enzymes in decapods (Gibson et al. 1979). In addition, cathepsin L existed in the large vacuole of B cell. It was the digestive cell and enzyme secretion cell of the hepatopancreas (Gibson et al. 1979). Moreover, CatL was also identified in



haemocyte and muscle. The results were corresponding to the transcription level in previous reports of *P. monodon* (Tassanakajon et al. 2006), *Litopenaeus vannamei* (Robalino et al. 2007) and *M. ensis* (Hu et al. 2007)

Furthermore, the lymphoid organ, first described in *Penaeus orientalis* by Oka (1969), acts as a filtering organ for the purposes of filtering and elimination of foreign particles and infectious agents from the haemolymph as well as for homeostatic improvement of the haemolymph filtrate (van de Braak et al. 2002; Duangsuwan et al. 2008). The lymphoid organ was a major site of bacterial uptake from the circulation and phagocytosis by haemocytes (Martin et al. 1987; Hose et al. 1992; van de Braak et al. 2002). Besides the function in bacteria elimination, the shrimp lymphoid organ was also involved in antiviral response (Anggraeni et al. 2000; van de Braak et al. 2002; Anantasomboon et al. 2008). The immunohistochemistry in lymphoid organ injected with WSSV revealed a decrease in CatL express at 24 h comparing with the lymphoid organ of the control shrimp. Generally, viruses are known to shut-off host transcription and/or translation to avoid metabolic competition while facilitating their own propagation, thereby, affecting cellular gene expression and cell functions (Lyles 2000; Bushell et al. 2002). The decline of the shrimp CatL level after WSSV infection might be the result of a direct or indirect virus shut-off mechanism or might be the result of an unsuccessful host defense. From the WSSV detection in lymphoid organ, WSSV was found in lymphoid organ tubule, but was not detected in lymphoid organ spheroid. While the localization of CatL in lymphoid organ was mainly in the spheroid. The presence of WSSV in the tubule was in agreement with the previous study of van de Braak et al. (2002) and Pantoja et al. (2003). Furthermore, Anantasomboon et al. (2008) found that the moribund shrimp was infected by yellow head virus (YHV) in the lymphoid organ tubule, whereas in the survival shrimp, YHV was rarely found in lymphoid organ spheroid. From the above reason, the presence of the CatL in the lymphoid organ spheroid suggested that it might involve in the shrimp immunity.

When shrimp was invaded by foreign particle or virus, the defense system involving the degradation in the infected cells by apoptosis was occurred to avoid the spreading of virus to normal cells. From the previous study, Pantoja and Lightner (2003) found that severe infection by WSSV may result in systemic apoptosis, and

apoptosis of the lymphoid organ, in particular, which is very similar to that caused by YHV. Like the result of Pantoja and Lightner, Anantasomboon et al. (2008) showed that the apoptosis of surviving shrimp was changed the position from the lymphoid organ tubule to the lymphoid organ spheroid. The presence of CatL in lymphoid organ, suggests the possible role of CatL in apoptosis so its function was further examined in cell culture.

Cell culture of *P. monodon* was prepared from lymphoid cells. First CatL inhibitor was incubated with shrimp cell culture and Cas3 inhibitor was also performed as positive control. After 2 h, the medium was completely removed and the apoptosis-inducer, AD was added. After 12 h, the apoptosis cells were observed in cell culture. Several apoptosis characteristics can be detected in apoptosis cells including DNA fragmentation, changes in cell size and granularity, changes in plasma membrane permeability, cell surface modification and formation of apoptotic bodies (Darzynkiewicz et al. 1997). The apoptotic bodies and changes in plasma membrane permeability were observed in this study. The highest numbers of apoptotic bodies were observed in cells which were induced with AD. Addition of both CatL and Cas3 inhibitors were able to inhibit the formation of apoptotic bodies. The changes of plasma membrane permeability were observed by dye exclusion method. Trypan blue which was absorbed by death cells can distinguish between death and viable cells (Yip et al. 1972). The death cells were counted in each experiment. The death cells were significantly decreased after the AD treated cells were incubated with CatL and Cas3 inhibitors. The appropriate concentrations of both inhibitors for apoptosis inhibition were 0.5  $\mu\text{M}$  and 1  $\mu\text{M}$  of Cas3 and CatL, respectively. The CatL inhibitor can inhibit apoptosis as well as the positive control, Cas3. Thus the results suggested that CatL probably involved in apoptosis as the Cas3. To confirm the death of cells in AD treatment, the DNA laddering assay was performed to detect apoptosis. The lymphoid cells were grown in order to extract the apoptotic DNA fragment by conventional phenol/chloroform extraction method with some modification. The characteristic apoptotic DNA ladder of approximately 200 bp could be seen. This is fragmentation of chromatin into units of single or multiple nucleosomes that is specific for apoptosis and one of the easiest ways to distinguish programmed cell death and toxic necrosis (Herrmann et al. 1994). Because programmed cell death was

normally found in the primary cells untreated with AD, the approximately 200-bp DNA fragment was found in all 40 nM AD treated cells with or without inhibitor as well as the control (untreated cells). But the intensity of the DNA fragment of all groups on agarose gel was not very different. Probably, this DNA fragmentation was caused by unsuitable DNA extraction technique. So, the DNA laddering assay was unsuccessful to confirm the apoptosis function of CatL. However, number of dead cell counted by dye exclusion method showed that CatL might involve in apoptosis.

To further characterize the activity of the lymphoid organ CatL. The full-length cDNA of CatL gene was over-expressed in *E. coli*. To protect the host cell from potentially disastrous consequences of uncontrolled degradative activity, essentially all proteases are synthesized as inactive proenzymes due to the presence of an N-terminal propeptide extension. In addition to its role as potent inhibitor of proteolytic activity, the prosegment of human CatL has been shown to be crucial for the correct folding of enzyme and to stabilize the protein to the denaturing effects of neutral to alkaline pH, which rapidly inactivates the enzyme (Coulombe et al. 1996). The procathepsin L gene of shrimp encoding the inhibitor region and the mature protein was cloned and expressed in *Escherichia coli* expression system using the pET21a(+) as vector. But the CatL gene could not be cloned directly in the pET21a(+) expression vector. Thus, this gene was first cloned into a pGEM-T easy vector and then subcloned into the the pET21a(+) vector. The cloning of the gene fragment between the 2 restriction sites, *Nhe* I and *Xho* I, put the CatL amino acid sequence downstream of the His-Tag sequence for the purification of the recombinant protein.

In order to over-express the recombinant protein, an *E. coli* strain BL21(DE3) was used as a host. The expression of protein of interest was driven by the T7 polymerase and controlled by the lac repressor which can be induced by a synthetic inducer, isopropyl thiogalactoside (IPTG). The bacterial expression system is particularly convenient for preparing very large quantities of protein under well-defined conditions. Unfortunately, bacterially expressed proteins are often difficult to purify because of their tendency to precipitate within the cell. The precipitated protein forms inclusion bodies, the dense, granular structures distributed throughout the cytoplasm (Marston 1986). The formation of inclusion bodies is especially common

for nonbacterial proteins. The recombinant CatL is no exception. The 37 kDa protein was thus expressed and aggregated in the cells as inclusion bodies.

The recombinant CatL was further purified. Two conditions had been used to solubilize the inclusion bodies, the denaturing and nondenaturing or native conditions. Under the denaturing condition, the inclusion bodies were solubilized using 6 M urea, and the recombinant protein was purified with the Ni-NTA agarose column for it was tagged at the C-terminus with polyhistidine (Delcarte et al. 2003). For the nondenaturing condition, the inclusion bodies were solubilized using the acetate buffer at pH 4.

Because the recombinant protein was expressed as the zymogens form, the crude protein was auto activated to mature enzyme at slightly acidic condition following the previous study of Cristofolletti et al. (2005). The autocatalytic processing of procathepsin L indicated that the acid activation was unsuccessful. In the previous study, Kramer et al. (2007) expressed the recombinant human procathepsin L and the recombinant protein was autoactivated by acidic condition. Moreover, pepsin was utilized in this activation by digesting between the inhibitor region and mature enzyme region. Thus, enzymatic digestion may be used for activation of shrimp CatL. The expression of mature protein without the inhibitor region probably offers a better alternative to obtain the active enzyme for future characterization.

## CHAPTER V

### CONCLUSIONS

1. Immunolocalization of cathepsin L (CatL) in various shrimp tissues showed that shrimp CatL was mainly localized in the hepatopancreas and lymphoid organ.
2. In hepatopancreas, CatL was observed in the epithelial cells of hepatopancreas, mainly in the B-cells. Where as in the lymphoid organ, CatL was found in the spheroids.
3. In WSSV infected shrimp, the expression of CatL protein in hepatopancreas decreased at 24 h and returned to normal level at 48 h and 84 h. Similar results were observed in the lymphoid organ of infected shrimp.
4. In the immunolocalization of WSSV, the virus was found in heart, stomach, gill, connective tissue, hepatopancreas and lymphoid organ of WSSV injected shrimp. In hepatopancreas, the apparent of staining levels was increased significantly from 24 h to 48 h while the levels of positive signals were declined at 84 h. The trend of WSSV detection in lymphoid organ was the same as in hepatopancreas. The WSSV was found in the stromal matrix and haemal sinuses of lymphoid tubule. The positive signal was increased from 24 to 84 h. No positive signal of WSSV as observed in lymphoid organ spheroid.
5. *P. monodon* CatL from lymphoid organ was successfully expressed in the *Escherichia coli* strain BL21 (DE3) expression system. The molecular mass of the recombinant CatL determined by using MALDI-TOF mass spectrometry is 37,483.190 Da. Under acidic condition, the auto autocatalytic processing of procathepsin L was unsuccessful.
6. The role of CatL in mediated apoptosis was investigated in the primary shrimp cell culture. The results showed that cells treated with either caspase or CatL inhibitors had lower percentage of dead cells than the control cells induced with actinomycin D alone. This suggests that CatL may be involved in apoptosis.

## REFERENCES

- Adams, J. M. and S. Cory (1998). "The Bcl-2 protein family: arbiters of cell survival." Science **281**(5381): 1322-6.
- Anantasomboon, G., R. Poonkhum, et al. (2008). "Low viral loads and lymphoid organ spheroids are associated with yellow head virus (YHV) tolerance in whiteleg shrimp *Penaeus vannamei*." Dev Comp Immunol **32**(6): 613-26.
- Anderson, I. (1993). The veterinary approach to marine prawns. Aquaculture for veterinarians: Fish husbandry and medicine. Brown. Amsterdam, Oxford Pergamon Press: 271-190.
- Anggraeni, M. S. and L. Owens (2000). "The haemocytic origin of lymphoid organ spheroid cells in the penaeid prawn *Penaeus monodon*." Dis Aquat Organ **40**(2): 85-92.
- Baily-Brook, J. H. and S. M. Moss (1992). Penaeid taxonomy, biology and zoogeography. Marine shrimp culture: Principles and practices. A. W. Fast and L. J. Lester. Amsterdam, Elsevier Science Publishers.
- Baskin-Bey, E. S., A. Canbay, et al. (2005). "Cathepsin B inactivation attenuates hepatocyte apoptosis and liver damage in steatotic livers after cold ischemia-warm reperfusion injury." Am J Physiol Gastrointest Liver Physiol **288**(2): G396-402.
- Bell, T. A. and D. V. Lightner (1988). A handbook of normal penaeid shrimp histology. Lawrence, Kansas, Allen Press, Inc.
- Briggs, M., S. F. Smith, et al. (2004). Introductions and movement of *Penaeus vannamei* and *Penaeus stylirostris* in Asia and the Pacific., FOOD AND AGRICULTURE ORGANIZATION OF THE UNITED NATIONS REGIONAL OFFICE FOR ASIA AND THE PACIFIC: 99.
- Broker, L. E., C. Huisman, et al. (2004). "Cathepsin B mediates caspase-independent cell death induced by microtubule stabilizing agents in non-small cell lung cancer cells." Cancer Res **64**(1): 27-30.
- Bushell, M. and P. Sarnow (2002). "Hijacking the translation apparatus by RNA viruses." J Cell Biol **158**(3): 395-9.

- Cain, K., S. B. Bratton, et al. (2000). "Apaf-1 oligomerizes into biologically active approximately 700-kDa and inactive approximately 1.4-MDa apoptosome complexes." J Biol Chem **275**(9): 6067-70.
- Chayaburakul, K., G. Nash, et al. (2004). "Multiple pathogens found in growth-retarded black tiger shrimp *Penaeus monodon* cultivated in Thailand." Dis Aquat Organ **60**(2): 89-96.
- Chen, L. L., H. C. Wang, et al. (2002). "Transcriptional analysis of the DNA polymerase gene of shrimp white spot syndrome virus." Virology **301**(1): 136-47.
- Chou, H. Y., C. Y. Huang, et al. (1995). "Pathogenicity of a baculovirus infection causing white spot syndrome in cultured shrimp in Taiwan." Dis Aquat Org **23**: 161-173.
- Chun, H. J., L. Zheng, et al. (2002). "Pleiotropic defects in lymphocyte activation caused by caspase-8 mutations lead to human immunodeficiency." Nature **419**(6905): 395-9.
- Chwieralski, C. E., T. Welte, et al. (2006). "Cathepsin-regulated apoptosis." Apoptosis **11**(2): 143-9.
- Cirman, T., K. Oresic, et al. (2004). "Selective disruption of lysosomes in HeLa cells triggers apoptosis mediated by cleavage of Bid by multiple papain-like lysosomal cathepsins." J Biol Chem **279**(5): 3578-87.
- Coulombe, R., P. Grochulski, et al. (1996). "Structure of human procathepsin L reveals the molecular basis of inhibition by the prosegment." Embo J **15**(20): 5492-503.
- Cristofolletti, P. T., A. F. Ribeiro, et al. (2005). "The cathepsin L-like proteinases from the midgut of *Tenebrio molitor* larvae: sequence, properties, immunocytochemical localization and function." Insect Biochem Mol Biol **35**(8): 883-901.
- Dall, W., B. J. Hill, et al. (1990). The Biology of the Penaeidae. Advances in Marine Biology. London, Academic Press.
- Darzynkiewicz, Z., G. Juan, et al. (1997). "Cytometry in cell necrobiology: analysis of apoptosis and accidental cell death (necrosis)." Cytometry **27**(1): 1-20.

- Delcarte, J., M. Fauconnier, et al. (2003). "Optimisation of expression and immobilized metal ion affinity chromatographic purification of recombinant (His)<sub>6</sub>-tagged cytochrome P450 hydroperoxide lyase in *Escherichia coli*." J Chromatogr B Analyt Technol Biomed Life Sci **786**(1-2): 229-36.
- Duangsuwan, P., I. Phoungpetchara, et al. (2008). "Histological and three dimensional organizations of lymphoid tubules in normal lymphoid organ of *Penaeus monodon*." Fish Shellfish Immunol **24**(4): 426-35.
- Fast, A. W. and L. J. Lester (1992). Marine shrimp culture : principles and practices. Amsterdam ; New York, Elsevier.
- Flegel, T. (1997). "Special topic review: Major viral diseases of black tiger prawn (*Penaeus monodon*) in Thailand." World J Microbiol Biotechnol **13**: 433-442.
- Flegel, T. W. (2006). "The special danger of viral pathogens in shrimp translocated for aquaculture." ScienceAsia **32**(3): 215-221.
- Flegel, T. W. and T. Pasharawipas (1998). "Active viral accommodation: A new concept for crustacean response to viral pathogens." Advances in Shrimp Biotechnology: 245-250.
- Foghsgaard, L., D. Wissing, et al. (2001). "Cathepsin B acts as a dominant execution protease in tumor cell apoptosis induced by tumor necrosis factor." J Cell Biol **153**(5): 999-1010.
- Galluzzi, L., M. C. Maiuri, et al. (2007). "Cell death modalities: classification and pathophysiological implications." Cell Death Differ **14**(7): 1237-43.
- Garnett, T. O., M. Filippova, et al. (2007). "Bid is cleaved upstream of caspase-8 activation during TRAIL-mediated apoptosis in human osteosarcoma cells." Apoptosis **12**(7): 1299-315.
- Gibson, R. and P. L. Barker (1979). "The decapod hepatopancreas." Oceanogr. Mar. Biol. Ann. Rev. **17**: 285-346.
- Goulet, B., A. Baruch, et al. (2004). "A cathepsin L isoform that is devoid of a signal peptide localizes to the nucleus in S phase and processes the CDP/Cux transcription factor." Mol Cell **14**(2): 207-19.
- Goulet, B., L. Sansregret, et al. (2007). "Increased expression and activity of nuclear cathepsin L in cancer cells suggests a novel mechanism of cell transformation." Mol Cancer Res **5**(9): 899-907.

- Guicciardi, M. E., S. F. Bronk, et al. (2005). "Bid is upstream of lysosome-mediated caspase 2 activation in tumor necrosis factor alpha-induced hepatocyte apoptosis." Gastroenterology **129**(1): 269-84.
- Guicciardi, M. E., J. Deussing, et al. (2000). "Cathepsin B contributes to TNF-alpha-mediated hepatocyte apoptosis by promoting mitochondrial release of cytochrome c." J Clin Invest **106**(9): 1127-37.
- Hameed, A. S. S., M. Sarathi, et al. (2006). "Quantitative assessment of apoptotic hemocytes in white spot syndrome virus (WSSV)-infected penaeid shrimp, *Penaeus monodon* and *Penaeus indicus*, by flow cytometric analysis." Aquaculture **256**(1-4): 111-120.
- He, N., Q. Qin, et al. (2005). "Differential profile of genes expressed in hemocytes of White Spot Syndrome Virus-resistant shrimp (*Penaeus japonicus*) by combining suppression subtractive hybridization and differential hybridization." Antiviral Res **66**(1): 39-45.
- Herrmann, M., H. M. Lorenz, et al. (1994). "A rapid and simple method for the isolation of apoptotic DNA fragments." Nucleic Acids Res **22**(24): 5506-7.
- Hose, J. E., G. G. Martin, et al. (1992). "Patterns of hemocyte production and release throughout the molt cycle in the penaeid shrimp *Sicyonia ingentis*." Biol. Bull. **183**: 185-199.
- Hu, K. J. and P. C. Leung (2004). "Shrimp cathepsin L encoded by an intronless gene has predominant expression in hepatopancreas, and occurs in the nucleus of oocyte." Comp Biochem Physiol B Biochem Mol Biol **137**(1): 21-33.
- Hu, K. J. and P. C. Leung (2007). "Food digestion by cathepsin L and digestion-related rapid cell differentiation in shrimp hepatopancreas." Comp Biochem Physiol B Biochem Mol Biol **146**(1): 69-80.
- Huang, C., X. Zhang, et al. (2002). "Characterization of a novel envelope protein (VP281) of shrimp white spot syndrome virus by mass spectrometry." J Gen Virol **83**(Pt 10): 2385-92.
- Inouye, K., S. Miwa, et al. (1994). "Mass mortalities of cultured Kuruma shrimp *Penaeus japonicus* in Japan in 1993: electron microscopic evidence of the causative virus." Fish Pathol **29**: 149-158.

- Jane, D. T., L. Morvay, et al. (2006). "Cathepsin B localizes to plasma membrane caveolae of differentiating myoblasts and is secreted in an active form at physiological pH." Biol Chem **387**(2): 223-34.
- Jeong, S. Y. and D. W. Seol (2008). "The role of mitochondria in apoptosis." BMB Rep **41**(1): 11-22.
- Jerala, R., E. Zerovnik, et al. (1998). "pH-induced conformational transitions of the propeptide of human cathepsin L. A role for a molten globule state in zymogen activation." J Biol Chem **273**(19): 11498-504.
- Jittivadhna, K. (2000). PCR-Based detection of hepatopancreatic parvovirus and white-spot syndrome virus in *Penaeus monodon*. Faculty of Graduate studies. Bangkok, Mahidol university: 150.
- Johnson, P. T. (1980). Histology of the blue crab, *Callinectes sapidus*. A model for the Decapoda. New York, Praeger.
- Kagedal, K., M. Zhao, et al. (2001). "Sphingosine-induced apoptosis is dependent on lysosomal proteases." Biochem J **359**(Pt 2): 335-43.
- Kerr, J. F., A. H. Wyllie, et al. (1972). "Apoptosis: a basic biological phenomenon with wide-ranging implications in tissue kinetics." Br J Cancer **26**(4): 239-57.
- Khanobdee, K., C. Soowannayan, et al. (2002). "Evidence for apoptosis correlated with mortality in the giant black tiger shrimp *Penaeus monodon* infected with yellow head virus." Dis Aquat Organ **48**(2): 79-90.
- Kiatpathomchai, W., S. Jitrapakdee, et al. (2004). "RT-PCR detection of yellow head virus (YHV) infection in *Penaeus monodon* using dried haemolymph spots." J Virol Methods **119**(1): 1-5.
- Kiatpathomchai, W., V. Boonsaeng, et al. (2001). "A non-stop, single-tube, semi-nested PCR technique for grading the severity of white spot syndrome virus infections in *Penaeus monodon*." Dis Aquat Organ **47**(3): 235-9.
- Kramer, G., A. Paul, et al. (2007). "Optimized folding and activation of recombinant procathepsin L and S produced in *Escherichia coli*." Protein Expr Purif **54**(1): 147-56.
- Krueger, A., S. C. Fas, et al. (2003). "The role of CD95 in the regulation of peripheral T-cell apoptosis." Immunol Rev **193**: 58-69.

- Laycock, M. V., T. Hirama, et al. (1989). "Purification and characterization of a digestive cysteine proteinase from the American lobster (*Homarus americanus*)." Biochem J **263**(2): 439-44.
- Laycock, M. V., R. M. MacKay, et al. (1991). "Molecular cloning of three cDNAs that encode cysteine proteinases in the digestive gland of the American lobster (*Homarus americanus*)." FEBS Lett **292**(1-2): 115-20.
- Le Boulay, C., A. Van Wormhoudt, et al. (1995). "Molecular cloning and sequencing of two cDNAs encoding cathepsin L-related cysteine proteinases in the nervous system and in the stomach of the Norway lobster (*Nephrops norvegicus*)." Comp Biochem Physiol B Biochem Mol Biol **111**(3): 353-9.
- Le Boulay, C., A. Van Wormhoudt, et al. (1996). "Cloning and expression of cathepsin L-like proteinases in the hepatopancreas of the shrimp *Penaeus vannamei* during the intermolt cycle." J Comp Physiol [B] **166**(5): 310-8.
- Lechner, A. M., I. Assfalg-Machleidt, et al. (2006). "RGD-dependent binding of procathepsin X to integrin alphavbeta3 mediates cell-adhesive properties." J Biol Chem **281**(51): 39588-97.
- Li, H., H. Zhu, et al. (1998). "Cleavage of BID by caspase 8 mediates the mitochondrial damage in the Fas pathway of apoptosis." Cell **94**(4): 491-501.
- Li, J. H. and J. S. Pober (2005). "The cathepsin B death pathway contributes to TNF plus IFN-gamma-mediated human endothelial injury." J Immunol **175**(3): 1858-66.
- Lightner, D. V. (1996). A Handbook of pathology and diagnostic procedures for disease of penaeid shrimp. Baton Rouge, LA, World Aquaculture Society.
- Linette, G. P., Y. Li, et al. (1996). "Cross talk between cell death and cell cycle progression: BCL-2 regulates NFAT-mediated activation." Proc Natl Acad Sci U S A **93**(18): 9545-52.
- Lotz, J. M. (1997). "Special review: Viruses, biosecurity and specific pathogen free stocks in shrimp aquaculture." World J Microbiol Biotechnol **13**: 405-403.
- Luo, T., X. Zhang, et al. (2003). "PmAV, a novel gene involved in virus resistance of shrimp *Penaeus monodon*." FEBS Lett **551**(1-3): 53-7.
- Lyles, D. S. (2000). "Cytopathogenesis and inhibition of host gene expression by RNA viruses." Microbiol Mol Biol Rev **64**(4): 709-24.

- Marston, F. A. (1986). "The purification of eukaryotic polypeptides synthesized in *Escherichia coli*." Biochem J **240**(1): 1-12.
- Martin, G. G., J. E. Hose, et al. (1987). "Structure of hematopoietic nodules in the ridgeback prawn, *Sicyonia ingentis*: Light and electron microscopic observations." J Morphol **192**: 193-204.
- Mayo, M. A. (2002). "A summary of taxonomic changes recently approved by ICTV." Arch Virol **147**(8): 1655-63.
- Menard, R., E. Carmona, et al. (1998). "Autocatalytic processing of recombinant human procathepsin L. Contribution of both intermolecular and unimolecular events in the processing of procathepsin L in vitro." J Biol Chem **273**(8): 4478-84.
- Michallet, M. C., F. Saltel, et al. (2003). "Cathepsin-B-dependent apoptosis triggered by antithymocyte globulins: a novel mechanism of T-cell depletion." Blood **102**(10): 3719-26.
- Mohan, C. V., K. M. Shankar, et al. (1998). "Histopathology of cultured shrimp showing gross signs of yellow head syndrome and white spot syndrome during 1994 Indian epizootics." Dis Aquat Organ **34**(1): 9-12.
- Musil, D., D. Zucic, et al. (1991). "The refined 2.15 Å X-ray crystal structure of human liver cathepsin B: the structural basis for its specificity." EMBO J **10**(9): 2321-30.
- Nagaraj, N. S., N. Vigneswaran, et al. (2006). "Cathepsin B mediates TRAIL-induced apoptosis in oral cancer cells." J Cancer Res Clin Oncol **132**(3): 171-83.
- Nielsen, H., J. Engelbrecht, et al. (1997). "A neural network method for identification of prokaryotic and eukaryotic signal peptides and prediction of their cleavage sites." Int J Neural Syst **8**(5-6): 581-99.
- Oka, M. (1969). "Studies on *Penaeus orientalis* Kishinouye VIII. Structure of newly found lymphoid organ." Bull Jpn Soc Sci Fish **35**: 245-250.
- Okumura, T., F. Nagai, et al. (2005). "Detection of white spot syndrome virus (WSSV) from hemolymph of Penaeid shrimps *Penaeus japonicus* by reverse passive latex agglutination assay using high-density latex particles." J Virol Methods **124**(1-2): 143-8.

- Overstreet, R. M., D. V. Lightner, et al. (1997). "Susceptibility to Taura Syndrome Virus of Some Penaeid Shrimp Species Native to the Gulf of Mexico and the Southeastern United States." J Invertebr Pathol **69**(2): 165-76.
- Pantoja, C. R. and D. V. Lightner (2003). "Similarity between the histopathology of white spot syndrome virus and yellow head syndrome virus and its relevance to diagnosis of YHV disease in the Americas." Aquaculture **218**(1-4): 47-54.
- Paris, C., J. Bertoglio, et al. (2007). "Lysosomal and mitochondrial pathways in miltefosine-induced apoptosis in U937 cells." Apoptosis **12**(7): 1257-67.
- Poulos, B. T., C. R. Pantoja, et al. (2001). "Development and application of monoclonal antibodies for the detection of white spot syndrome virus of penaeid shrimp." Dis Aquat Organ **47**(1): 13-23.
- Primavera, J. H. (1990). External and internal anatomy of adult penaeid prawns/shrimps, SEAFDEC, Aquaculture Department.
- Quere, R., T. Commes, et al. (2002). "White spot syndrome virus and infectious hypodermal and hematopoietic necrosis virus simultaneous diagnosis by miniarray system with colorimetry detection." J Virol Methods **105**(2): 189-96.
- Robalino, J., J. S. Almeida, et al. (2007). "Insights into the immune transcriptome of the shrimp *Litopenaeus vannamei*: tissue-specific expression profiles and transcriptomic responses to immune challenge." Physiol Genomics **29**(1): 44-56.
- Roberts, L. R., H. Kurosawa, et al. (1997). "Cathepsin B contributes to bile salt-induced apoptosis of rat hepatocytes." Gastroenterology **113**(5): 1714-26.
- Rosenberry, B. (1997). World Shrimp Farming 1997. Shrimp News International. San Diego.
- Roshy, S., B. F. Sloane, et al. (2003). "Pericellular cathepsin B and malignant progression." Cancer Metastasis Rev **22**(2-3): 271-86.
- Rossi, A., Q. Deveraux, et al. (2004). "Comprehensive search for cysteine cathepsins in the human genome." Biological Chemistry **385**(5): 363-372.
- Sahtout, A. H., M. D. Hassan, et al. (2001). "DNA fragmentation, an indicator of apoptosis, in cultured black tiger shrimp *Penaeus monodon* infected with white spot syndrome virus (WSSV)." Dis Aquat Organ **44**(2): 155-9.

- Salmena, L., B. Lemmers, et al. (2003). "Essential role for caspase 8 in T-cell homeostasis and T-cell-mediated immunity." Genes Dev **17**(7): 883-95.
- Sambrook, J. and D. W. Russell (2001). Molecular cloning : a laboratory manual. Cold Spring Harbor, N.Y., Cold Spring Harbor Laboratory Press.
- Sanchez-Martinez, J. G., G. Aguirre-Guzman, et al. (2007). "White Spot Syndrome Virus in cultured shrimp: A review." Aquaculture Research **38**(13): 1339-1354.
- Sithigorngul, P., P. Chauyuchwong, et al. (2000). "Development of a monoclonal antibody specific to yellow head virus (YHV) from *Penaeus monodon*." Dis Aquat Organ **42**(1): 27-34.
- Solis, N. B. (1988). Biology and ecology. Biology and culture of *Penaeus monodon*. Y. Taki, J. H. Premavara and J. Lobrera, Aquaculture Department, Southeast Asian Fisheries Development Center.
- Soowannayan, C., T. W. Flegel, et al. (2003). "Detection and differentiation of yellow head complex viruses using monoclonal antibodies." Dis Aquat Organ **57**(3): 193-200.
- Span, K. M. (1997). "Special topic review: Viral diseases of penaeid shrimp with particular reference to four viruses recently found in shrimp from Queensland." World J Microbiol Biotechnol **13**: 419-426.
- Stoka, V., B. Turk, et al. (2001). "Lysosomal protease pathways to apoptosis. Cleavage of bid, not pro-caspases, is the most likely route." J Biol Chem **276**(5): 3149-57.
- Stoka, V., V. Turk, et al. (2007). "Lysosomal cysteine cathepsins: signaling pathways in apoptosis." Biol Chem **388**(6): 555-60.
- Strasser, A. (2001). "BH3-only members of the Bcl-2 family are critical inducers of apoptosis and preclude autoimmunity." Keystone Symposium on Molecular Mechanisms of Apoptosis.
- Sukhumsirichart, W., W. Kiatpathomchai, et al. (2002). "Detection of hepatopancreatic parvovirus (HPV) infection in *Penaeus monodon* using PCR-ELISA." Mol Cell Probes **16**(6): 409-13.
- Taatjes, D. J., B. E. Sobel, et al. (2008). "Morphological and cytochemical determination of cell death by apoptosis." Histochem Cell Biol **129**(1): 33-43.

- Tapay, L. M., E. C. Nadala, Jr., et al. (1999). "A polymerase chain reaction protocol for the detection of various geographical isolates of white spot virus." J Virol Methods **82**(1): 39-43.
- Tardy, C., P. Codogno, et al. (2006). "Lysosomes and lysosomal proteins in cancer cell death (new players of an old struggle)." Biochim Biophys Acta **1765**(2): 101-25.
- Tassanakajon, A., S. Klinbunga, et al. (2006). "*Penaeus monodon* gene discovery project: The generation of an EST collection and establishment of a database." Gene **384**(1-2): 104-112.
- Tassanakajon, A., S. Klinbunga, et al. (2006). "*Penaeus monodon* gene discovery project: The generation of an EST collection and establishment of a database." Gene **384**(1-2): 104-112.
- Thiele, D. L. and P. E. Lipsky (1990). "Mechanism of L-leucyl-L-leucine methyl ester-mediated killing of cytotoxic lymphocytes: dependence on a lysosomal thiol protease, dipeptidyl peptidase I, that is enriched in these cells." Proc Natl Acad Sci U S A **87**(1): 83-7.
- Tirasophon, W., Y. Roshorm, et al. (2005). "Silencing of yellow head virus replication in penaeid shrimp cells by dsRNA." Biochem Biophys Res Commun **334**(1): 102-7.
- Tsai, J. M., H. C. Wang, et al. (2006). "Identification of the nucleocapsid, tegument, and envelope proteins of the shrimp white spot syndrome virus virion." J Virol **80**(6): 3021-9.
- Turk, B., D. Turk, et al. (2000). "Lysosomal cysteine proteases: more than scavengers." Biochim Biophys Acta **1477**(1-2): 98-111.
- Turk, V., B. Turk, et al. (2002). "Lysosomal cathepsins: structure, role in antigen processing and presentation, and cancer." Adv Enzyme Regul **42**: 285-303.
- Turk, D., B. Turk, et al. (2003). "Papain-like lysosomal cysteine proteases and their inhibitors: drug discovery targets?" Biochem Soc Symp(70): 15-30.
- van de Braak, C. B., M. H. Botterblom, et al. (2002). "Preliminary study on haemocyte response to white spot syndrome virus infection in black tiger shrimp *Penaeus monodon*." Dis Aquat Organ **51**(2): 149-55.

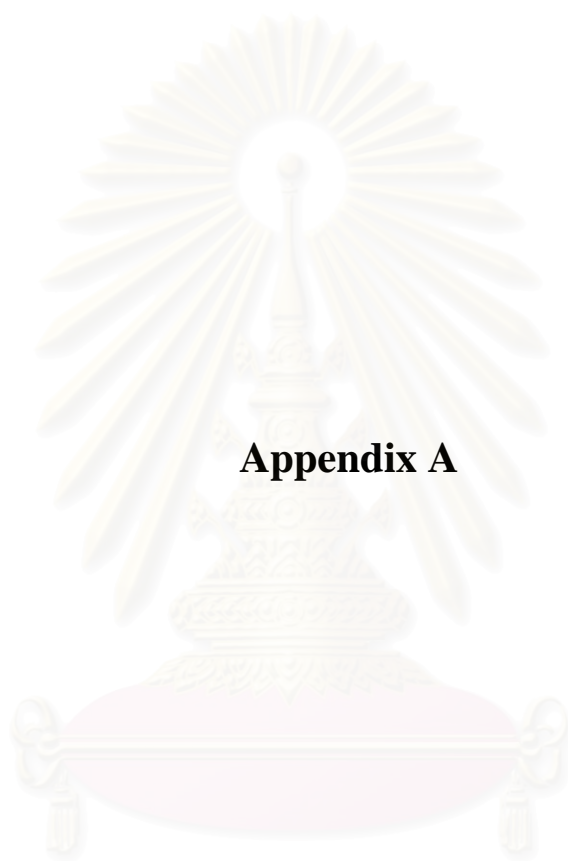
- van de Braak, C. B., M. H. Botterblom, et al. (2002). "The roles of haemocytes and the lymphoid organ in the clearance of injected *Vibrio* bacteria in *Penaeus monodon* shrimp." Fish Shellfish Immunol **13**(4): 293-309.
- van Hulten, M. C., J. Witteveldt, et al. (2001). "The white spot syndrome virus DNA genome sequence." Virology **286**(1): 7-22.
- van Hulten, M. C., J. Witteveldt, et al. (2001). "White spot syndrome virus envelope protein VP28 is involved in the systemic infection of shrimp." Virology **285**(2): 228-33.
- Vasiljeva, O., M. Dolinar, et al. (2003). "Recombinant human cathepsin H lacking the mini chain is an endopeptidase." Biochemistry **42**(46): 13522-8.
- Vasiljeva, O., T. Reinheckel, et al. (2007). "Emerging roles of cysteine cathepsins in disease and their potential as drug targets." Curr Pharm Des **13**(4): 387-403.
- Vasiljeva, O. and B. Turk (2008). "Dual contrasting roles of cysteine cathepsins in cancer progression: apoptosis versus tumour invasion." Biochimie **90**(2): 380-6.
- Wang, C. S., Y. J. Tsai, et al. (1998). "Detection of white spot disease virus (WSDV) infection in shrimp using in situ hybridization." J Invertebr Pathol **72**(2): 170-3.
- Wang, Z. M., L. B. Hu, et al. (2004). "ORF390 of white spot syndrome virus genome is identified as a novel anti-apoptosis gene." Biochemical and Biophysical Research Communications **325**(3): 899-907.
- White, C., C. Li, et al. (2005). "The endoplasmic reticulum gateway to apoptosis by Bcl-X(L) modulation of the InsP3R." Nat Cell Biol **7**(10): 1021-8.
- Wikstrom, J. D., S. M. Katzman, et al. (2007). "beta-Cell mitochondria exhibit membrane potential heterogeneity that can be altered by stimulatory or toxic fuel levels." Diabetes **56**(10): 2569-78.
- Witteveldt, J., A. M. Vermeesch, et al. (2005). "Nucleocapsid protein VP15 is the basic DNA binding protein of white spot syndrome virus of shrimp." Arch Virol.
- Wongprasert, K., K. Khanobdee, et al. (2003). "Time-course and levels of apoptosis in various tissues of black tiger shrimp *Penaeus monodon* infected with white-spot syndrome virus." Diseases of Aquatic Organisms **55**(1): 3-10.

- Wongteerasupaya, C., P. Pungchai, et al. (2003). "High variation in repetitive DNA fragment length for white spot syndrome virus (WSSV) isolates in Thailand." Dis Aquat Organ **54**(3): 253-7.
- Wu, J. L. and K. Muroga (2004). "Apoptosis does not play an important role in the resistance of 'immune' *Penaeus japonicus* against white spot syndrome virus." Journal of Fish Diseases **27**(1): 15-21.
- Wu, W., L. Wang, et al. (2005). "Identification of white spot syndrome virus (WSSV) envelope proteins involved in shrimp infection." Virology **332**(2): 578-83.
- Wyllie, A. H., J. F. Kerr, et al. (1980). "Cell death: the significance of apoptosis." Int Rev Cytol **68**: 251-306.
- Yip, D. K. and N. Auersperg (1972). "The dye-exclusion test for cell viability: persistence of differential staining following fixation." In Vitro **7**(5): 323-9.
- Zhang, X., C. Huang, et al. (2004). "Antiviral properties of hemocyanin isolated from shrimp *Penaeus monodon*." Antiviral Res **61**(2): 93-9.
- Zhao, M., F. Antunes, et al. (2003). "Lysosomal enzymes promote mitochondrial oxidant production, cytochrome c release and apoptosis." Eur J Biochem **270**(18): 3778-86.



**APPENDICES**

สถาบันวิทยบริการ  
จุฬาลงกรณ์มหาวิทยาลัย

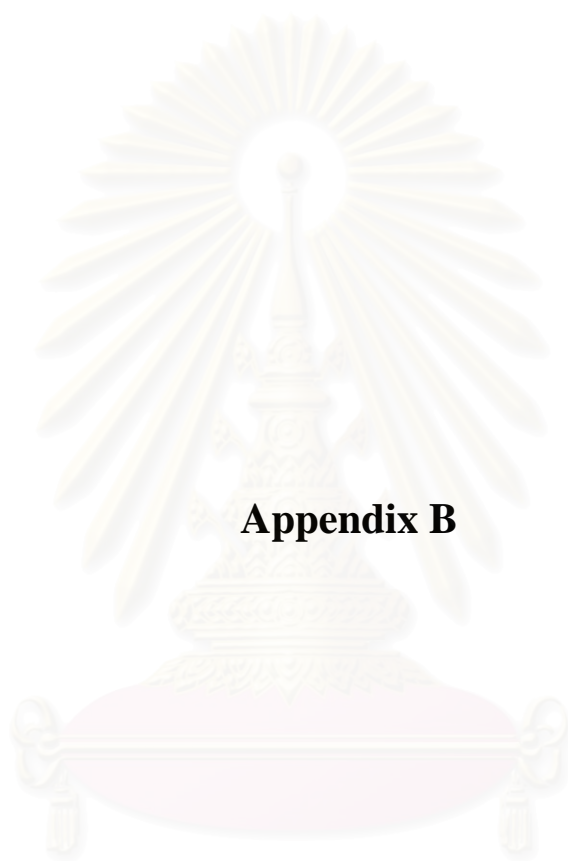


## Appendix A

สถาบันวิทยบริการ  
จุฬาลงกรณ์มหาวิทยาลัย

**Phenol-Chloroform extraction of DNA**

1. Add an equal volume (equal to sample volume) of Phenol-Chloroform (1:1) to sample.
2. Mix (shake, don't vortex).
3. Take aqueous (upper) layer. (If dirty sample, repeat Phenol-Chloroform step until interface is fairly clean).
4. Add equal volume chloroform, mix (shake, don't vortex).
5. Spin 3 min.
6. Take aqueous (upper) layer. (Optional: repeat Chloroform steps).
7. Add 1/10 volume 3 M Sodium acetate mix (shake).
8. Add 2 volumes ice-cold ethanol (100 %), mix (shake).
9. Incubate on ice for 15 to 30 minutes. (Can store on ice or at -20 °C at this step).
10. Spin 10 minutes, 4 °C.
11. Remove supernatant, being careful not to disturb pellet (DNA).
12. Half-fill tube with 70 % EtOH, spin at least 2 minutes at 4 °C. (Optional: Re-rinse and spin again).
13. Pipet off the supernatant, careful not to touch pellet.
14. Air-dry (~ 1 hour).
15. Redissolve in 40 µl of TE buffer



## Appendix B

สถาบันวิทยบริการ  
จุฬาลงกรณ์มหาวิทยาลัย

## Preparation for polyacrylamide gel electrophoresis

### 1. Stock reagents

#### 30 % Acrylamide, 0.8 % bis-acrylamide, 100 ml

Acrylamide	29.2	g
N, N'-methylene-bis-acrylamide	0.8	g

Adjust volume to 100 ml with distilled water.

#### 1.5 M Tris-HCl pH 8.8

Tris (hydroxymethyl)-aminomethane	18.17	g
-----------------------------------	-------	---

Adjust pH to 8.8 with 1 M HCl and adjust volume to 100 ml with distilled water.

#### 2.0 M Tris-HCl pH 8.8

Tris (hydroxymethyl)-aminomethane	24.2	g
-----------------------------------	------	---

Adjust pH to 8.8 with 1 M HCl and adjust volume to 100 ml with distilled water.

#### 0.5 M Tris-HCl pH 6.8

Tris (hydroxymethyl)-aminomethane	6.06	g
-----------------------------------	------	---

Adjust pH to 6.8 with 1 M HCl and adjust volume to 100 ml with distilled water.

#### 1.0 M Tris-HCl pH 6.8

Tris (hydroxymethyl)-aminomethane	12.1	g
-----------------------------------	------	---

Adjust pH to 6.8 with 1 M HCl and adjust volume to 100 ml with distilled water.

#### Solution B (SDS PAGE)

2.0 M Tris-HCl pH 8.8	75	ml
10 % SDS	4	ml
Distilled water	21	ml

#### Solution C (SDS PAGE)

1.0 M Tris-HCl pH 8.8	50	ml
10 % SDS	4	ml
Distilled water	46	ml

## 2. SDS-PAGE

### 15 % Separating gel

30 % Acrylamide/ml solution	5.0	ml
Solution B	2.5	ml
Distilled water	2.5	ml
10 % $(\text{NH}_4)_2\text{S}_2\text{O}_8$	50	$\mu\text{l}$
TEMED	10	$\mu\text{l}$

### 5.0 % Stacking gel

30 % Acrylamide/ml solution	0.67	ml
Solution C	1.0	ml
Distilled water	2.3	ml
10 % $(\text{NH}_4)_2\text{S}_2\text{O}_8$	30	$\mu\text{l}$
TEMED	5.0	$\mu\text{l}$

### 5X Sample buffer

1 M Tris-HCl pH 6.8	0.6	ml
50 % Glycerol	5.0	ml
10 % SDS	2.0	ml
2-Mercaptoethanol	0.5	ml
1 % Bromophenol blue	1.0	ml
Distilled water	0.9	ml

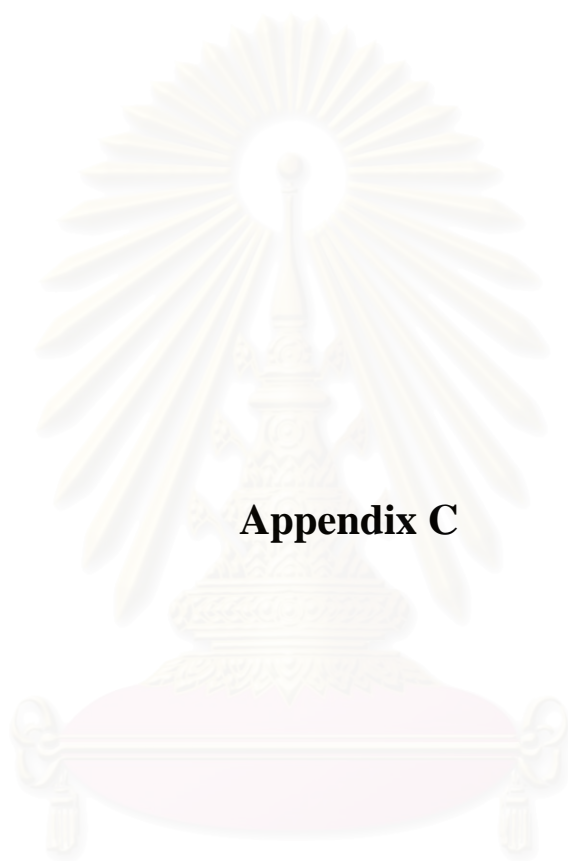
One part of sample buffer was added to four parts of sample. The mixture was heated 5 min. in boiling water before loading to the gel.

## 3. Electrophoresis buffer, 1 litre

(25 mM Tris, 192 mM glycine)

Tris (hydroxymethyl)-aminomethane	3.03	g
Glycine	14.40	g
SDS	1.0	g

Dissolve in distilled water to 1 litre. Do not adjust pH with acid or base (final pH should be 8.3).

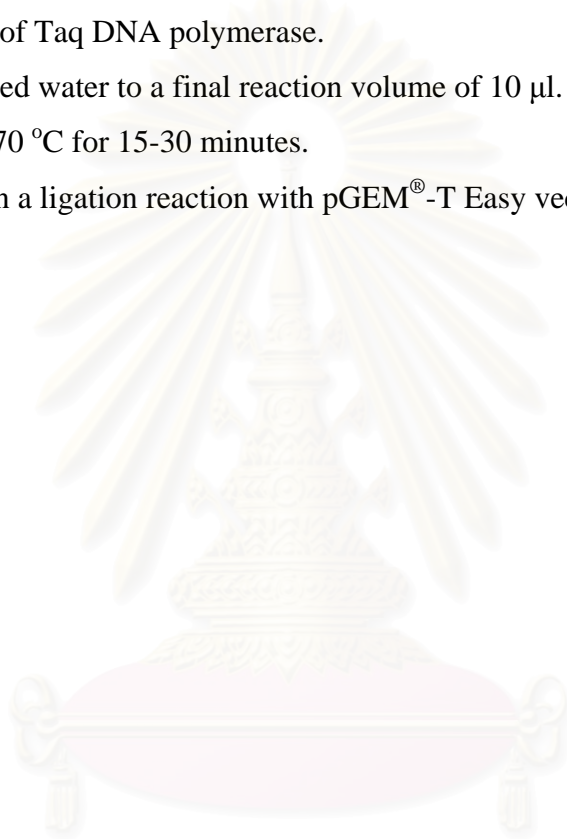


## Appendix C

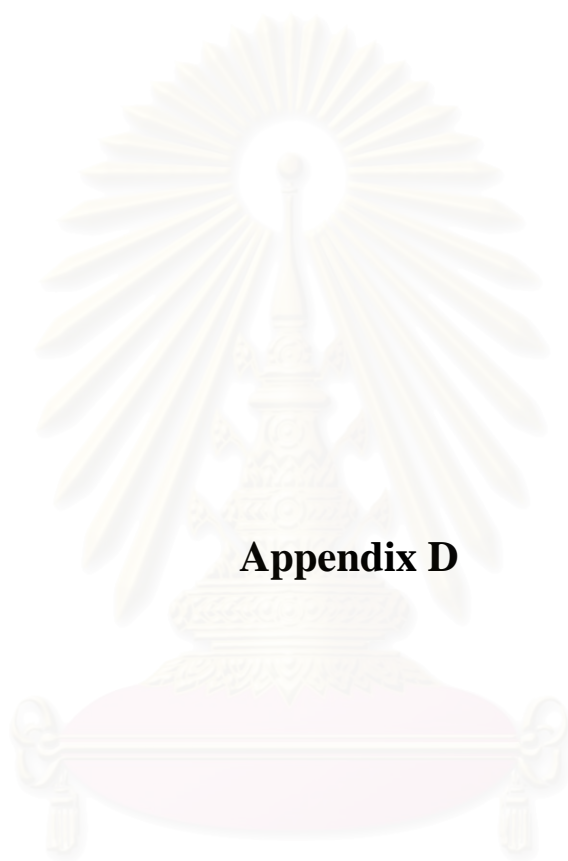
สถาบันวิทยบริการ  
จุฬาลงกรณ์มหาวิทยาลัย

**A-tailing procedure for blunt-ended PCR fragments**

1. Start with 1-7  $\mu\text{l}$  of purified PCR fragment generated by a proofreading polymerase, *Pfu* DNA polymerase.
2. Add 1  $\mu\text{l}$  Taq DNA polymerase 10x Reaction Buffer with  $\text{MgCl}_2$ .
3. Add dATP to a final concentration of 0.2 mM.
4. Add 5 units of Taq DNA polymerase.
5. Add deionized water to a final reaction volume of 10  $\mu\text{l}$ .
6. Incubate at 70 °C for 15-30 minutes.
7. Use 1-2  $\mu\text{l}$  in a ligation reaction with pGEM<sup>®</sup>-T Easy vector



สถาบันวิทยบริการ  
จุฬาลงกรณ์มหาวิทยาลัย



## Appendix D

สถาบันวิทยบริการ  
จุฬาลงกรณ์มหาวิทยาลัย

**LB Broth** (per Liter)

10 g of NaCl

10 g of tryptone

5 g of yeast extract

Add deionized H<sub>2</sub>O to a final volume of 1 liter and autoclave**LB Agar** (per Liter)

10 g of NaCl

10 g of tryptone

5 g of yeast extract

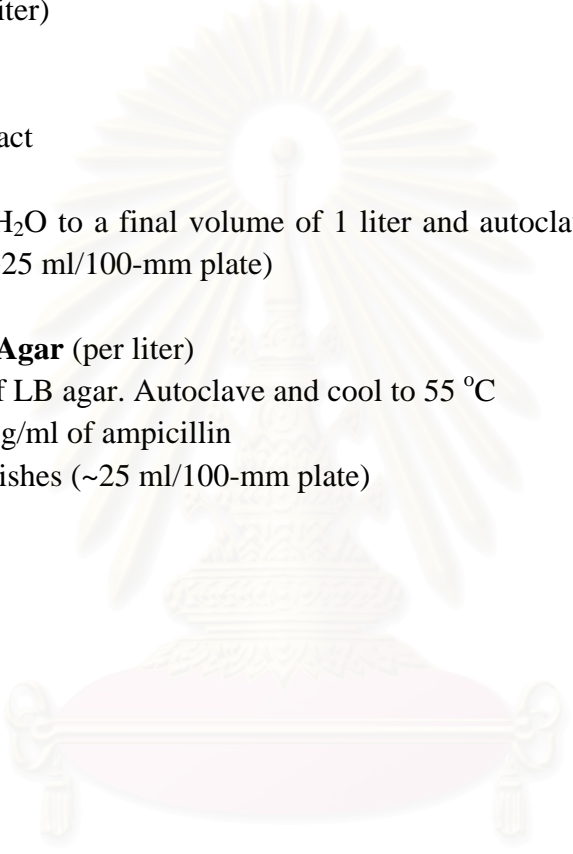
15 g pf agar

Add deionized H<sub>2</sub>O to a final volume of 1 liter and autoclave. After, pour into petri dishes (~25 ml/100-mm plate)**LB-Ampicillin Agar** (per liter)

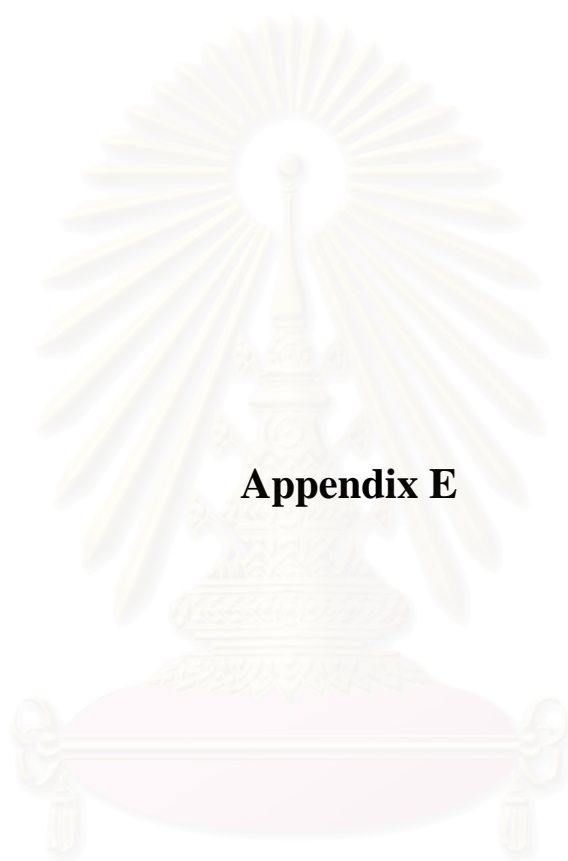
Prepare 1 liter of LB agar. Autoclave and cool to 55 °C

Add 1 ml of 0.1 g/ml of ampicillin

Pour into petri dishes (~25 ml/100-mm plate)



สถาบันวิทยบริการ  
จุฬาลงกรณ์มหาวิทยาลัย



## Appendix E

สถาบันวิทยบริการ  
จุฬาลงกรณ์มหาวิทยาลัย

pGEM<sup>®</sup> T-EASY vector map (Promega, USA)



II.C. pGEM<sup>®</sup>-T Easy Vector Map and Sequence Reference Points

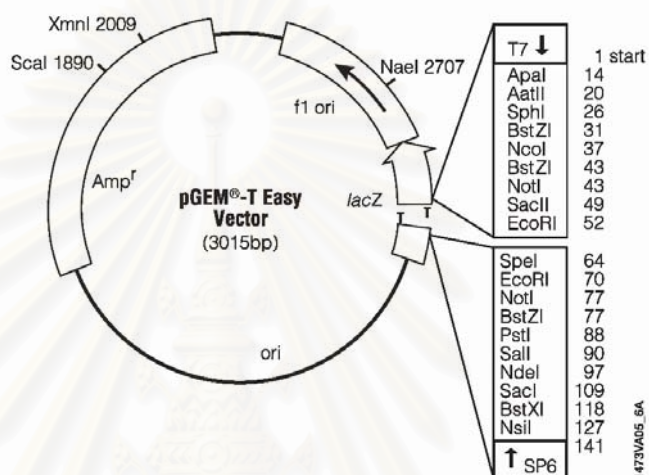


Figure 3. pGEM<sup>®</sup>-T Easy Vector circle map and sequence reference points.

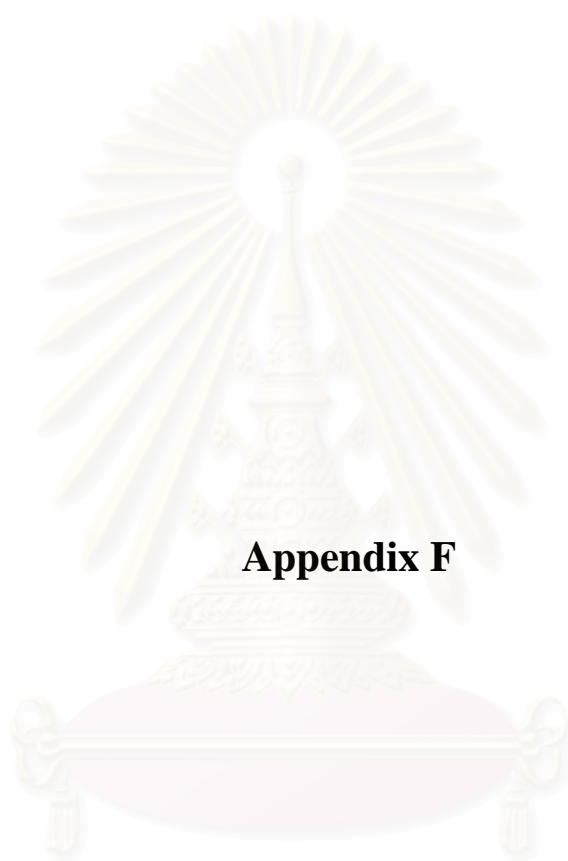
pGEM<sup>®</sup>-T Easy Vector sequence reference points:

T7 RNA polymerase transcription initiation site	1
multiple cloning region	10-128
SP6 RNA polymerase promoter (-17 to +3)	139-158
SP6 RNA polymerase transcription initiation site	141
pUC/M13 Reverse Sequencing Primer binding site	176-197
<i>lacZ</i> start codon	180
<i>lac</i> operator	200-216
β-lactamase coding region	1337-2197
phage f1 region	2380-2835
<i>lac</i> operon sequences	2836-2996, 166-395
pUC/M13 Forward Sequencing Primer binding site	2949-2972
T7 RNA polymerase promoter (-17 to +3)	2999-3

**Note:** Inserts can be sequenced using the SP6 Promoter Primer (Cat.# Q5011), T7 Promoter Primer (Cat.# Q5021), pUC/M13 Forward Primer (Cat.# Q5601), or pUC/M13 Reverse Primer (Cat.# Q5421).



**Note:** A single digest with BstZI (Cat.# R6881), EcoRI (Cat.# R6011) or NotI (Cat.# R6431) will release inserts cloned into the pGEM<sup>®</sup>-T Easy Vector. Double digests can also be used to release inserts.



## Appendix F

สถาบันวิทยบริการ  
จุฬาลงกรณ์มหาวิทยาลัย



## BIOGRAPHY

Mr. Arthit Chalorsrikul was born on Aug 15, 1982 in Bangkok province, Thailand. He graduated with a Bachelor of Science degree in Biochemistry, Faculty of Science, Chulalongkorn University in 2004. He has further studied for the Master degree in Biochemistry, Faculty of Science, Chulalongkorn University since 2004.



สถาบันวิทยบริการ  
จุฬาลงกรณ์มหาวิทยาลัย